UNIVERSIDADE DA BEIRA INTERIOR
Ciências da Saúde

Purification of supercoiled HPV-16 E6/E7 plasmid using a modified monolithic support

Lúcia Filipa Alves Amorim

Dissertação para a obtenção do Grau de Mestre em
Ciências Biomédicas
(2º Ciclo de estudos)

Orientadora: Profª. Doutora Ângela Sousa
Coorientadora: Profª. Doutora Carla Cruz

Covilhã, junho de 2014

To my parents

Acknowledgments

Firstly, I would like to thank to my supervisors Doctor Ângela Sousa and Doctor Carla Cruz, for all their guidance, advice, availability throughout this year, and continuous help in the development of this work. It was a privilege to work and learn with them.

I would also like to acknowledge to University of Beira Interior, in particular the Health Sciences Research Centre, where all the work was developed.

I am also grateful to all my colleagues in the Biotechnology and Biomolecular Sciences group for all the help, advice and support.

Thanks to my friends, for all the laughter and pranks, that always made a difficult day easier, for all the coffees and the patience.

Finally, I am deeply thankful to my parents, for everything they taught me, for all the sacrifices they have made, for all the support, the advices, for believing in me and for their love.

Resumo

Cerca de 15% dos cancros em humanos são causados por vírus. Por exemplo, o Vírus do Papiloma Humano encontra-se associado a mais de 99% dos casos de cancro do colo do útero. As vacinas preventivas contra o Vírus do Papiloma Humano existentes no mercado apenas induzem imunidade mediada por anticorpos e são completamente ineficazes na presença de infeção. Deste modo, os problemas associados a infecções pelo Vírus do Papiloma Humano e progressões tumorais continuam a aumentar. A necessidade de atenuar as lesões associadas ao Vírus do Papiloma Humano levou ao desenvolvimento de vacinas de DNA.

As vacinas de DNA surgiram como uma estratégia versátil para induzir respostas imunes, quer celulares, quer humorais. Para além disso, o DNA plasmídico (pDNA) surge como um transportador promissor para entrega de genes, uma vez que é produzido de forma simples, com elevado grau de pureza e baixo custo, e apresenta capacidade de transfectar células eucarióticas com níveis de expressão satisfatórios.

Assim sendo, nos últimos anos, os níveis de plasmídeo necessário para aplicações farmacêuticas levaram ao desenvolvimento de novos suportes cromatográficos, com elevada capacidade de ligação e seletividade pela isoforma superenrolada do plasmídeo. As matrizes monolíticas são consideradas ideais para purificar biomoléculas como o pDNA. Estes suportes apresentam estruturas tridimensionais de poros interconectados que permitem a transferência de massa por convecção e fornecem elevadas capacidades de ligação, o que torna estas matrizes inovadoras. Por outro lado, a cromatografia de afinidade com aminoácidos revelou-se uma abordagem promissora devido ao bioreconhecimento seletivo da isoforma superenrolada do pDNA, uma vez que esta estratégia se baseia na ocorrência natural de várias interações entre proteínas e ácidos nucleicos, em organismos biológicos, que maioritariamente envolvem aminoácidos básicos como a L-histidina.

As interações entre aminoácidos imobilizados e as diferentes isoformas de plasmideos podem ser estudadas por ressonância de plasma de superfície (RPS). O conhecimento prévio da afinidade aminoácido/pDNA pode posteriormente ser explorado na purificação através da cromatografia de afinidade.

Desta forma, um dos objetivos deste trabalho é utilizar a técnica de RPS para selecionar o aminoácido L-histidina ou um dos seus derivados, benzil-L-histidina e metil-L-histidina, que tem maior afinidade com o pDNA, para posteriormente imobilizar o ligando mais promissor numa matriz monolítica.

Inicialmente foram realizadas várias experiências de RPS utilizando três plasmídeos de tamanhos diferentes (6,05, 8,70 e 14 quilo pares de bases) e com as isoformas previamente separadas (circular aberta, superenrolada e linear). Os resultados revelaram que, no geral, a afinidade dos plasmídeos para o ligando de L-histidina e seus derivados, era elevada (K_D >10^{-8} M) e a afinidade mais elevada ocorreu com a isoforma linear do HPV-16 E6/E7/L-histidina,

$3,34 \times 10^{-10} \pm 0,0209$ M. Desta forma, a L-histidina foi o aminoácido selecionado para ser imobilizado na matriz monolítica.

Após preparação do suporte monolítico de L-histidina, foram realizados vários estudos cromatográficos com amostras mencionadas anteriormente. No geral, a isoforma superenrolada promoveu interações fortes com o monolito de L-histidina e a separação das isoformas foi conseguida. A separação das isoformas dos plasmídeos não se alterou com variação da taxa de fluxo. Estudos de capacidade de ligação dinâmica do monolito L-histidina revelaram que a sua capacidade de ligação máxima foi 11,03 mg/mL, com uma taxa de fluxo de 0,5 mL/min e uma solução de plasmídeo de 0,05 mg/mL. Estes resultados foram comparados com os valores de capacidade do suporte convencional de L-histidina-agarose, de um monolito não modificado e um monolito modificado com outro aminoácido, a aginina. A maior diferença nos resultados foi verificada com a matriz convencional de L-histidina-agarose, em que a capacidade do monolito de L-histidina foi cerca de vinte e nove vezes maior do que a capacidade da matriz convencional, usando as mesmas condições de saturação. Em relação ao monolito não modificado e à matriz monolítica modificada com o aminoácido arginina, os valores de capacidade do monolito de L-histidina revelaram ser ligeiramente superiores, em ambos os casos.

De um modo geral, a cromatografia de afinidade pode beneficiar das análises de afinidade exploradas por RPS. A combinação do ligando de L-histidina com o suporte monolítico permitiu a separação da isoforma superenrolada do plasmídeo HPV-16 E6/E7.

Palavras-chave

Capacidade dinâmica de ligação, DNA plasmídico superenrolado, Ligandos de afinidade, Monolito de L-histidina, Ressonância de plasma de superficíe, Vírus do Papiloma Humano.

Abstract

About 15% of human cancers are caused by viruses. For instance, the particular case of the high-risk human papillomavirus (HPV) is associated with more than 99% of cervical carcinomas. The preventive vaccines for HPV infection available in the market only induce the antibody immunity and are completely ineffective when the infection is already present. Therefore, the problematic associated to HPV infections and tumor progressions continue to be unsolved. Thus, the urge to attenuate the HPV associated lesions led to the development of DNA vaccines.

DNA vaccines emerged as a versatile strategy to induce both humoural and cellular immune immune responses. In addition, plasmid DNA (pDNA) arose as a promising vehicle for gene delivery, due to its simple manufacturing process with high purity degree and low cost, as well as its ability to transfect eukaryotic cells with satisfactory expression levels.

Therefore, in the last years, the growing demand of pharmaceutical-grade pDNA fostered the development of new chromatographic supports, allowing high capacity and selectivity by the supercoiled (sc) pDNA. The innovative monolithic matrices are considered advantageous supports to purify large biomolecules, such as pDNA, due to their tridimensional characteristics of interconnected pores, which allows good mass transfer properties and binding capacity. Amino acid-affinity chromatography has revealed to be a promise approach that selectively recognizes the sc pDNA, since this strategy is based on natural occurrence of multiple interactions between proteins and nucleic acids in biological organisms, which mainly involve basic amino acids such as L-histidine.

Surface Plasmon Resonance (SPR) Biosensor can be used to exploit the interactions between immobilized amino acids and different plasmid topologies to provide further structural information for affinity chromatography purification.

Thus, the aim of this work was to perform a screening of L-histidine amino acid and their derivatives, Im-benzyl-L-histidine and L-methyl-L-histidine, employing the SPR technique in order to modify a monolithic support with the selected ligand, to purify pDNA. Several experiments were performed with three plasmids of different sizes (6.05, 8.70 and 14 kilo base pairs) and different isoforms (open circular, sc and linear), separately. The results revealed that the overall affinity of plasmids to L-histidine ligand and their derivatives was high (K_D >10^{-8} M) and the highest affinity was found for HPV-16 E6/E7/L-histidine interaction, 3.34 x 10^{-10} ± 0.0209 M. Therefore, L-histidine was selected for immobilization on a monolithic matrix.

After preparation of the histidine monolithic support, chromatographic studies were also accomplished with the aforementioned samples. In general, the sc isoform developed strong interactions with the support and the separation of plasmid isoforms was achieved by decreasing ammonium sulfate concentration. The separation of plasmid isoforms remained

unchanged by flow rate variations. The breakthrough experiments of L-histidine monolith revealed satisfactory dynamic binding capacity when compared to other matrices.
Overall, affinity chromatography can benefit from affinity analysis experiments provided by SPR biosensor, and the combination of L-histidine ligand with the monolithic support can be a promising strategy to purify the sc pDNA with the desirable purity degree for pharmaceutical applications, such as the DNA vaccines directed against the HPVs.

Keywords

Affinity ligands, Dynamic binding capacity, Human papillomavirus, L-Histidine monolith, Supercoiled plasmid DNA, Surface Plasmon Resonance.

Table of Contents

Chapter I- Introduction 1

1.Gene therapy and DNA vaccines 3

1.1.Delivery systems 4

1.1.1.Viral and non-viral delivery systems: advantages and limitations 6

1.1.1.1.Viral delivery systems 6

1.1.1.2.Non-viral delivery systems 7

2.Therapeutic applications 9

2.1.Human papillomavirus 10

3.Plasmid DNA technology 12

3.1.Plasmid DNA biosynthesis 12

3.2.Downstream processing 12

3.2.1.Primary isolation 13

3.3.Plasmid DNA purification 13

3.3.1.Chromatographic techniques 14

3.3.1.1.Size exclusion chromatography 14

3.3.1.2.Ion exchange chromatography 14

3.3.1.3.Hydrophobic interaction chromatography 15

3.3.1.4.Affinity chromatography 15

3.3.2.Ligands selection 17

3.3.2.1.L-Histidine and derivatives 17

3.3.2.2.Surface Plasmon Resonance 18

3.3.3.Stationary phase 19

3.3.3.1.Monoliths 19

4.Aims 20

Chapter II – Materials and methods 23

2.1.Materials 25

2.1.1.Reagents 25

2.1.2.Plasmids 25

2.1.3.Instrumentation 25

2.1.4.Specifications 26

2.2.Methods 26

2.2.1.Plasmid amplification by bacterial production 26

2.2.2.Alkaline lysis and pre-purification of pDNA samples with NZYTech Kit 27

2.2.3.Plasmid isoforms preparation 27

2.2.3.1.Supercoiled isoform 27

2.2.3.2.Linear isoform 27

2.2.3.3.Open circular isoform 27
2.2.4.Agarose gel electrophoresis 28
2.2.5.SPR studies 28
2.2.5.1.Amino acids immobilization 28
2.2.5.2. Affinity analysis 29
2.2.6.^{1}H NMR experiments 29
2.2.7.Cromatographic studies 29
2.2.7.1. Amino acid immobilization 29
2.2.7.2.Linear gradients 29
2.2.7.3.Stepwise gradients 30
2.2.7.4.Dynamic binding capacity 30
2.2.7.5.Monolith regeneration 31
Chapter III – Results and discussion 33
3.Ligands screening 35
3.1. Amino acid immobilization 35
3.2.SPR binding experiments 35
3.2.1.Running buffer selection for affinity experiments 35
3.2.2.Affinity data analysis 37
4.Cromatographic experiments 40
4.1.L-Histidine immobilization 40
4.2.Evaluation of elution conditions on pDNA retention 41
4.2.1.Elution buffer composition 41
4.2.2.Ionic strength influence 42
4.2.3.pH influence 42
4.3.Chromatographic profile of different plasmid isoforms 43
4.3.1.pVAX1-*LacZ* (6.05 kbp) 44
4.3.1.1.pVAX1-*LacZ* linear isoform 44
4.3.1.2.pVAX1-*LacZ* open circular isoform 44
4.3.1.3.pVAX1-*LacZ* supercoiled isoform 45
4.3.2.HPV-16 E6/E7 (8.70 kbp) 46
4.3.2.1. HPV-16 E6/E7 linear isoform 46
4.3.2.2. HPV-16 E6/E7 open circular isoform 47
4.3.2.3. HPV-16 E6/E7 supercoiled isoform 48
4.3.3.pcDNA3-based plasmid (14 kbp) 48
4.3.3.1.pcDNA3-based plasmid linear isoform 48
4.3.3.2.pcDNA3-based plasmid open circular isoform 49
4.3.3.3.pcDNA3-based plasmid supercoiled isoform 50
4.4.Plasmid isoforms separation 51
4.4.1.pVAX1-*LacZ* 51
4.4.2.HPV-16 E6/E7 52

4.4.3.pcDNA3-based plasmid 52
4.5.Effect of flow rates on plasmid isoforms separation 54
4.6.Dynamic binding capacity 56
Chapter IV – Conclusions and future perspectives 61
Chapter V – Bibliography 67
Chapter VI – Appendix: submitted manuscript 77

List of Figures

Chapter I- Introduction

Figure 1. Gene therapy and DNA vaccines. 3
Figure 2. Barriers to delivery systems. 5
Figure 3. Distribution of delivery systems used in clinical trials. 6
Figure 4. Indications addressed by gene therapy clinical trials. 9
Figure 5. HPV genome: structure and organization. 10
Figure 6. Graphical representation of the main goals in the present work. 20

Chapter III- Results and discussion

Figure 7. Examples of sensorgrams in which no signal was detected. 36
Figure 8. Examples of sensorgrams and equilibrium binding analyses. 38
Figure 9. Decreasing linear gradients performed with non-immobilized epoxy disk and L-histidine modified monolith. 40
Figure 10. Decreasing linear gradient performed with HEPES buffer. 41
Figure 11. Increasing linear gradient performed with NaCl. 42
Figure 12. Decreasing linear gradient performed with elution buffer at pH 6.0. 43
Figure 13. Decreasing linear gradient performed with pVAX1-*LacZ* linear isoform sample. 44
Figure 14. Decreasing linear gradient performed with pVAX1-*LacZ* open circular isoform sample. 45
Figure 15. Decreasing linear gradient performed with pVAX1-*LacZ* supercoiled isoform sample. 46
Figure 16. Decreasing linear gradient performed with HPV-16 E6/E7 linear isoform sample. 47
Figure 17. Decreasing linear gradient performed with HPV-16 E6/E7 open circular isoform sample. 47
Figure 18. Decreasing linear gradient performed with HPV-16 E6/E7 supercoiled isoform sample. 48
Figure 19. Decreasing linear gradient performed with pcDNA3-based plasmid linear isoform sample. 49
Figure 20. Decreasing linear gradient performed with pcDNA3-based plasmid open circular isoform sample. 49
Figure 21. Decreasing linear gradient performed with pcDNA3-based plasmid supercoiled isoform sample. 50
Figure 22. Stepwise gradient used in pVAX1-*LacZ* plasmid isoforms separation (2.99 M and 0M ammonium sulfate). 51

Figure 23. Stepwise gradient used in HPV-16 E6/E7 plasmid isoforms separation (2.94 M and 0M ammonium sulfate). 52
Figure 24. Stepwise gradient used in pcDNA3-based plasmid isoforms separation (2.91 M and 0M ammonium sulfate). 53
Figure 25. Flow rate effect on pVAX1-*LacZ* isoforms separation. 55

List of Tables

Chapter I- Introduction

Table 1. Main limitations and advantages of the most widely used viral delivery systems. 7

Table 2. Regulatory agencies specifications. 12

Table 3. Affinity chromatography methodologies for nucleic acids purification. 16

Chapter III- Results and discussion

Table 4. Equilibrium data analysis of plasmids in 10 mM of HEPES pH 7.4. 39

Table 5. Dynamic binding capacity results of L-histidine monolith at 0.5 and 1 mL/min. 56

List of Acronyms

BCA	Bicinchoninic acid
ºC	Celsius degree
CDI	CarbonylDiImidazole
DBC	Dynamic binding capacity
D_2H	Deuterated water
cm	Centimeter
DNA	Desoxirribonucleic acid
E. coli	*Escherichia coli*
EDC	1-ethyl-3-(3- dimethylaminopropyl) carbodiimide
EDTA	Ethylene-diamine tetraacetic acid
EU	Endotoxin Units
g	gram
gDNA	Genomic DNA
HBS-EP	HEPES, NaCl, P20 surfactant, EDTA
HIV	Human Immunodeficiency Virus
^{1}H NMR	Proton Nuclear Magnetic Resonance
HPV	Human Pappilomavirus
kbp	kilo base pairs
KH_2PO_4	Monopotassium phosphate
K_2HPO_4	Dipotassium phosphate
K_D	Dissociation constant
L	liter
LAL	Limulus amebocyte lysate
LB	Luria-Broth
ln	Linear
M	Molar
mM	milimolar
MHz	Megahertz
min	minutes
mL	milliliter
mRNA	Messenger RNA
NaCl	Sodium chloride
NaOH	Sodium hydroxide
NHS	N-hydroxysuccinimide
$(NH_4)_2SO_4$	Ammonium sulfate
oc	Open circular
OD_{600}	Optical density at 600 nm
PCR	Polymerase chain reaction
pDNA	Plasmid DNA
RNA	Ribonucleic acid
RU	Ressonance Units
s	Seconds
sc	Supercoiled
SD	Standard Deviation

SDS	Sodium dodecylsulfate
siRNA	Small interfering RNA
SPR	Surface Plasmon Resonace
TAE	Tris, acetic acid, EDTA
Tris	Tris(hydroxymethyl) aminomethane
URR	Upstream regulatory region
UV	Ultraviolet
V	volt
µL	microliter

Chapter I – Introduction

1. Gene therapy and DNA vaccines

Gene therapy may be defined as the cure, treatment or prevention of human diseases using nucleic acids. This can be achieved by gene addition, gene correction and gene knockdown, depending on the type of disease, being the gene addition the most attempted strategy, since the other aforementioned strategies are technically more difficult (Kauffman *et al.*, 2013).

Gene therapy can be categorized into germ line and somatic gene therapy. In the somatic gene therapy approach, the changes resulting from insertion of genetic material in some target cells will not pass along to the next generation, whereas in germ line gene therapy approach, the therapeutic or modified gene will be passed onto the next generation, but regulatory agencies do not allow such approach due to technical and ethical reasons (Haritha *et al*, 2012).

Somatic gene therapy can be performed using two different strategies to vector administration, *in vivo* and *ex vivo* (Kauffman *et al.*, 2013; Haritha *et al*, 2012). The *in vitro* strategy involves the direct vector delivery into the target cells of the patient, as shown in figure 1. The therapy achievement relies on efficient uptake of the therapeutic gene by the target cells, and its prior uptake by nucleus, intracellular degradation and its expression capability. The *ex vivo* strategy involves the target cells isolation from the patient, genetic modification outside the body and autologous transplant of the modified cells into the patient (figure1), being less likely to trigger immune responses (Naldini, 2011).

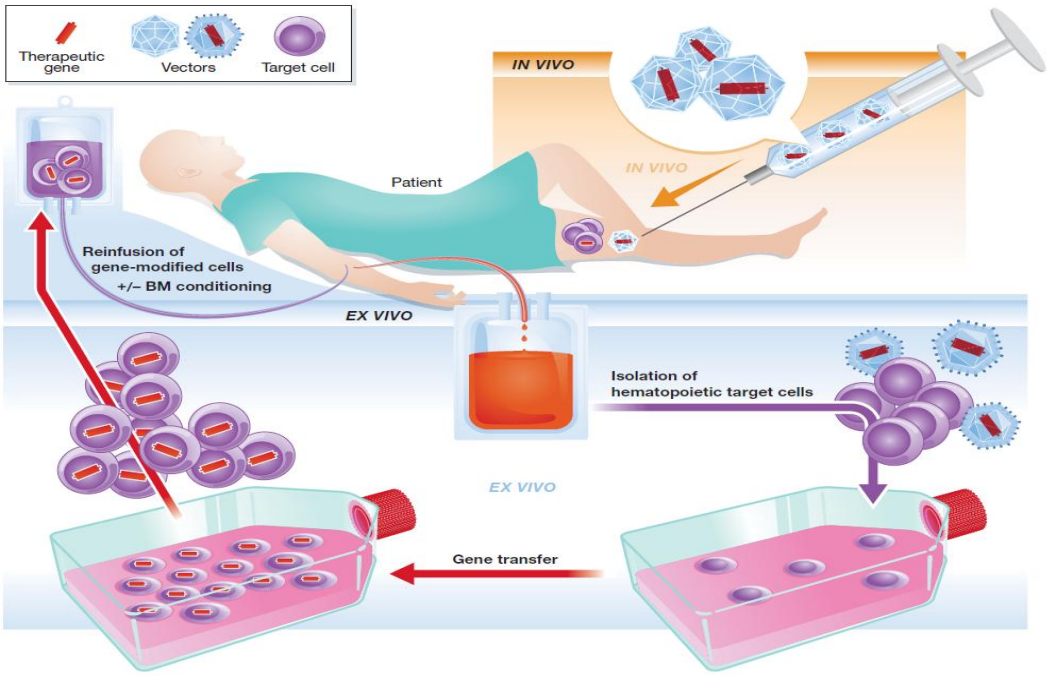

Figure 1. Gene transfer strategies. (A) *in vivo* strategy: Direct vector delivery to patient cells. (B) *ex vivo* strategy: Isolation, genetic modification and transplantation of modified cells into the patient (Kauffman *et al.*, 2013).

On the other hand, DNA vaccines are based on the conventional vaccines principle, since they are used to produce immunological responses against infectious agents. Nevertheless, conventional protein based vaccines only induce an humoral response from the immune system and vaccines derived from live attenuated organisms induce cellular immune response, while DNA vaccines are able to stimulate both antibodies and cell-mediated components (Liu, 2011).

DNA vaccines take advantage of genetic information that is delivered by a system able to induce an immune response against a given antigen. Upon inoculation, the individual shall produce a strong and enduring immune response against the encoded protein antigen, associated to the pathology (Liu, 2010). Therefore, DNA vaccines may be advantageous in terms of safety when compared with conventional vaccines, such as conventional live virus vaccines, since can reverse to a pathogenic form. Besides, DNA vaccines can be manufactured in a relatively cost-effective manner and easily stored. Other advantages are the versatility and rapid design of DNA vaccines, since multiple antigenic genes can be given in one formulation (Liu, 2010; Saade *et al.*, 2012).

1.1. Delivery systems

Several delivery systems have been developed over the years to transport the therapeutic gene to the target cells. Therapeutic genes can be categorized into gene inhibitors or gene inductors.
The gene inhibitors category include: oligonucleotides, ribozymes, DNAzymes, aptamers and small interfering RNAs (siRNAs). Oligonucleotides are short single-stranded segments of DNA able to selectively inhibit the expression of a single protein; ribozymes interact at the mRNA level, the RNA molecules are capable of sequence specific cleaving of mRNA; DNAzymes present strong catalytic activity and have high potential as gene suppression agents; aptamers are small single-stranded or double-stranded nucleic acid segments that can directly interact with proteins; siRNAs are short double-stranded RNA segments which nucleotide bases are complementary to the mRNA sequence of the protein whose transcription is blocked. Gene inductors, such as plasmids containing transgenes, are high molecular weight, double-stranded DNA constructs, with transgenes that encode specific proteins (Patil *et al.*, 2005).

Although some limitations and problems have been solved or minimized, some barriers to deliver the naked therapeutic nucleic acids still remain unsolved (Kay, 2011). Those barriers are the vector uptake, transport and uncoating, vector genome persistence, sustained transcriptional expression and the host immune response, as it is represented in figure 2.

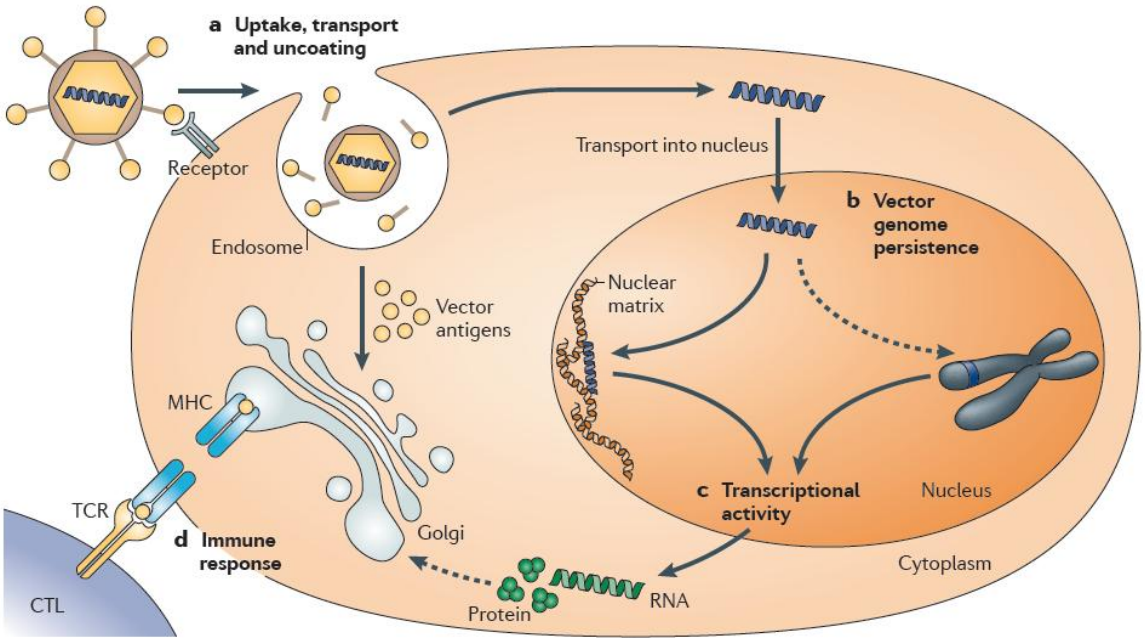

Figure 2. Barriers to delivery systems: a) vector uptake, transport and uncoating, vectors are internalized by various processes and they must reach escape the endosome to reach the nucleus without being degraded. b) Vector genome persistence, the DNA can exist as an episomal molecule or be integrated into the host chromosome. c) Sustained transcriptional expression that should match the time required to treat the target disease. d) The host immune response can limit the gene therapy success (Kay, 2011).

After vector administration, several parameters influence successful transgene expression of therapeutic levels, namely the vascular supply, endothelial barriers, vector size and interactions between host cell receptors and the vector ligand. The cell membrane, endosomal escape and the nuclear membrane are the three barriers that non-viral delivery systems have to overcome until to reach the nucleus, while virus have efficient mechanisms to enter the cell and localize the nucleus (Thomas *et al.*, 2003; Kay, 2011).

The vector genome persistence depends whether it integrates into host cellular chromatin or predominantly persists in the cell nucleus as extrachromosomal episomes. Non-integrating vectors can mediate persistent transgene expression in non-proliferating cells, but integrating vectors are more widely used when the genetic alteration should remain stable in dividing cells (Thomas *et al.*, 2003), although they present the risk of insertional mutagenesis (Biasco *et al.*, 2012).

Sustained transcriptional expression refers to the fact that the transgene expression may be desired during lifetime or limited periods, depending on the specific target disease (Thomas *et al.*, 2003; Kay, 2011).

The transgene product or the vector may be recognized by the host immune system as foreigner and therefore, an immune response can be triggered, limiting the transgene product expression (Thomas *et al.*, 2003; Kay, 2011).

These aforementioned limitations illustrate the importance of correct selection of a suitable delivery system to carry the therapeutic nucleic acid for a specific purpose. Nevertheless, the delivery systems can be categorized under viral delivery systems and non-viral delivery systems and each category present advantages and limitations.

1.1.1. Viral and non-viral delivery systems: advantages and limitations

The most widely used vectors are the viral delivery systems, adenovirus and retrovirus, followed by the non-viral delivery system, plasmid DNA (figure 3) that has received significant attention over the last years, becoming increasingly common (Ginn *et al.*, 2013).

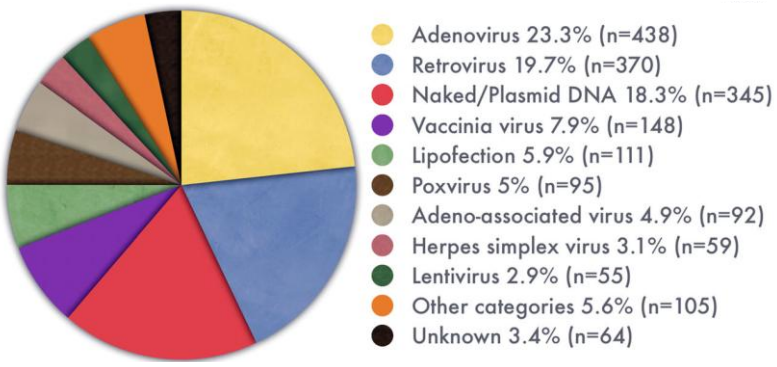

Figure 3. Distribution of delivery systems used in clinical trials (Ginn *et al.*, 2013).

The plasmid DNA (pDNA) emerges as a promising vehicle for gene delivery because it is a double-stranded biomolecule with high molecular weight, easily constructed with any trangenes of interest, obtained in large scale under satisfactory purity degree by a simple manufacturing process with low cost, and able to transfect eukaryotic cells with satisfactory expression levels. A more detailed description of pDNA technology is presented in section 3. The obstacle of naked pDNA clinical application is the efficiency to cross the extra- and intracellular barriers, but this problem is being addressed with delivery techniques, addition of adjuvants, and various prime-boost strategies (Saade and Petrovsky, 2012; Coban *et al.*, 2008).

1.1.1.1. Viral delivery systems

The virus mediated gene transfer is highly efficient because gain easily access to host cells and make use of their machinery to facilitate the replication. Viral delivery systems such as retrovirus, lentivirus, adenovirus, adeno-associated virus, and herpes simplex virus have been widely used in clinical trials (Walter and Stein, 2000) and their main advantages and limitations are summarized in table 1.

Table 1. Main limitations and advantages of the most widely used viral delivery systems (adapted from Thomas *et al.*, 2003).

Viral vector	Main limitations	Main advantages
Retrovirus	Only transduces dividing cells; integration might induce oncogenesis in some applications; Small packaging capacity	Persistent gene transfer in dividing cells
Lentivirus	Integration might induce oncogenesis in some applications; Small packaging capacity	Persistent gene transfer in most tissues
Herpes simplex virus	Transient transgene expression in cells other than neurons; high inflammatory potential	Large packaging capacity
Adeno-associated virus	Small packaging capacity; Require a helper virus for replication and completion of their life cycle	Non-inflammatory ; non-pathogenic
Adenovirus	Capsid mediates a potent inflammatory response; Small packaging capacity	Extremely efficient transduction of most tissues

Other limitations associated with viral delivery systems include hampered production, repeated administrations due to host inflammatory responses and potential insertional mutagenesis of some viral delivery systems (Haritha *et al.*, 2012).

1.1.1.2. Non-viral delivery systems

The use of non-viral delivery systems became popular to overcome the bottlenecks associated with the use of viral delivery. Non-viral delivery consists on synthetic or natural compounds or physical forces to deliver the therapeutic nucleic acid into the cell. They are considered less toxic and immunogenic, since they do not contain viral contaminants. The non-viral gene delivery offers other advantages, once there is no size limit on the amount of genes that they can deliver. They are also easily produced and allow repeated administration, without triggering inflammatory responses (Al-Dosari and Gao, 2009).

The major drawbacks associated with non-viral delivery systems, such as the low efficacy of cell invasion when compared with viral vectors and the short-lived gene expression, are being addressed with constant developments in the field (Kamimura *et al.*, 2011).

The non-viral gene delivery methods can be divided into physical and chemical-based non-viral delivery methods.

The use of physical forces to improve the gene transfer can be performed by jet injection, hydrodynamic gene transfer, gene gun, electroporation and sonoporation. Jet injection is accomplished through a high-speed stream of therapeutic nucleic acid solution driven by a pressurized gas to penetrate the skin and the underlying tissues. This injection methodology does not induce tissue damage or significant inflammatory reactions at jet-injection sites (Ren *et al.*, 2002). The hydrodynamic gene transfer is based on the injection of a large therapeutic nucleic acid volume in short period of time, which leads to a reversible permeability change in the endothelial lining and the generation of transient pores. This invasive procedure has been modified in order to achieve its clinical applicability (Fabre *et al.*, 2008). The gene gun delivery method depends on the impact of heavy metal particles coated with the therapeutic nucleic acid on target tissues (Uchida *et al.*, 2002). These particles are accelerated by highly pressurized inert gas and can easily cross the cell and nuclear membranes, releasing the nucleic acid adsorbed on their surface into the nucleus. Electroporation uses an electric field to alter the cell permeability. The therapeutic nucleic acid is injected to the target tissues and then electric pulses are applied (Marti *et al.*, 2004). On the other hand, sonoporation uses ultrasound waves to create plasma membrane defects by acoustic cavitation (Nomikou *et al.*, 2013).

Examples of chemical-based delivery systems are cationic lipids and cationic polymers. These vectors form condensed complexes with therapeutic nucleic acids, negatively charged, through electrostatic interactions. The complexes facilitate cell uptake and intracellular delivery and protect the therapeutic nucleic acid (Morille *et al.*, 2008).

Overall, an ideal carrier has low toxicity and immunogenicity and higher efficiency. However it has not yet been achieved; despite several efforts continue to be made to develop hybrid carriers. The large array of novel carriers is in continuous investigation to improve safety and enhanced therapeutic efficacy. In these carriers, new abilities are added or certain undesirable elements are replaced (Thomas *et al.*, 2003; Huang and Kamihira, 2013).

2. Therapeutic applications

From the beginning, gene therapy substantial progresses have been made in this field. Important milestones were achieved, as for example, China became the first country to approve a gene therapy based product for clinical use, Gendicine, an adenoviral vector for the treatment of head- and neck squamous cell carcinoma (Zhaohui, 2005). In Europe, gene therapy has also taken the next step with approval of Glybera, an adeno-associated viral vector for the treatment of familial lipoprotein lipase deficiency (Wirth and Yla-Herttuala, 2013). These achievements open perspectives of more gene-based therapies in near future.
Cancer, cardiovascular disease and inherited monogenic diseases lead the ranking of diseases addressed in clinical trials by gene therapy (Ginn *et al.*, 2013), as can be seen in figure 4.

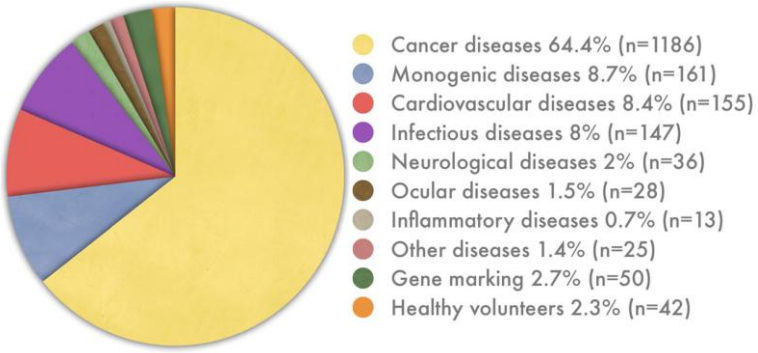

Figure 4. Indications addressed by gene therapy clinical trials (Ginn *et al.*, 2013).

However, due to the enormous therapeutic potential of gene therapy, several other conditions can be addressed.

A broad range of viral and non viral diseases are being addressed in DNA vaccine clinical trials. The majority of clinical trials are focused in human immunodeficiency virus (HIV) and cancers. Influenza, hepatitis B, hepatitis C, malaria and human papillomavirus (HPV) are also being exploited in clinical trials (Ferraro *et al.*, 2011).

The preventive HPV vaccines in the market, Gardasil and Cervarix do not induce appreciable levels of cellular immune responses, and thus, the burden of HPV infections or HPV-associated lesions proceeds to increase (Ferraro *et al.*, 2011). Therefore, strong cellular responses are required and DNA vaccines appear promising candidates to induce the desired immune response.

2.1. Human papillomavirus

About 15% of all human cancers are caused by viruses. Human papillomaviruses are responsible for at least 5% of tumors worldwide, although not sufficient cause of cervical cancer, the HPV infection represents the major etiologic factor in the neoplasia development (Tota *et al.*, 2011). Other cancer subsets like oropharyngeal, penile, vaginal, vulvar and anal cancer are also attributed to HPV (Trottier and Burchell, 2009), which is currently one of the most common sexually transmitted infections worldwide (Dunne *et al.*, 2007).

Human papillomavirus are small, circular and double-stranded DNA virus, members of the Papillomaviridae family. All HPV show a pronounced tropism for epithelial cells, and infections by these viruses are associated with hyperproliferative lesions of mucosa and skin (Howley and Lowry, 2007). These mucosal HPVs can be classified as low- or high-risk, according to the outcome of associated lesions. Low-risk HPVs, such as HPV6 or HPV11, cause genital warts, benign lesions, whereas high-risk HPVs, like HPV16 or HPV18, cause intraephitelial lesions with the propensity for malignant progression (Schlecht *et al.*, 2001). High-risk HPVs are associated with greater than 99% of cervical carcinomas (Schiffman *et al.*, 2007).

All HPV viruses share a common genome organization of about 7.9 kbp. The circular DNA can be divided into three functional regions: a non-coding regulatory region, known as the upstream regulatory region (URR), which modulates viral DNA replication and gene transcription; a region composed by HPV early genes (E1,E2, E3, E4, E5, E6,E7), which code for proteins related with viral genome transcription, replication, persistence and regulation of cell proliferation. And finally, a region that codes for HPV late genes (L1 and L2) and structural genes, which is responsible for the major and minor capsid proteins codification (as shown in figure 5) (Doorslaer and Burk, 2010).

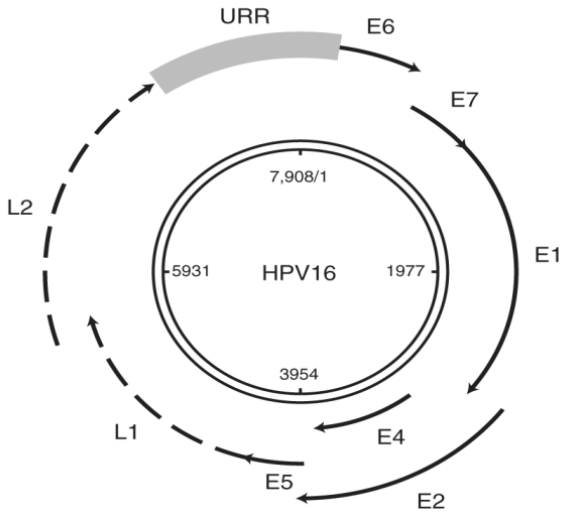

Figure 5. HPV genome: structure and organization. The gray box represents the upstream regulatory region; the dashed arrows represent early genes and solid arrows the late genes (Doorslaer and Burk, 2010).

HPV life cycle is associated with epithelial differentiation. The basal epithelial cells are initially infected by HPVs, where the viral episome is maintained extrachromosomally at low copy number (viral genome is maintained at about 100 copies per cell). A productive infection with genome amplification, capsid protein expression and virion mounting occurs in cells from the suprabasal layers. On one hand, cells above the basal layer are terminally differentiated, on the other HPV does not code for its own set of replication proteins. Thus, the HPV has to induce host cells re-entry in S-phase to take advantage of host replication machinery (Doorslaer and Burk, 2010).

The products of E6 and E7 early genes are essential in the process of HPV induced cellular immortalization and transformation (DeFilippis *et al.*, 2003). The E7 expression, the major HPV oncoprotein, is sufficient to immortalize primary human epithelial cells at low frequency. E7 interacts with cellular regulatory protein complexes and alters or neutralizes their normal functions, leading to impaired cell cycle arrest responses and deregulation of cellular differentiation and apoptosis mechanisms. E7 interacts with retinoblastoma protein and mediates its degradation, affecting its growth-suppressive function. As consequence, transcriptional genes necessary for S-phase entry and progression are activated. The E6 oncoprotein targets the tumor suppressor p53, leading to its proteosomal degradation (Howie et al, 2009; McLaughlin-Drubin and Münger, 2009).

3. Plasmid DNA technology

3.1. Plasmid DNA biosynthesis

The demand for clinical grade pDNA application has led to technology development in the pDNA manufacturing. Efforts to achieve high upstream plasmid yields have been made in vector design (Huang and Kamihira, 2013), host strain (Carnes *et al.*, 2006) and fermentation processes (Williams *et al.,* 2009a).

The origin of replication and selection marker are the most important prokaryotic vector elements that are functionally necessary for host production and directly influence the outcome of manufacturing process. The origin of replication is essential to propagate the plasmid as an extrachromosomal DNA element in the host cells, and the selection marker is essential to select bacterial clones carrying the plasmid, through the plasmids antibiotic-resistance gene (Williams *et al.*, 2009b; Tolmachov, 2009).

Plasmids, encoding the gene of interest, are generally biosynthesized by autonomous replication in *Escherichia coli* (*E. coli*) hosts, a bacterium widely used in recombinant proteins safe production. The fermentation process key parameters are cell density, plasmid copy number, homogeneity and yield that are strongly influenced by medium-composition and harvesting point (Carnes et al., 2011). Plasmid yield is maximized by the increase of cell density measured by optical density units (dry or wet cell mass per unit culture volume). The optimum harvesting time point is critical in order to obtain high sc isoform homogeneity at the end of the fermentation process, since other plasmid topologies can arise by the action of nucleases and they are difficult to separate from the sc isoform (Williams, 2013).

3.2. Downstream processing

The downstream process is intended to remove host impurities, such as RNA, gDNA and endotoxins to acceptable levels (table 2 summarizes impurity levels acceptable by regulatory agencies).

Table 2. Regulatory agencies specifications (Stadler *et al.*, 2004; Ferreira *et al.*, 2000).

Impurity	FDA specifications
Appearance	Clear, colorless solution
Plasmid homogeneity	<97% supercoiled
Proteins	Not detectable (by micro-BCA method)
RNA	Not detectable (by 0.8% agarose gel)
gDNA	<2 μg/mg plasmid (by PCR)
Endotoxins	<0.1 EU/ng plasmid (by LAL assay)

The main challenge of this step remains in common characteristics shared by pDNA and host impurities, namely the negative charge (RNA, gDNA and endotoxins), molecular mass (gDNA and endotoxins) and hydrophobicity (endotoxins) (Stadler et al., 2004; Ferreira, 2005).

The presence of impurities may detrimentally affect the vaccine performance. For instance, impurities like endotoxins may reduce the transfection efficiency, produce cytotoxic effects on mammalian cells and, if present in large amounts *in vivo*, can produce symptoms of toxic shock syndrome (Davis *et al.*, 1996).

3.2.1. Primary isolation

Following fermentation, the host cells are disintegrated and the plasmids are released for the extracellular medium. Several processes have been developed to disrupt the bacterial cells and release their content but the method of choice and more widely used is alkaline lysis, firstly described by Birnboim and Doly (Birnboim and Doly, 1979), or its variations (Holmes and Quigley, 1981).

In alkaline lysis, the cell disruption is achieved at high pH (pH 12) with sodium hydroxide (NaOH) and sodium dodecylsulfate (SDS) to disintegrate the cell walls. In this process the pH value and the residence time have to be accurately controlled to avoid plasmid degradation, since these alkaline conditions also promote sc pDNA unwind. If the lysis process is carried out above pH 12.5 or if in pH extremes, the anchor base pairs, that prevented the complete separation of complementary strains, may be lost, resulting in denatured pDNA. Potassium acetate is subsequent applied to neutralization, which precipitates SDS together with denatured gDNA and cellular debris. Thus, precipitated impurities can be removed by filtration or centrifugation and the majority of pDNA remains in the supernatant. During these steps, mixing procedures have to be done with care since shear forces can induce damages in the supercoiled plasmid isoform (Prather, 2003).

3.3. Plasmid DNA purification

The recovery and purification of pDNA from a clarified cell lysate may involve several techniques. The techniques most widely used in this process are precipitation and pDNA extraction by organic solvents, ultrafiltration and predominately different chromatographic processes (Prather, 2003; Prazeres and Ferreira, 2004). In general, the lysate sample can be first concentrated by an alcohol precipitation and then clarified by a chaotropic salt precipitation.

Chromatography techniques have been used, singly or combined, to achieve a final pDNA product that respects the regulatory agencies recommendations to be used as a biotherapeutic agent (Prazeres and Ferreira, 2004). Analytical chromatography is also a very useful tool to monitor the pDNA quality through the production process (Diogo *et al.*, 2003).

3.3.1. Chromatographic techniques

In separation and purification of pDNA by chromatography, the analytes are distributed between the stationary and mobile phase. This technique exploits different types of interactions that the analyte can develop with the stationary or mobile phases. The analyte with relative affinity for both phases determines the interaction magnitude. The analyte that strongly interact with stationary phase will be retained longer in the chromatographic system.

The successful chromatographic separation depends upon the selection of the most appropriate chromatographic process followed by the optimization of the binding and elution conditions associated with the separation (Urthaler *et al.*, 2005).

3.3.1.1. Size exclusion chromatography

The principle of the size exclusion chromatography involves separation of molecules based on their molecular size and shape. The analytes are passed through the column particles with a narrow range of pore sizes. Larger analytes will be excluded from the pores and will pass through the interstitial spaces between the particles, being the firsts to appear in the eluate. Smaller analytes will be distributed between the mobile phase, inside and outside the particles, and will therefore pass the column at slower rate, being eluted in last. Size exclusion chromatography can be used to separate pDNA on basis of size and can be used separately or sequentially with other chromatographic methods. Since this method shows some drawbacks, such as limited capacity and selectivity for pDNA (Prazeres and Ferreira, 2004; Horn *et al.*, 1995), it is not preferred as an initial purification step but as an ideal polishing step, enabling residual contaminants removal with simultaneous buffer exchange into an appropriate buffer for storage or formulation.

3.3.1.2. Ion exchange chromatography

Ion exchange chromatography is frequently chosen for the separation and purification of charged molecules (proteins, peptides, nucleic acids, polynucleotides), based on the attraction between oppositely charged ion exchanger, the stationary phase and analyte. There are two types of ion exchangers, cation and anion exchangers. The negatively charged groups will attract positively charged cations and the positively charged groups will attract negatively charged anions, respectively. Anion exchange chromatography can be applied for pDNA separation, the negatively charged phosphate groups on the pDNA backbone will interact with the positively charged groups on the stationary phase. By an increasing salt

gradient, the different nucleic acids should elute according of the increase charge density, depending on their chain length and conformation (Quaak *et al.*, 2009). The main challenge to achieve pDNA purification with a single anion exchange chromatography step is the lack of selectivity, owing to similar binding affinities between the pDNA and impurities (Lyddiat and O'Sullivan, 1998; Ongkudon and Dankuah, 2011).

3.3.1.3. Hydrophobic interaction chromatography

This technique takes advantage of the higher hydrophobicity of single stranded nucleic acids and endotoxins. The pDNA have the hydrophobic bases packed inside the double helix, and thus, the hydrophobic interaction of pDNA with the stationary phase is minimal, whereas single stranded nucleic acid impurities show a higher exposure of the hydrophobic groups (Ferreira, 2005; Urthaler *et al.*, 2005). The major drawback of hydrophobic interaction chromatography is associated with high salt concentration used in the binding and elution strategies (Iuliano *et al.*, 2002).

3.3.1.4. Affinity chromatography

Affinity chromatography is the most specific separation technique. As a classical definition, this technique is based on a selective association between the solute and a complementary molecule, the ligand. The association is reversible and therefore the solute can recovered in the active conformation.

The ligands, with affinity to target molecules on the solute, are covalently attached on a chromatographic matrix. The target molecules elution can be promoted by competitive agent addition or pH, ionic strength or polarity conditions change (Roque and Lowe, 2008).

The natural biological processes, such as molecular recognition, are exploited by several affinity chromatographic modalities employed in pDNA purification. Immobilized metal-ion, triple-helix, protein-DNA and amino acid-DNA affinity chromatography have been employed with a specific ligand to separate pDNA on the basis of its biological function or chemical structure (Ghanem *et al.*, 2013). Table 3 summarizes the principle, disadvantages and advantages of these four affinity chromatography methodologies.

Table 3. Affinity chromatography methodologies for nucleic acids purification (adapted from Sousa *et al.*, 2008a).

Affinity type	Principle	Specific binding	Advantages	Limitations
Immobilized metal-ion	Chelating ligands charged with divalent metal ions specifically interact with aromatic nitrogen atoms	Single-stranded nucleic acids	Efficient resolution of RNA from gDNA and pDNA; high endotoxin removal; separation of denatured pDNA	pDNA in the flowthrough; incomplete RNA capture in complex mixtures; co-elution of all DNA forms
Triple-helix	Specific sequences present on DNA are recognized by an immobilized oligonucleotide, forming a triple-helix	Double-stranded DNA	Discrimination of different plasmids based on their sequence; sc pDNa isolation in one chromatographic step: reduction of RNA, gDNA and endotoxin levels; possibility for scale-up	Loss of pDNA during wash step; low yields; slow kinetics of triple-helix formation; long chromatographic run times
Protein-DNA	A protein or protein complex immobilized on the matrix specifically recognizes a DNA motif	pDNA	Discrimination of different plasmids based on their sequence; pDNA isolation from clarified lysates; Elimination of proteins and RNA from preparation	Relatively low yields; contamination with gDNA
Amino acid-DNA	Multiple interactions occur between immobilized amino acids and nucleic acids	sc pDNA	Sc pDNA purification in a single chromatographic step; efficient elimination of RNA, gDNA, proteins and endotoxins	Elution with high salt concentration and relatively low yields

These methodologies have the power to eliminate additional steps while increasing yields and improving process economics.

The selection of the amino acids as affinity ligands was based on natural occurrence of many different interactions between proteins and nucleic acids in biological organisms, which mainly involve basic amino acids such as L-histidine or L-arginine (Sousa *et al.*, 2010).
Due to the common characteristics shared by pDNA and host impurities, several chromatographic steps had to be applied in order to obtain the purified sc pDNA isoform. Therefore, amino acid-DNA affinity chromatography has revealed to be a promissory approach, since allows a specific binding with sc pDNA isoform in a single chromatographic step, through specific amino acids bound to the agarose matrix, such as L-histidine (Sousa *et al.*, 2006), L-arginine (Soares *et al.*, 2008b) and L-lysine (Sousa *et al.*, 2009), eliminating the remaining pDNA isoforms and all the impurities present on sc pDNA-containing extract.

3.3.2. Ligands selection

Selectivity and specificity are the key characteristics of a suitable ligand for pDNA purification (Sousa *et al.*, 2010). Therefore, understanding the physicochemical

characteristics of pDNA becomes relevant in order to select suitable ligands for purification strategies.

Briefly, plasmids are DNA molecules double stranded and covalently closed, forming a closed loop. Each strand of a pDNA molecule consists of a linear polymer of deoxyribonucleotides linked by phosphodiester bonds. When pH<4, the phosphate groups are negatively charged. The two anti-parallel strands are connected to each other by hydrogen bounds between complementary nucleotides in each strand and the two strands wind around a common axis originating the right handed double helix structure. This structure has highly hydrophobic grooves, due to the close packing of the aromatic bases, with accessible aromatic electrons and available sites for hydrogen bounding, which can be reached by solvent and ligand molecules. These structural and physicochemical characteristics can be exploited in purification strategies, namely to select appropriate ligands to interact with pDNA (Ferreira, 2005).

Synthetic and natural compounds such as dyes (Clonis et al., 2000), metal chelates (Yuchi et al., 2000) and amino acids can be used as affinity ligands. In addition, several atomic studies have described preferential interactions occurring between particular positively charged amino acids and nucleic acid bases (Hoffman *et al.*, 2004). Although L-histidine, L-arginine and L-lysine belong to the positively charged amino acids group, the agarose matrices with these immobilized ligands applied on pDNA chromatography have showed different elution behavior.

3.3.2.1. L-histidine and derivatives

The use of L-histidine as an affinity ligand was first reported in a variety of peptides and proteins purification (Amourache and Vijayalakshmi, 1984) and more recently, as above mentioned, in pDNA purification using an agarose conventional matrix (Sousa *et al.*, 2006).

The versatility of L-histidine in molecular interactions arises from its unique structure, which distinguishes it among the twenty natural amino acids. The imidazole group in L-histidine side chain plays a major role in interactions. The molecular interactions of L-histidine can be classified into cation- π interactions (the imidazole motif is an aromatic ring that can interact with metallic cations or organic cations), π-π stacking interactions and hydrogen-π interactions (since the structure of L-histidine aromatic ring allow π-π stacking interactions and the polar hydrogen atom of L-histidine can form hydrogen-π bonds with other aromatic structures), coordinate bond interactions (due to the lone electron pair in the nitrogen atom of imidazole ring) and hydrogen bond interactions (since imidazole system is a hydrogen bond donor and acceptor) (Caramelo-Nunes *et al.*, 2014; Liao *et al.*, 2013).

These L-histidine features derived from the imidazole ring characteristics, which highlighted the potential of this amino acid as a suitable ligand for chromatographic purposes. The use of

L-histidine derivatives, such as Im-benzyl-L-histidine and L-methyl-L-histidine, composed by benzyl and methyl groups in position 1 of imidazole ring appear as promising ligands as well.

3.3.2.2. Surface plasmon resonance

The reversible biomolecular interactions between amino acids and pDNA molecules can be assessed by a label-free method, surface plasmon resonance (SPR). Thus, this method can be used to perform a screening of suitable ligands for affinity chromatography.

The SPR main components are the optical light source, a sensor chip and a detection system. The sensor chip, the biorecognition transducer, has a thin gold layer coupled to a glass layer; the glass layer has higher refractive index than gold. When a light beam propagates in a medium of high refractive index (glass) and encounters an interface at a medium of low refractive index (gold) is totally reflected at a specific angle, this physical phenomenon is called total internal reflection. Despite the light being fully reflected, the electromagnetic field component penetrates over a short distance into the medium that has the lower refractive index (gold). The leaked electromagnetic field component is referred as the evanescent field, and the wave amplitude attenuates exponentially from the interface. The evanescent wave excites electrons within the gold layer, yielding surface plasmons that propagate parallel to the interface. The ligands are immobilized on the sensor chip gold surface (coated chemically to enhance surface immobilization) and the analytes are injected into a continuous flow of running buffer. Once the analyte interacts non-covalently with the immobilized ligand, a change in molecular weight occurs and therefore the resonance angle shifts (Grupta and Verma, 2009; Ritzefeld and Sewald, 2011). A change in the SPR angle of 0.1 degrees corresponds to a change of 1000 RU (resonance units) in SPR signal (Thillaivinayagalingam *et al.*, 2010).

Biacore (GE Healthcare) is the main supplier in the SPR market (Rich and Myszka, 2010) and every standard device is equipped with an integrated microfluidic cartridge that forms four flow cells on the sensor chip. Usually the first flow cell is used as blank, to subtract the responses obtained in the other three flow cells, which can be used to immobilize three different ligands (Majka and Speck, 2007).

There are several sensor chips available in market, all with the common gold surface but coated chemically different. The sensor chip CM5, from Biacore, is the most versatile chip with a matrix carboxymethylated dextran, covalently attached to the gold surface, in order to promote a hydrophilic environment for interaction with biomolecules, without interfering with the SPR signal. Advantageous for interactions involving small molecules with high surface stability, providing accuracy and precision and allowing repeated analysis on the same surface, accordingly to manufacturer's instructions.

Therefore, small molecules like L-histidine and their derivatives can be immobilized on the

sensor chip CM5 surface, using amine coupling (Fischer, 2010), and the pDNA can be injected on the surface, in order to evaluate the affinity of interactions, label-free and with low sample consumption. SPR becomes a valuable tool to select suitable ligands for chromatographic experiments.

3.3.3. Stationary phase

A ligand with high selectivity will aid in the pDNA chromatography, however conventional matrices exhibit some limitations that will only be surpassed with a suitable chromatographic matrix.

Over the last years, several efforts have been made to overcome the chromatography bottlenecks associated with the stationary phases. An ideal matrix would be inexpensive, able to preserve the sensitive three-dimensional structure of large biomolecules but rigid enough, in order to avoid swelling or shrinking due to higher flow rates. More rigid stationary phases would resist to higher pressures and consequently higher linear velocities, enabling faster separations. At this point, the main barrier to fast chromatographic procedures would be the mass transfer between the mobile and stationary phases (Mihelic *et al*, 2000; Sousa *et al.*, 2012). Thus, functionally distinct from porous particle-based columns, the monolithic columns appeared as attractive supports for chromatographic purification procedures, especially of large biomolecules (Endres *et al.*, 2003).

3.3.3.1. Monoliths

The monolithic support is a rigid macroporous polymer column, made by in-situ polymerization within the confines of a chromatographic column, requiring no packing operations. The polymerization procedure allows optimization of porous properties of the monolith in terms of amount and pore size, depending on the polymerization temperature, which enable a plethora of applications (Merhar *et al.*, 2003; Vlakh and Tennikova, 2007). Moreover, monoliths are highly porous (Svec, 2010) and the pores are interconnected, forming a network of channels with large binding area (Endres *et al.*, 2003). The entire mobile phase is forced to flow through the monolith and convection becomes the dominant transport mechanism. Mass transport based on convection by laminar flow is an important feature on the separation of large biomolecules, such as pDNA. This results in flow-unaffected resolution and dynamic binding capacity that enables fast chromatographic procedures with low back pressure (Yamamoto and Kita, 2005). Time is a crucial factor in plasmid purification due to the possible pDNA degradation that may affect its structure and conformation. Besides the crucial role of these parameters on interaction, the desired conformation for clinical proposes (sc isoform) may be affected by longer chromatographic procedures.

Overall, the combination of the versatility and capacity of monolithic supports with the selectivity and specificity of amino acid ligands becomes a promising strategy to find the ideal chromatographic support, to recognize and purify the sc pDNA isoform from the non-effective pDNA topologies and host components, with high purity degree and productivity.

4. Aims

Given the importance of DNA vaccines and the use of pDNA vectors previously mentioned, the main goals of the present work are: the use of the SPR technique to perform a screening of binding affinity between three suitable ligands (L-Histidine, Im-benzyl-L-histidine and L-methyl-L-histidine) and pDNA samples; the immobilization of the selected ligand on a CIM™ epoxy monolithic disk; Isoforms separation of three plasmids with different sizes; evaluation of the flow rate effect on isoforms separation; assessment of the dynamic binding capacity of the modified monolith. Figure 6 represents graphically the general aims of this work.

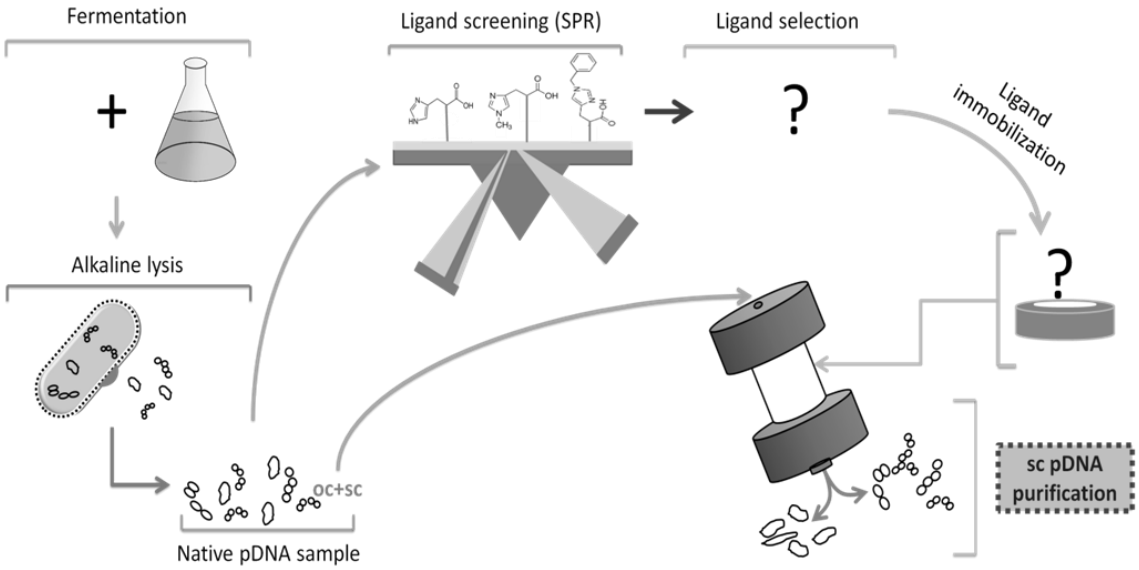

Figure 6. Graphical representation of the main goals in the present work.

Chapter II - Materials and methods

2.1. Materials

2.1.1. Reagents

The Hind III restriction enzyme, the GreenSafe Premium and the NZYTech Plasmid Maxi Columns were purchased from NZYTech (Lisbon, Portugal). Hyper Ladder I (Bioline, London, UK) was used as a DNA molecular weight marker.
Sodium chloride and ammonium sulfate were purchased from Panreac (Barcelona, Spain), tris(hydroxymethyl) aminomethane (Tris) from Merck (Darmstadt, Germany), 4-(2-hydroxyethyl)-1-piperazineethanesulfonic acid (HEPES) and borate buffer were from Sigma Aldrich (St.Louis, MO, USA).

2.1.2. Plasmids

The 6.05 kbp pVAX1-*LacZ* plasmid was provided by Invitrogen (Carlsband, CA, USA), the 8.702 kbp HPV-16 E6/E7 plasmid, Addgene plasmid 8641 (Münger *et al.*, 1989), and the 14 kbp pcDNA3-myc-FLNa S2152A plasmid, Addgene plasmid 8983, (pcDNA3-based plasmid) (Woo *et al.*, 2004) were provided by Addgene (Cambrige, USA).

2.1.3. Instrumentation

Ultrospec 3000 UV/Visible Spectrophotometer (Pharmacia Biotech, Cambridge, England) was used to determine samples concentration of nucleic acids.
Agarose gels were revealed under UV light in a transilluminator system (ILC Lda, Lisbon, Portugal).
All SPR experiments were performed using a BIAcore T200 system and the BIAevaluation software was used for data analysis.
The ^{1}H NMR spectra were recorded on a Bruker Avance III 600 MHz spectrometer equipped with a four-channel Quadruple (QCI) resonance probe and all spectra were processed with the software topspin 3.1 (Bruker).
Chromatographic experiments were performed by using the AKTA Purifier system (GE Healthcare Biosciences Uppsala, Sweden) and the control system software was Unicorn version 5.11.

2.1.4. Specifications

All solutions, used in SPR and chromatographic experiments, were freshly prepared using deionized ultra-pure grade water, purified with a Mili-Q system from Millipore (Billerica, MA, USA) and analytical grade reagents were used. Elution buffers were filtered through a 0.20 µm pore size membrane (Schleicher Schuell, Dassel, Germany) and degassed ultrasonically.

Chromatographic experiments were carried out with monolithic disks of 0.34 mL bed volume (average pore size of 1500 nm in diameter) modified with L-histidine amino acid and kindly provided by BIA Separations (Ajdovščina, Slovenia).
All experiments were conducted at room temperature unless otherwise stated.

2.2. Methods

2.2.1. Plasmids amplification by bacterial production

The pVAX1-*LacZ,* HPV-16 E6/E7 and pcDNA3-based plasmid amplification were performed by autonomous replication in *Escherichia coli* (*E. coli*) DH5α, after transformation. To ensure the exclusive growth of transformed cells, antibiotics were applied as selection markers. The medium was supplemented with 30 µg kanamycin/mL for cells transformed with pVAX1-*LacZ,* 100 µg ampicillin/mL for cells transformed with HPV-16 E6/E7 and 100 µg ampicillin/mL and 50 µg Neomycin/mL for cells transformed with pcDNA3-based plasmid.
The transformed cells harboring each plasmid were separately grown in plates at 37 ºC and the medium used was Luria-Broth (LB) agar, supplemented with the aforementioned antibiotics in accordance with the plasmid of transformed cells. In pre-fermentation, strides from plates of each plasmid were inoculated into 250 mL shake flasks with 62.5 mL of Terrific Broth (TB) medium (20 g/L tryptone, 24 g/L yeast extract, 4 mL/L glycerol, 0.017 M KH_2PO_4 and 0.072 M K_2HPO_4), with the respective selection marker for each plasmid. The pre-fermentation was carried out at 37 ºC under 250 rpm shaking.
The optical density of the culture medium at a wavelength of 600 nm (OD_{600}) was used to evaluate the transformed cells growth. When OD_{600} reached approximately a value of 2.6, the appropriate amount of pre-fermentation was inoculated in fresh TB medium, in order to start the fermentation with an OD_{600} of approximately 0.2. Growth was carried out under the same conditions but in 1L shake flasks with 250 mL of fermentation medium in order to maintain the same oxygenation conditions of pre-fermentation. Growth was suspended at the mid-log phase (OD_{600}~7) in order to achieve cells enriched with sc pDNA isoform.
Cells were recovered by centrifugation at 4500 g and 4 ºC. Supernatants were discarded and bacterial pellets were stored at -20 ºC.

2.2.2. Alkaline lysis and pre-purification of pDNA samples with NZYTech Kit

The alkaline lysis of pelleted bacteria was performed by a modified alkaline method and the plasmid samples were pre-purified according to NZYTech Plasmid Maxi kit manufacturer's instructions. The kit was designed for the rapid and large-scale preparation of highly pure pDNA from recombinant *E.coli* strains.

Briefly, after the alkaline lysis, the precipitated cell debris were eliminated by centrifugation, and then, the impurities are removed by a medium-salt wash after plasmid DNA binding to the NZYTech silica-based anion-exchange resin. All contaminants are washed from the column. Then, the pDNA elution occurs when a high-salt buffer is added. In last, the pDNA is concentrated by isopropanol precipitation.

The pDNA pellet was dissolved in appropriate buffer to future use.

2.2.3. Plasmid isoforms preparation

Three plasmid conformations, namely sc, linear (ln) and open circular (oc) isoforms of each plasmid, were prepared to be used in SPR and chromatographic experiments.

2.2.3.1. Supercoiled isoform

The sc samples of pVAX1-*LacZ*, HPV-16 E6/E7 and pcDNA3-based plasmid were directly obtained by alkaline lysis, as described above, according to manufacturer's instructions. The bacterial growth was suspended with OD_{600}~7 to obtain sc-enriched samples. The plasmid yield was assessed by UV spectrophotometry and the sc isoform integrity was confirmed by agarose gel electrophoresis.

2.2.3.2. Linear isoform

The sc samples of pVAX1-*LacZ*, HPV-16 E6/E7 and pcDNA3-based plasmid were also used to prepare ln pure samples of each plasmid. For this propose, an enzymatic digestion with Hind III, 1 h at 37 ºC was accomplished according to the manufacturer´s protocol. The sample conversion was confirmed by agarose gel electrophoresis.

2.2.3.3. Open circular isoform

PVAX1-LacZ, HPV-16 E6/E7 and pcDNA3-based plasmid samples, obtained by alkaline lysis, were also used to prepare oc pure samples. In order to convert sc into oc isoform, the plasmids were incubated at room temperature, and monitored over the time by agarose electrophoresis, until total sample conversion (about 3 days).

2.2.4. Agarose gel electrophoresis

The conformation and the relative purity of different isoforms of three plasmids were analyzed by horizontal electrophoresis using 15-cm-long 0.8% agarose gels (Hoefer, San Francisco, CA, USA), stained with GreenSafe Premium (1µg/mL). The GreenSafe Premium was incorporated in agarose gel during its preparation and appears as a safer alternative to the traditional ethidium bromide stain to detect nucleic acids.
Electrophoresis was performed at 100 V, for 30 minutes, with TAE buffer (40 mM Tris base, 20 mM acetic acid and 1 mM EDTA, pH 8.0) and agarose gels were revealed under UV light.
The fractions recovered from chromatographic experiments were also analyzed by agarose gel electrophoresis.

2.2.5. SPR studies

2.2.5.1. Amino acids immobilization

L-histidine, Im-benzyl-L-histidine and L-methyl-L-histidine, were dissolved in 100 mM borate solution, at pH 9, with a final concentration of 340 mM, 21 mM and 350 mM, respectively to be immobilized on a carboxymethylated dextran-coated sensor chip (CM5 research grade).
The sensor chip was docked on the Biacore T200 system after being equilibrated at room temperature to prevent condensation on the chip surface. The detector was normalized with BIAnormalizing solution (70% glycerol, GE Healthcare).
The running buffer for ligands immobilization was HBS-EP (10 mM HEPES, 150 mM NaCl, 0.05% P20 surfactant, 3 mM EDTA, pH 7.4), purchased from Biacore. The coupling method to covalently attach L-histidine, Im-benzyl-L-histidine and L-methyl-L-histidine to the sensor chip surface was amine coupling. The $-NH_2$ functional group of ligands was covalently bound to the NH esters on the dextran coating the sensor chip surface, with that purpose the sensor chip surface was activated with 1-ethyl-3-(3- dimethylaminopropyl) carbodiimide (EDC) and N-hydroxysuccinimide (NHS). After ligands injection the sensor surface was blocked with ethanolamine and injections with HBS-EP were performed to stabilize the baseline.
L-methyl-L-histidine was immobilized on flow cell 2 with a final response of 207.6 RU, Im-benzyl-L-histidine was immobilized on flow cell 3 with a final 229.8 RU as final response and in flow cell 4 was immobilized the L-histidine with a final response of 183.5 RU.
The CM5 chip flow cell 1 was left unmodified to act as reference and samples were tested for binding in duplicate.

2.2.5.2. Affinity analysis

After immobilization, different running buffers were tested: 10 mM Tris-HCl, pH 8, 500 mM ammonium sulfate in 10 mM Tris-HCl, pH 8, 500 mM ammonium sulfate, 100 mM of HEPES, pH 7.4 and 10 mM of HEPES, pH 7.4.
The affinity data was collected with HEPES 10 mM pH 7.4. Samples of pVAX1-*LacZ*, HPV-16 E6/E7 and pcDNA3-based plasmid isoforms (sc, oc and ln) were injected at concentrations ranging from 0.55μM to 4.3×10^{-6} μM. After each run the plasmid was removed from the surface without requiring a regeneration solution.
A steady state affinity study was performed with the binding data collected, averaging the resonance unit values (RU) in the plateau region of the sensorgrams over 350-400 s and the data were fit to an 1:1 interaction model using BIAevaluation software.

2.2.6. ^{1}H NMR experiments

The L-histidine 0.34 M was dissolve in solution of HEPES (10 mM and 100 mM) with 10 % D_2O at pH 7.4. The proton resonances of L-histidine were first assigned. The ^{1}H NMR spectra were recorded at a temperature of 298 K on a Bruker Avance III 600 MHz spectrometer operating at 14.09 Tesla observing ^{1}H at 600.13 MHz. The spectrometer was equipped with a four-channel Quadruple (QCI) resonance probe and all spectra were processed with the software topspin 3.1 (Bruker).

2.2.7. Chromatographic studies

All chromatographic runs were monitored at 260 nm and the fractions pooled were concentrated and desalted for further analysis with agarose electrophoresis.

2.2.7.1. Amino acid immobilization

The ligand, L-histidine, was dissolved in 4 mL of NaOH, in order to be immobilized in a CIM™ epoxy disk. The L-histidine and NaOH solution was pumped through the monolithic disk followed by 72h thermostating of the column at 60 ºC.
Finally, the monolithic disk was washed with water and the remaining epoxy groups were hydrolyzed in diol groups by soaking with 0.5 M H_2SO_4 for 30 min.

2.2.7.2. Linear gradients

Linear gradients were performed by decreasing the ammonium sulfate concentration from 3.5 to 0 M and increasing the sodium chloride concentration from 0 to 3 M. In these chromatographic experiments the L-histidine monolith was equilibrated with the binding

buffer at a flow rate of 1 mL/min and the plasmid samples, pre-purified with the NZYTech kit, were injected (100 µL) at the same flow rate.

2.2.7.3. Stepwise gradients

Stepwise gradients of decreasing ammonium sulfate were explored to separate isoforms of pVAX1-*LacZ*, HPV-16 E6/E7 and pcDNA3-based plasmid. In these chromatographic experiments, the L-histidine monolith was equilibrated with 2.99 M ammonium sulfate for pVAX1-*LacZ*, 2.94 M for HPV-16 E6/E7 and 2.91 M for pcDNA3-based plasmid at a flow rate of 1 mL/min. Plasmid samples were injected in 100 µL loop at the same flow rate.

Different flow rates were applied to study the flow rate effect on plasmid isoforms separation. The L-histidine monolith was equilibrated with 2.99 M ammonium sulfate and the stepwise gradients were performed at a flow rate of 1mL/min, 2mL/min and 4mL/min with the pVAX1-*LacZ* plasmid.

2.2.7.4. Dynamic binding capacity

After several alkaline lysis with the NZYTech kit, a solution with 0.05 mg/mL pVAX1-*LacZ* was prepared to perform breakthrough experiments. The experiments were conducted to assess the L-histidine monolith dynamic binding capacity for pDNA. Briefly, L-histidine monolith was equilibrated with 3.5 M ammonium sulfate in 10 mM Tris-HCl buffer and 10 mM EDTA, pH 8. After the column saturation with pDNA prepared in the same equilibrium buffer, the elution was obtained by decreasing the ammonium sulfate concentration to 0 M. The L-histidine monolith was also overloaded at different flow rates, 1 mL/min and 0.5 mL/min.

Dynamic binding capacity assessment was carried out, after data normalization, by calculating the amount of bound pDNA per mL of support at 10%, 50% and 100% of breakthrough curves and subtracting the respective value obtained under non-binding conditions.

2.2.7.5. Monolith regeneration

After some chromatographic experiments, the monolith regeneration was conducted through washing with deionized water followed by 5 column volumes of 0.5 M NaOH at flow rate of 0.5 mL/min. In order to restore the proper pH, L-histidine monolith was again thoroughly washed with the deionized water.

Chapter III - Results and discussion

3. Ligands screening

L-histidine was already successfully used in previous studies with an agarose conventional matrix to efficiently purify the sc pDNA from a clarified lysate (Sousa *et al.*, 2006). However, low capacity and low diffusivity for pDNA are disadvantages associated with the abovementioned conventional matrix (Sousa *et al.*, 2012). These limitations can be surpassed by using the innovative monolithic supports. Thus, the L-histidine amino acid and two derivatives with the imidazole ring functionalized with methyl and benzyl are considered promising affinity ligands to combine with monoliths for pDNA purification.
Therefore, in this work, the suitability of L-histidine and their derivatives, Im-benzyl-L-histidine and L-methyl-L-histidine, was assessed by SPR in order to select the ligand for immobilization on a modified monolith.

3.1. Amino acids immobilization

In order to perform the SPR experiments, L-histidine, Im-benzyl-L-histidine and L-methyl-L-histidine were immobilized on Sensor Chip CM5 via amine coupling (McWhirter and Löfas, 2006). The carboxylic groups on the carboxymethylated (CM)-dextran matrix -coated sensor chip surface were activated with 1-ethyl-3-(3-dimethylaminopropyl) carbodiimide (EDC) and N-hydroxysuccinimide (NHS). The ligands were dissolved in 100 mM of borate solution, pH 9.0 and the running buffer used for ligands immobilization was HBS-EP (10 mM HEPES, 150 mM NaCl, 0.05% P20 surfactant, 3 mM EDTA, pH 7.4). After that, the unreacted NHS-esters were blocked with solution of 1 M ethanolamine. Throughout the experiments, the flow cell 1 acts as a control reference (without amino acid immobilized) and is used to correct the bulk refractive index changes and non-specific binding at the sensor surfaces.

3.2. SPR binding experiments

3.2.1. Running buffer selection for affinity experiments

After ligands immobilization on the chip, different running buffers were tested to chose the most suitable to perform the affinity assay.
The first running buffer tested was 10 mM Tris-HCl, pH 8.0, however no signal was detected. The same occurred with running buffers ammonium sulfate 500 mM in 10 mM Tris-HCl, pH 8 and 500 mM of ammonium sulfate.

In figure 7 are showed two sensorgrams were the response was negative, both were obtained with Im-benzyl-L-histidine, one with the sc isoform of pVAX1-*LacZ* in ammonium sulfate as

running buffer, figure 7 (A), the second example was accomplished with the sc isoform of pcDNA3-based plasmid in Tris-HCl as running buffer, figure 7 (B).

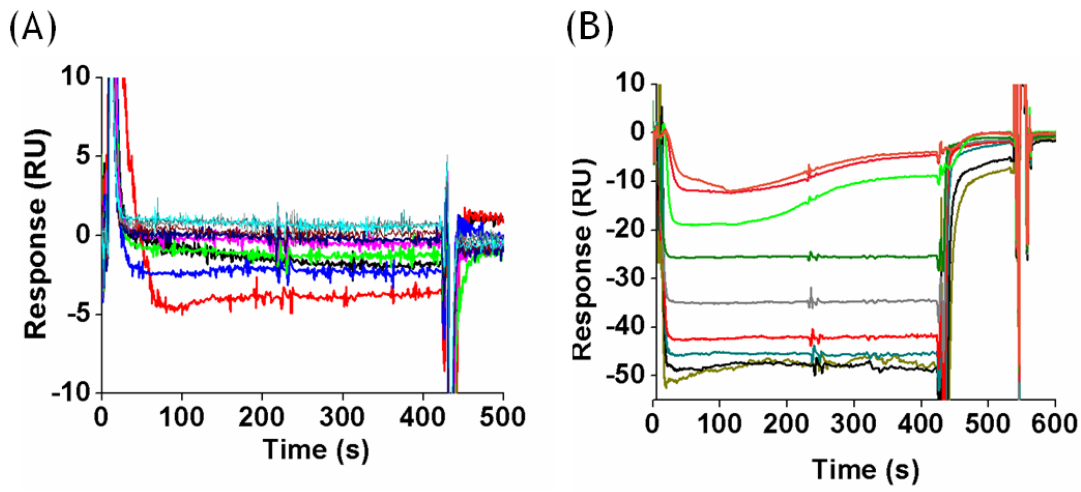

Figure 7. Sensorgrams obtained with two different plasmids and two different running buffers, which no signal was detected.

Nonetheless, with each running buffer tested, several isoforms from plasmids of different sizes were injected in order to discriminate the lack of signal due to plasmid size or conformation.

The different plasmid isoforms were interacting with the reference and those interactions were more significantly than to the amino acid surfaces. Since the final response is the result from the plasmid isoforms interaction with the amino acid surfaces minus the plasmid isoforms interaction with the reference surface, the signal obtained was negative.

In order to decrease the non-specific binding with the reference, the running buffer was changed to HEPES 10 mM, pH 7.4, since it has been described as a running buffer to reduce the non-specific binding with nucleic acids (Fischer, 2010).The responses were detectable and reproducible in some ligands/plasmid complexes, not all, due to remaining non-specific binding.

Another strategy to decrease the unspecific binding was to increase the running buffer concentration of HEPES (Fischer, 2010) for 100 mM, pH 7.4. However no binding response was detected.

^{1}H NMR experiments were performed with solutions of 10 mM and 100 mM of HEPES at pH 7.4, in order to understand the concentration effect on the binding with L-histidine. The L-histidine was dissolved in solution of HEPES (10 mM and 100 mM) with 10 % D_2O at pH 7.4. The ^{1}H NMR spectra showed chemical shift variation in imidazole protons only with HEPES 100 mM. This can be attributed to the fact that the imidazole ring of L-histidine interacted preferentially with HEPES buffer 100 mM indicating that imidazole protons are not free to interact with the target biomolecule. This result is in concordance with the described

previously (Caramelo-Nunes *et al.*, 2014) where the aromatic side chain of L-histidine is the structural feature that mainly interact with plasmid isoforms.

3.2.2. Affinity data analysis

HEPES 10 mM, pH 7.4 was the running buffer selected to collect the affinity data when different plasmid isoforms were injected over the surface, since it was the one that promoted less unspecific binding with the blank cell.

The SPR binding profile was identical for all complexes indicating that the plasmid isoforms associate and dissociate rapidly from the amino acid surfaces. By this way only steady-state studies were performed. The sensorgram examples are given in figure 8.

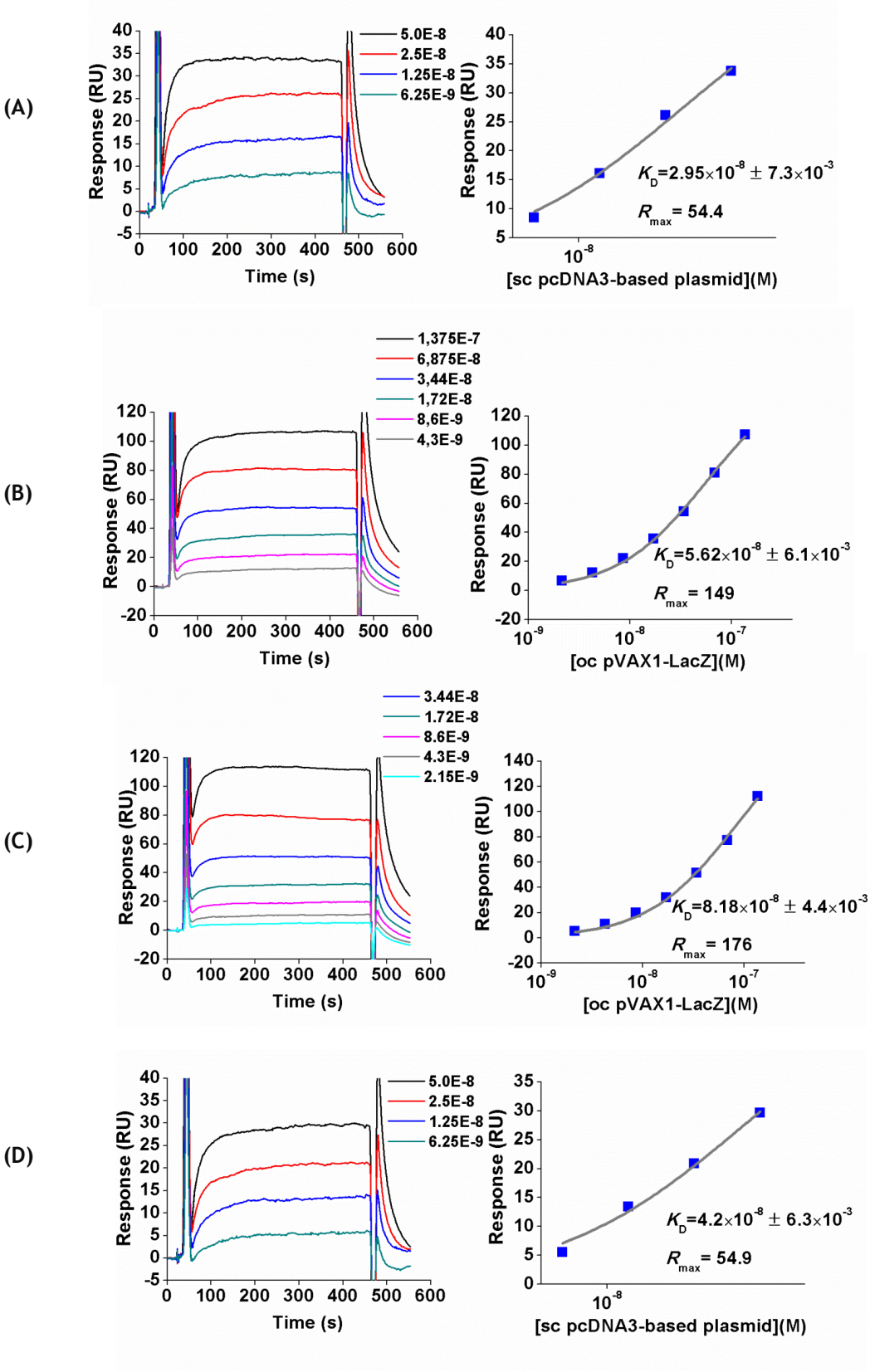

Figure 8. Sensorgrams and equilibrium-binding analysis of immobilized Im-benzyl-L-histidine to **(A)** sc isoform of pcDNA3-based plasmid **(B)** oc isoform of pVAX1-*LacZ* and immobilized L-histidine to **(C)** oc isoform of pVAX1-*LacZ* and **(D)** sc isoform of pcDNA3-based plasmid in HEPES 10mM pH 7.4.

A steady-state study was carried out by averaging the resonance unit values (RU) in the plateau region of the sensorgrams over a 350 to 400 s. Nonspecific binding was detected in the reference surface, to the NH esters. Therefore, affinity calculations of some plasmid isoforms were unfeasible. The equilibrium dissociation constants (K_D) are presented in table 4 and are significantly higher (10^{-10}-10^{-8} M range) with the highest affinity found for HPV-16 E6/E7 linear/L-histidine, 3.34 x10^{-10}±0.0209 M, while the supercoiled isoform of the pcDNA3-based plasmid shows the lowest binding.

Table 4. Equilibrium data analysis of plasmids in 10 mM of HEPES pH 7.4. K_D-dissociation constant; **SD**-standard deviation.

Plasmid samples		K_D(M) ± SD		
		L-methyl-L-histidine	**Im-benzyl-Lhistidine**	**L-histidine**
pVAX1-*LacZ*	Sc	5.05×10^{-8} ±0.00613	6.03×10^{-9} ±0.00595	5.79×10^{-8} ±0.0131
	Oc	*	5.62×10^{-8} ±0.00607	8.18×10^{-8} ±0.00441
	Ln	*	*	*
HPV-16 E6/E7	Sc	*	*	*
	Oc	1.1×10^{-10} ±0.00573	*	*
	Ln	*	*	3.34×10^{-10} ±0.0209
pcDNA3-based plasmid	Sc	*	2.95×10^{-8} ±0.00734	4.2×10^{-8} ±0.00629
	Oc	*	*	*
	Ln	*	1.68×10^{-9} ±0.00702	244×10^{-9} ±0.00848

The linear isoform of pcDNA3-based plasmid have lowest affinity than linear isoform of HPV-16 E6/E7 plasmid, these results suggest a non-linear tendency between plasmid size and binding affinity.

Overall, the maximum response was found for L-histidine surface, when compared with its derivatives indicating that L-histidine might be the most promising ligand for purification of pVAX1-*LacZ*, HPV-16 E6/E7 and pcDNA3-based plasmids, for affinity chromatography.

4. Chromatographic experiments

4.1. L-Histidine immobilization

The monolithic matrices present several advantages over the conventional matrices, including their tridimensional characteristics of interconnected pores that allow good mass transfer properties and binding capacity for large biomolecules, such as pDNA (Endres *et al.*, 2003).
Considering the analysis of the SPR results obtained previously, the ligand chosen to be immobilized on the monolithic support was L-histidine.
Therefore, combining the innovative monolithic matrices with the specificity and selectivity of the L-histidine ligand can be a valuable and promising strategy towards sc pDNA purification.
The L-histidine ligand was immobilized on a CIM^{TM} epoxy disk according to the procedure described in chapter 2. The monolith modification was evaluated by comparing the pDNA elution behavior in the non-grafted epoxy monolith with the monolith modified with L-histidine ligands. A decreasing linear gradient of ammonium sulfate, from 3.5 M to 0 M in 10 mM Tris-HCl and 10 mM EDTA pH 8.0 was performed with both monoliths, loading a pVAX1-*LacZ* plasmid sample (100 µL) at flow rate of 1 mL/min. The binding condition promoted the pDNA retention to the epoxy groups on the non-grafted monolith (figure 9 (A)) and the pDNA retention to the L-histidine ligands on the L-histidine monolith (figure 9 (B)). The pDNA was then eluted in both cases during the linear gradient.
As shown in figure 9, the elution profiles are different, as well as, the pDNA retention time. The differences in the elution profile can be due to the presence of L-histidine ligand on the modified monolith (figure 9 (B)). All peaks achieved during both chromatographic assays were recovered and analyzed by agarose electrophoresis.The results indicated that the pDNA was completely retained to the monolithic supports, being eluted during the linear gradients.

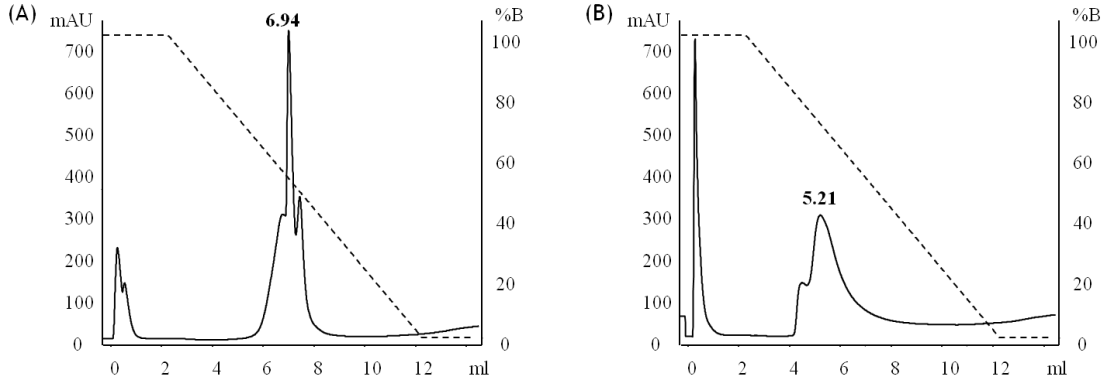

Figure 9. Chromatographic profiles of decreasing linear gradients from 3.5 M to 0 M ammonium sulfate in 10 mM Tris-HCl and 10 mM EDTA, pH 8.0 with the **(A)** non-immobilized epoxy monolith and **(B)** the L-histidine monolith. The assays were performed at 1 mL/min with pVAX1-*LacZ* plasmid sample, pre-purified with NZYTech kit. The labels in the peaks represent the pDNA retention time.

4.2. Evaluation of elution conditions on pDNA retention

In order to establish the ideal binding and elution conditions to be used for further separations of plasmid isoforms, the influence of buffer composition, ionic strength and pH was studied by affinity chromatography.

4.2.1. Elution buffer composition

HEPES 10 mM pH 7.4 was the running buffer more suitable to perform the SPR analysis. Therefore the role of this buffer in pDNA retention was also evaluated in chromatographic preliminary studies.

A decreasing linear gradient of ammonium sulfate in 10 mM HEPES and 10 mM EDTA, at pH 7.4, from 3.5 M to 0 M, was performed, by loading 100 µL of pVAX1-*LacZ* plasmid sample at flow rate of 1 mL/min. As the aim of this study was to observe the influence of the HEPES buffer in the pDNA retention, the elution strategy used was similar to the strategy previously used with the Tris-HCl (previous section, figure 9 (B)). As it is visible in figure 10, the pDNA elution profile obtained with HEPES buffer was the same observed in the Tris-HCl.

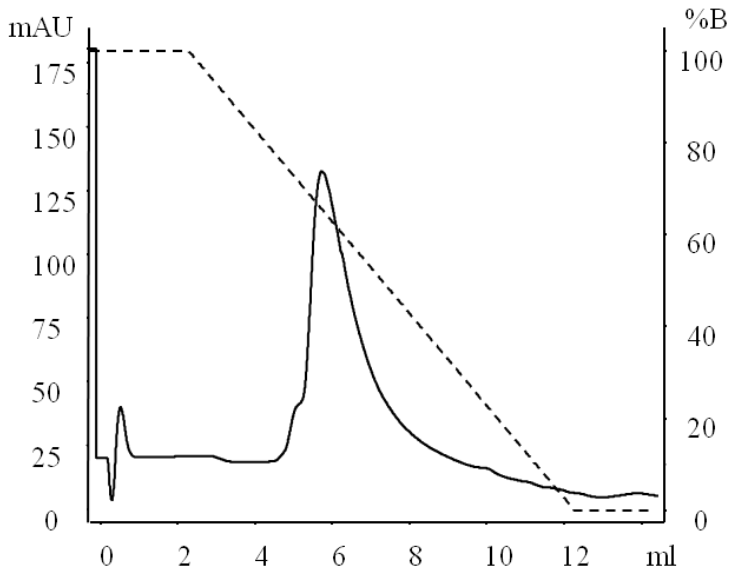

Figure 10. Chromatographic profile of decreasing linear gradient from 3.5 M to 0 M (NH4)2SO4 in 10 mM HEPES and 10 mM EDTA, pH 7.4 with the L-histidine monolith. The assay was performed at 1 mL/min with pVAX1-LacZ plasmid sample, pre-purified with NZYTech kit.

4.2.2. Ionic strength influence

Another study was conducted to evaluate the influence of ionic strength in the plasmid retention to the L-histidine monolith. An increasing linear gradient from 0 to 3 M of sodium chloride in 10 mM Tris-HCl and 10 mM EDTA, pH 8.0 was performed at flow rate of 1mL/min. After the injection of the pVAX1-*LacZ* plasmid sample, a first and unique peak was rapidly attained in the flow-through due to the elution of unbound species, as can be seen in figure 11. During the increasing linear gradient of NaCl no specie was eluted.

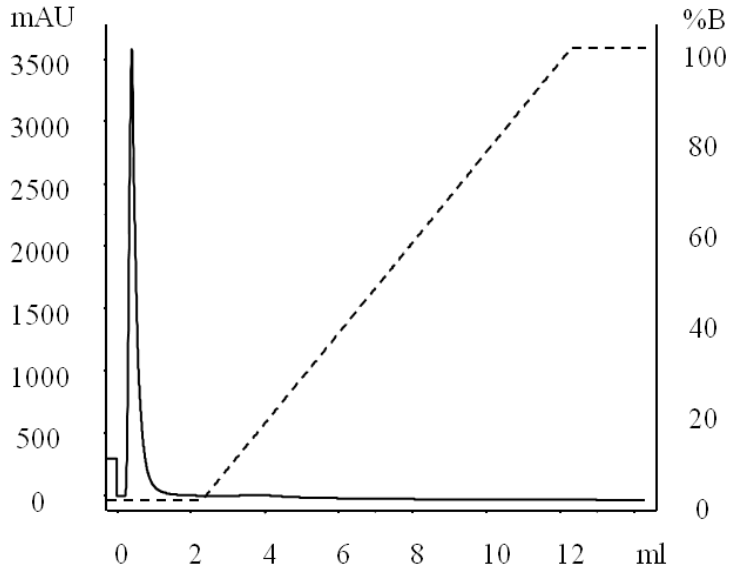

Figure 11. Chromatographic profile of an increasing linear gradient from 0 M to 3 M NaCl in 10 mM Tris-HCl and 10 mM EDTA, pH 8.0. The assay was performed at 1 mL/min, using the L-histidine monolith with the pVAX1-*LacZ* plasmid sample, pre-purified with the NZYTech kit.

In fact, this result indicates no pDNA retention was obtained at low salt concentrations, and consequently, it is concluded that ionic interactions are not the prevalent forces between pDNA and the L-histidine monolith.

4.2.3. pH influence

The pH influence on oligonucleotides retention was reported in a previous study by using the L-histidine-agarose support (Sousa *et al.*, 2009). Therefore, to obtain enhanced binding/elution conditions, the pH influence on the plasmid retention was also evaluated.

A solution with 3.5 M ammonium sulfate in 10 mM Tris-HCl buffer and 10 mM EDTA, pH 6.0 was prepared and a decreasing linear gradient was established from 3.5 M to 0 to observe the acidic pH influence on pDNA retention. The chromatographic profile obtained is showed in figure 12. As it is observed, the pDNA retention time slightly increased to 5.59 when compared with the same assay at pH 8.0 (5.21, figure 9 (B)).

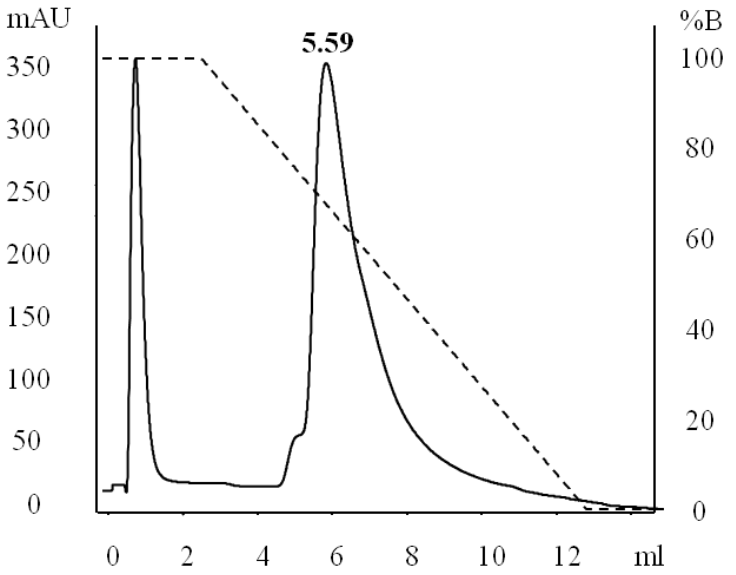

Figure 12. Decreasing linear gradient from 3.5 M to 0 M ammonium sulfate in 10 mM Tris-HCl and 10 mM EDTA, pH 6.0, with the L-histidine monolith. The assay was performed at 1 mL/min with pVAX1-*LacZ* plasmid sample (100 µL), pre-purified with the NZYTech kit. The label in the peak represent the pDNA retention time.

Due to the high ammonium sulphate concentrations used, the predominance of hydrophobic interactions is evidenced. However, this result suggests the presence of other interactions, which affect the plasmid retention. Given that the pKa of L-histidine is 6.5, acidic pH environment can favor the protonation of imidazole ring, which enables the involvement of π-π stacking and cation π interactions with plasmid aromatic bases (Caramelo-Nunes *et al.*, 2014).

4.3. Chromatographic profile of different plasmid isoforms

Similarly to what was evaluated in SPR, several chromatographic experiments were accomplished through a screening of different isoforms (oc, sc and ln) of pVAX1-*LacZ*, HPV-16 E6/E7 and pcDNA3-based plasmid, separately injected. The elution conditions were chosen

through the results achieved in previous assays. Thus, a decreasing linear gradient from 3.5 M to 0 M ammonium sulfate in 10 mM Tris-HCl and 10 mM EDTA pH 8.0 was applied for each pDNA isoform. Their retention behavior was analyzed in order to characterize the L-histidine monolith and assess the separation of the sc pDNA isoform when present in a mixture of isoforms.

4.3.1. pVAX1-*LacZ* (6.05 kbp)

4.3.1.1. pVAX1-*LacZ* linear isoform

The first pVAX1-*LacZ* isoform evaluated was the ln isoform. The ln pVAX1-*LacZ* plasmid sample was obtained through enzymatic digestion, as described in chapter 2. A decreasing linear gradient from 3.5 M to 0 M $(NH_4)_2SO_4$ in 10 mM Tris-HCl and 10 mM EDTA pH 8.0 was performed at 1 mL/min. As shown in figure 13, after injection step, the sample was eluted in a single peak during the flowthrough at 3.5 M of ammonium sulfate, indicating that these conditions do not favor the ln isoform retention.

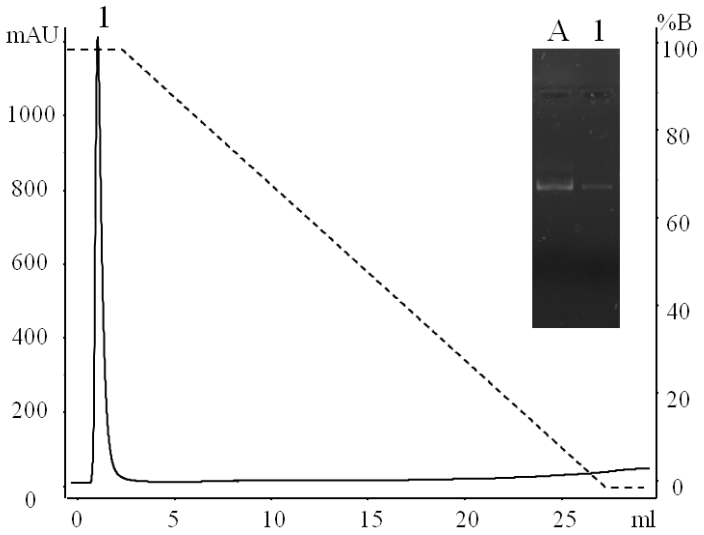

Figure 13. Decreasing linear gradient from 3.5 M to 0 M ammonium sulfate in 10 mM Tris-HCl and 10 mM EDTA, pH 8.0, at 1mL/min. The ln pVAX1-*LacZ* plasmid sample was prepared from a sample pre-purified with NZYTech kit by enzymatic digestion. In the agarose gel electrophoresis, the lane A represents the ln sample injected (100 µL) and lane 1 corresponds to peak 1.

4.3.1.2. pVAX1-*LacZ* open circular isoform

The same conditions were used to evaluate the pVAX1-*LacZ* open circular isoform. This isoform was obtained by incubating the sc pVAX1-*LacZ* sample at room temperature until total sample conversion. The oc pDNA sample was injected under the elution conditions previously refereed, and the resultant chromatographic profile is presented in figure 14. The first peak,

eluted at 3.5 M ammonium sulfate, corresponds to unbound species and the second peak, eluted during the linear gradient, represents some species that remained bound. The agarose gel electrophoresis shows the content of each peak, indicating that in the first peak was eluted most part of the oc isoform, but a partial retention of this isoform also occurred. Considering this chromatographic behavior and comparing the peaks size, it can be suggested that the majority of the oc isoform was eluted in the first peak, and therefore, this isoform did not effectively bind to L-histidine monolith under the elution conditions established.

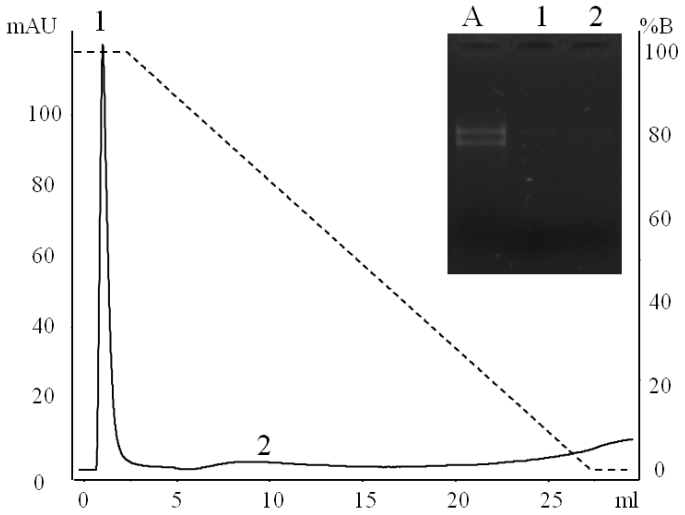

Figure 14. Decreasing linear gradient from 3.5 M to 0 M ammonium sulfate in 10 mM Tris-HCl and 10 mM EDTA, pH 8.0, at 1mL/min. The oc pVAX1-*LacZ* plasmid sample was prepared from a sample pre-purified with NZYTech kit by room temperature incubation. In the agarose gel electrophoresis, the lane A represents the oc sample injected (100 µL), lane 1 corresponds to peak 1 and lane 2 to peak 2.

4.3.1.3. pVAX1-*LacZ* supercoiled isoform

A supercoiled pVAX1-*LacZ* sample was also injected in the L-histidine monolith with a decreasing linear gradient from 3.5 M to 0 M ammonium sulfate in 10 mM Tris-HCl and 10 mM EDTA pH 8.0 at 1 mL/min. The chromatographic profile obtained with the sc-enriched sample (figure 15) differs significantly from the ones previously presented for oc and ln isoforms of the pVAX1-*LacZ* plasmid. The chromatogram reveals a small peak during the flowthrough and a larger peak eluted during the linear gradient that corresponds to species retained into the L-histidine monolith, under these conditions.

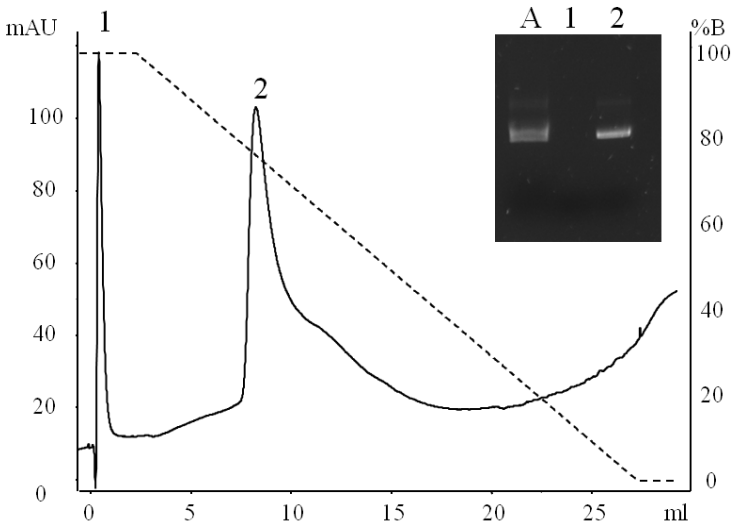

Figure 15. Decreasing linear gradient from 3.5 M to 0 M ammonium sulfate in 10 mM Tris-HCl and 10 mM EDTA, pH 8.0, at 1mL/min. The sc-enriched pVAX1-*LacZ* plasmid sample was pre-purified with NZYTech kit. In the agarose gel electrophoresis, the lane A represents the sc-enriched sample injected (100 µL), lane 1 corresponds to peak 1 and lane 2 corresponds to peak 2.

The peak content was evaluated by agarose gel electrophoresis but the results indicated that the first peak does not present nucleic acids, while the second peak reveals a bright sc pDNA band. These results suggest that the sc isoform was completely retained to the L-histidine monolith and the same behavior was not extended to the other plasmid topologies.

4.3.2. HPV-16 E6/E7 (8.70 kbp)

4.3.2.1. HPV-16 E6/E7 linear isoform

A decreasing linear gradient was also performed with an HPV-16 E6/E7 linear sample, using the aforementioned conditions. The elution behavior for HPV-16 E6/E7 linear isoform is slightly different from the elution behavior previously observed with the ln pVAX1-*LacZ* sample. The HPV-16 E6/E7 chromatographic profile shows two consecutive peaks in the flowthrough (figure 16). Nonetheless, the electrophoretic analysis revealed that the ln isoform was mostly eluted in the second peak, which seems to be delayed in the column. However, no retention of HPV-16 E6/E7 ln pDNA to the L-histidine was observed under these elution conditions.

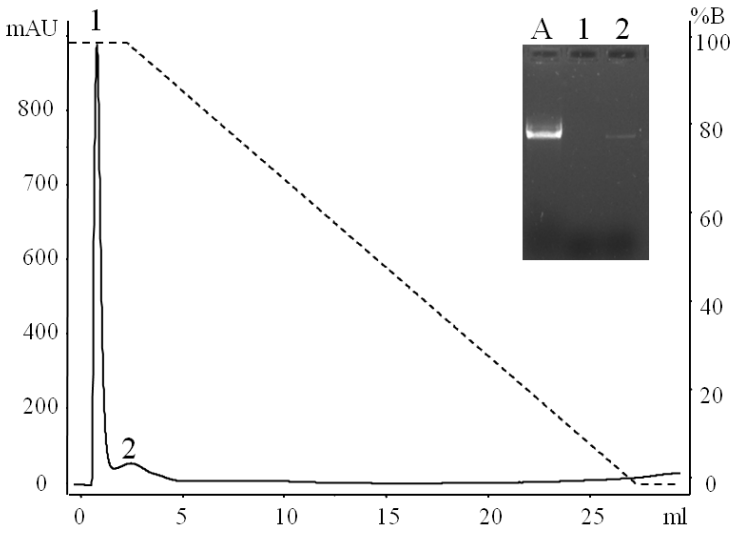

Figure 16. Decreasing linear gradient from 3.5 M to 0 M ammonium sulfate in 10 mM Tris-HCl and 10 mM EDTA, pH 8.0, at 1mL/min. The HPV-16 E6/E7 ln plasmid sample was prepared from a sample pre-purified with NZYTech kit by enzymatic digestion. In the agarose gel electrophoresis, the lane A represents the ln sample injected (100 µL); lane 1:peak 1; lane 2: peak 2.

4.3.2.2. HPV-16 E6/E7 open circular isoform

Using the same elution strategy, a HPV-16 E6/E7 oc sample was injected to evaluate the chromatographic profile of this isoform. The obtained profile was similar to the elution profile of the pVAX1-*LacZ* oc isoform. Thus, by agarose electrophoresis analysis it was observed that the HPV-16 E6/E7 oc isoform is present in both peaks (figure 17). Also in this case, the oc isoform retention to the modified monolithic matrix was not effective.

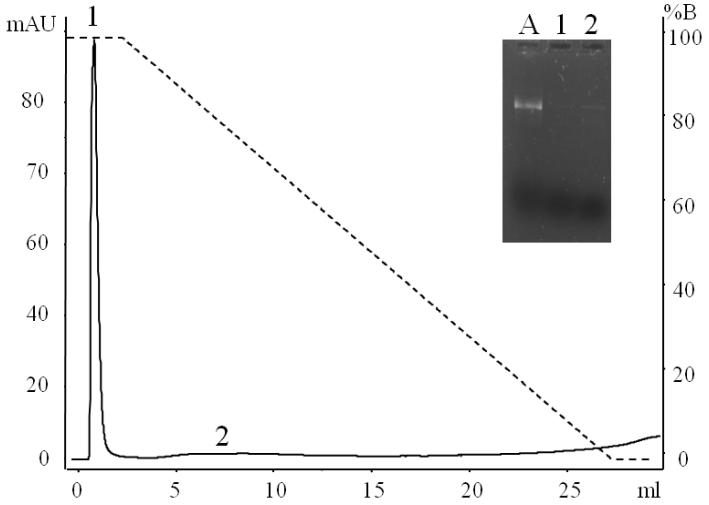

Figure 17. Decreasing linear gradient from 3.5 M to 0 M ammonium sulfate in 10 mM Tris-HCl and 10 mM EDTA, pH 8.0, at 1mL/min. In the agarose gel electrophoresis, the lane A represents the oc sample injected (100 µL), lane 1 content corresponds to peak 1 and lane 2 corresponds to peak 2.

4.3.2.3. HPV-16 E6/E7 supercoiled isoform

The chromatographic behavior of the HPV-16 E6/E7 supercoiled isoform was also studied through the decreasing ammonium sulfate gradient. The elution profile of the HPV-16 E6/E7 sc isoform revealed to be similar to the pVAX1-*LacZ* sc isoform, previously shown. The similarity can be seen in figure 18 and also the electrophoretic analysis revealed that the sc isoform completely bound to the L-histidine monolith, being eluted in the peak 2 during the linear gradient (confirmed by lane 2 of the electrophoresis).

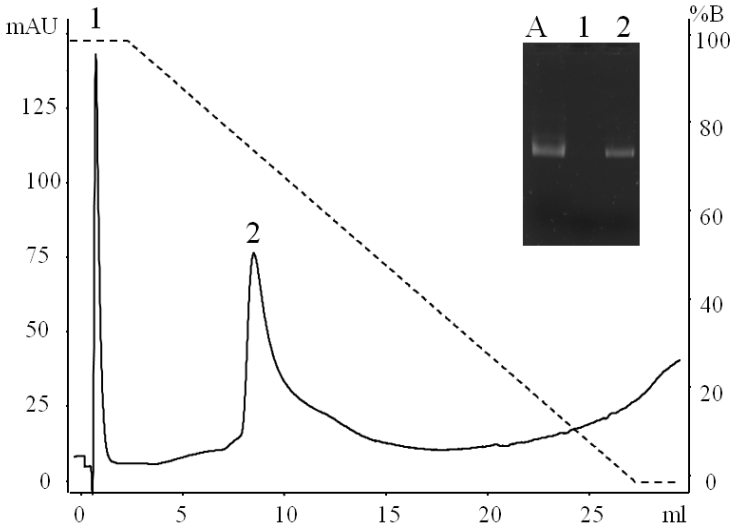

Figure 18. Decreasing linear gradient from 3.5 M to 0 M ammonium sulfate in 10 mM Tris-HCl and 10 mM EDTA, pH 8.0, at 1mL/min. The sc-enriched plasmid sample was pre-purified with NZYTech kit. In the agarose gel electrophoresis, the lane A represents the sc-enriched sample injected (100 µL), lane 1 corresponds to peak 1 and lane 2 corresponds to peak 2.

4.3.3. pcDNA3-based plasmid (14 kbp)

4.3.3.1. pcDNA3-based plasmid linear isoform

The elution conditions previously mentioned were also applied to accomplish the chromatographic study of the pcDNA3-based plasmid linear isoform. After the ln sample injection, two consecutive peaks were eluted (figure 19). The elution profile presents similarities with the HPV-16 E6/E7 linear isoform profile. The peak content was revealed by agarose gel electrophoresis in figure 18, and the linear isoform was eluted in the first and second peaks. Thus, the pcDNA3-based plasmid linear isoform was partially delayed into the L-histidine monolith. This behavior suggests that the time required for the isoform pass through the column is influenced by the pDNA molecular size and conformation, being observed long time for larger molecules.

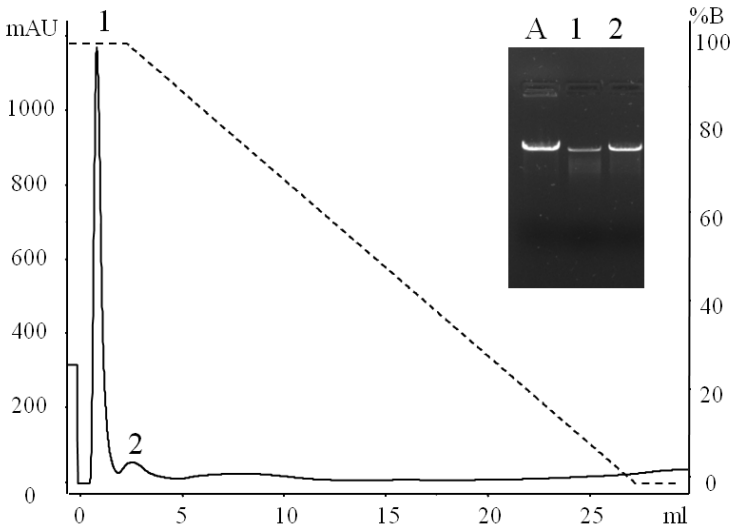

Figure 19. Decreasing linear gradient from 3.5 M to 0 M ammonium sulfate in 10 mM Tris-HCl and 10 mM EDTA, pH 8.0, at 1 mL/min. The HPV-16 E6/E7 ln plasmid sample was prepared from a sample pre-purified with NZYTech kit by enzymatic digestion. In the agarose gel electrophoresis, the lane A represents the ln sample injected (100 µL); lane 1: peak 1; lane 2: peak 2.

4.3.3.2. pcDNA3-based plasmid open circular isoform

The linear gradient used to assess the open circular isoform behavior of the pcDNA3-based plasmid revealed two peaks (figure 20). Comparing the chromatographic profile of this plasmid topology with the profiles already shown for the same topology but different plasmids, the behavior is slightly modified, since the second peak is increased. However, by agarose gel electrophoresis the oc pcDNA3-based plasmid seems to be partially eluted in both peaks.

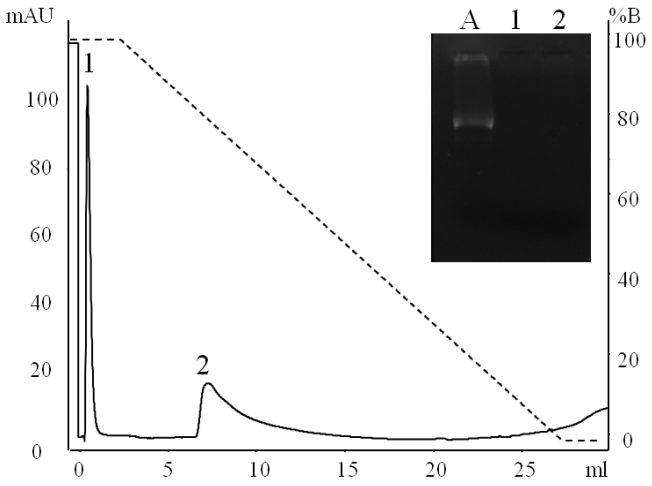

Figure 20. Decreasing linear gradient from 3.5 M to 0 M ammonium sulfate in 10 mM Tris-HCl and 10 mM EDTA, pH 8.0, at 1mL/min. In the agarose gel electrophoresis, the lane A represents the oc sample injected (100 µL), lane 1 content corresponds to peak 1 and lane 2 corresponds to peak 2.

4.3.3.3. pcDNA3-based plasmid supercoiled isoform

The pcDNA3-based plasmid supercoiled isoform was also evaluated under the elution conditions established. The decreasing linear gradient preformed during 25 minutes revealed that the unbound species were eluted in the first minutes (figure 21), during the flowthrough, at 3.5 M ammonium sulfate. The second peak, eluted during the linear gradient, corresponds majorly to the plasmid supercoiled isoform, as revealed in the agarose gel electrophoresis.

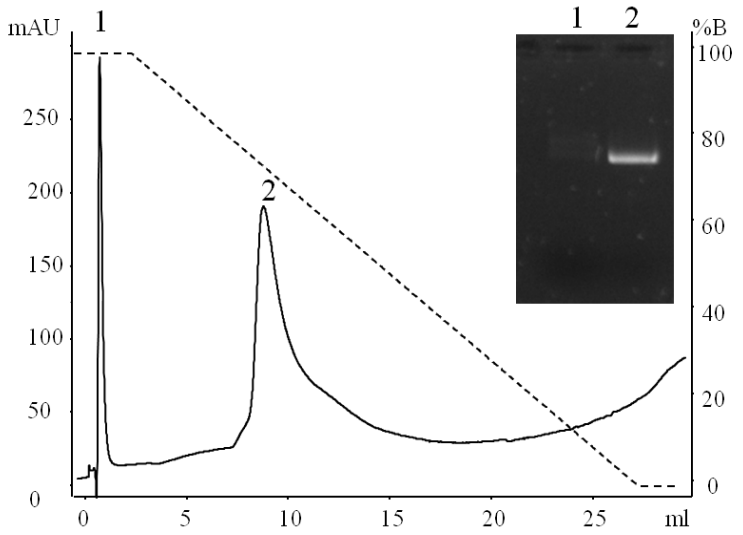

Figure 21. Decreasing linear gradient from 3.5 M to 0 M ammonium sulfate in 10 mM Tris-HCl and 10 mM EDTA, pH 8.0, at 1mL/min. The sc-enriched plasmid sample was pre-purified with NZYTech kit. In the agarose gel electrophoresis, lane 1 content corresponds to peak 1 and lane 2 corresponds to peak 2.

Thus, the results revealed that the L-histidine monolith specifically interacts with the sc pDNA isoform of the three plasmids with different sizes, while other plasmid topologies are not effectively retained in the modified monolith. This preferential interaction can be explained by the different base exposure degree, due to the deformations induced by the torsional strain, which are responsible for the supercoiled conformation (Tanigawa and Okada, 1998). Therefore, the bases of the sc isoform are more exposed and available to interact with the ligand (Strick *et al.*, 1998; Sousa *et al.*, 2005).

The retention behavior of each pDNA isoform suggests that it can be possible the separation of the respective sc pDNA when present in a mixture of isoforms.

4.4. Plasmid isoforms separation

Several stepwise gradients of ammonium sulfate were performed in order to optimize the separation of sc pDNA from the other topologies, using the three plasmids with different sizes. Additional washing steps were also performed between each experiment.

4.4.1. pVAX1-*LacZ*

In order to isolate the pVAX1-*LacZ* sc isoform, the L-histidine monolith was equilibrated with 2.99 M ammonium sulfate in 10 mM Tris-HCl buffer and 10 mM EDTA, pH 8.0, at a flow rate of 1 mL/min. Then, the pVAX1-*LacZ* plasmid sample pre-purified with the NZYTech kit was injected (100 µL). After injection, a first peak was eluted during the flowthrough, which corresponds to unbound species (figure 22 (A)). A second step was established with 0 M of ammonium sulfate for elution of bound species in a second peak. The fractions from each peak were recovered, desalted with concentrators and analyzed by agarose gel electrophoresis (figure 22 (B)). The results revealed that the elution of oc isoform occurred in the first peak (figure 22 (B), lane 1) with high ionic strength, and the sc isoform was achieved in the second peak with the decrease of ionic strength (figure 22 (B), lane 2).

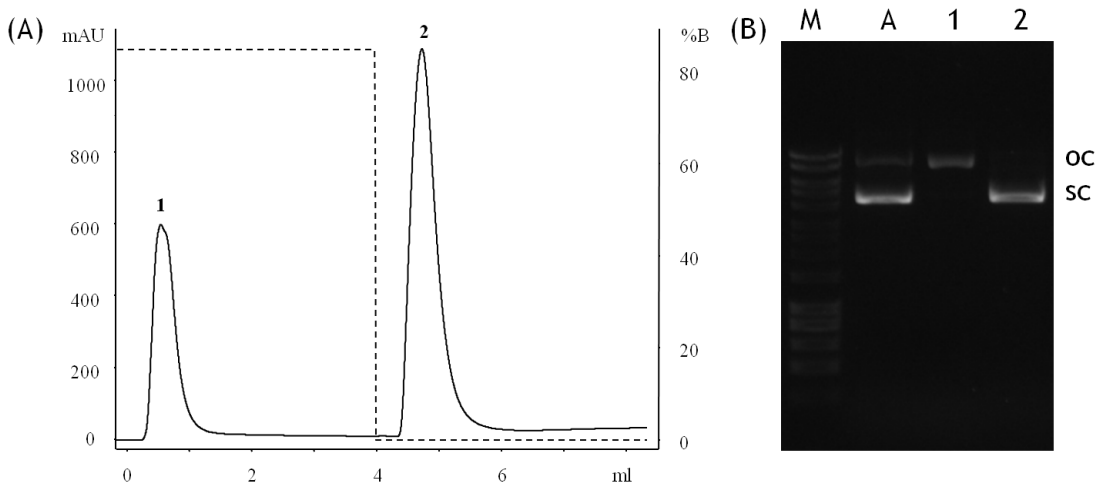

Figure 22. Separation of pVAX1-*LacZ* plasmid isoforms with the L-histidine monolith. **(A)** Chromatographic profile with the ammonium sulfate concentration optimized for the isoforms separation of pVAX1-*LacZ*, (stepwise gradient of 2.99 M and 0 M of ammonium sulfate). UV detection at 260 nm. Injection volume was 100 µL. **(B)** Agarose gel electrophoresis of each peak resultant from the respective chromatogram. Lane M: molecular weight marker; lane A: pVAX1-*LacZ* injected onto the column (oc+sc); lane 1: oc isoform; lane 2: sc isoform.

4.4.2. HPV-16 E6/E7

The previous elution strategy was also explored in order to achieve the isolation of the sc HPV-16 E6/E7 isoform. Curiously, the initial ammonium sulfate concentration used to equilibrate the L-histidine monolith and promote the sc pDNA retention was gently decreased. The column was equilibrated with 2.94 M ammonium sulfate in 10 mM Tris-HCl buffer and 10 mM EDTA, pH 8.0 and after the elution of the unbound species a second step with 0 M ammonium sulfate was performed to elute the bound species (figure 23 (A)). The fractions pooled from each peak were analyzed by agarose gel electrophoresis, reveling that the unbound species eluted in the first peak correspond to oc isoform (figure 23 (B), lane 1), and the second peak obtained at 0 M ammonium sulfate corresponds to the sc isoform (figure 23 (B), lane 2).

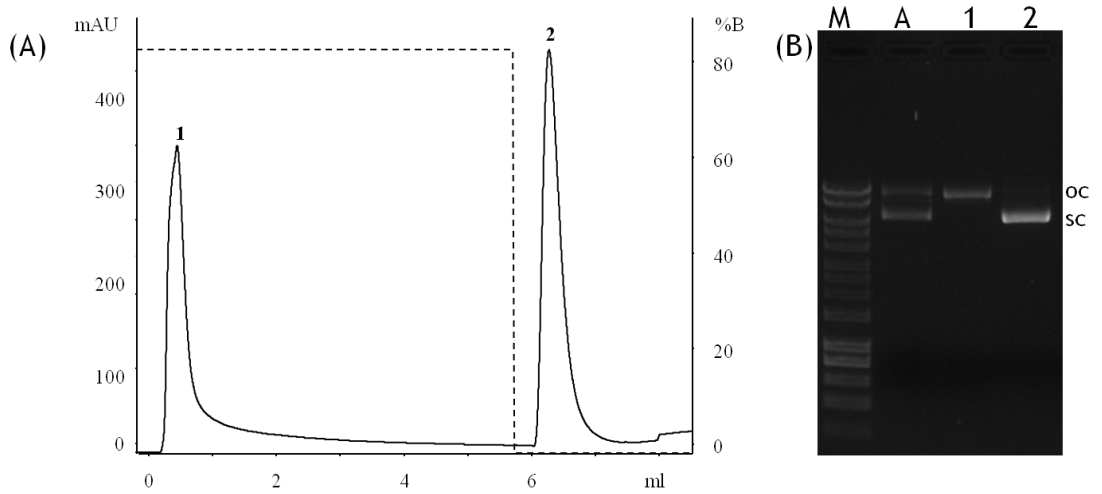

Figure 23. Separation of HPV-16 E6/E7 plasmid isoforms with the L-histidine monolith. **(A)** The stepwise gradient was optimized for the isoforms separation. The monolith was equilibrated with 2.94 M ammonium sulfate and after the elution of the first peak the buffer was changed to 0 M ammonium sulfate. UV detection at 260 nm. Injection volume was 100 µL. **(B)** Agarose gel electrophoresis of each peak resultant from the respective chromatogram. Lane M: molecular weight marker; lane A: HPV-16 E6/E7 injected onto the column (oc+sc); lane 1: oc isoform; lane 2: sc isoform.

4.4.3. pcDNA3-based plasmid

For the sc pcDNA3-based plasmid isoform separation, the modified monolith was first equilibrated with 2.91 M ammonium sulfate in 10 mM Tris-HCl buffer and 10 mM EDTA, pH 8.0. A first peak was eluted and the buffer was changed to 10 mM Tris-HCl buffer and 10 mM EDTA, pH 8.0, in order to decrease the ionic strength, and therefore, to promote the elution of bound species (figure 24 (A)). Agarose gel confirmed that the oc isoform was eluted in the

first peak (figure 24 (B), lane 1) and with the ionic strength decrease to 0 M ammonium sulfate, the sc isoform was eluted in the second peak (figure 24 (B), lane 2).

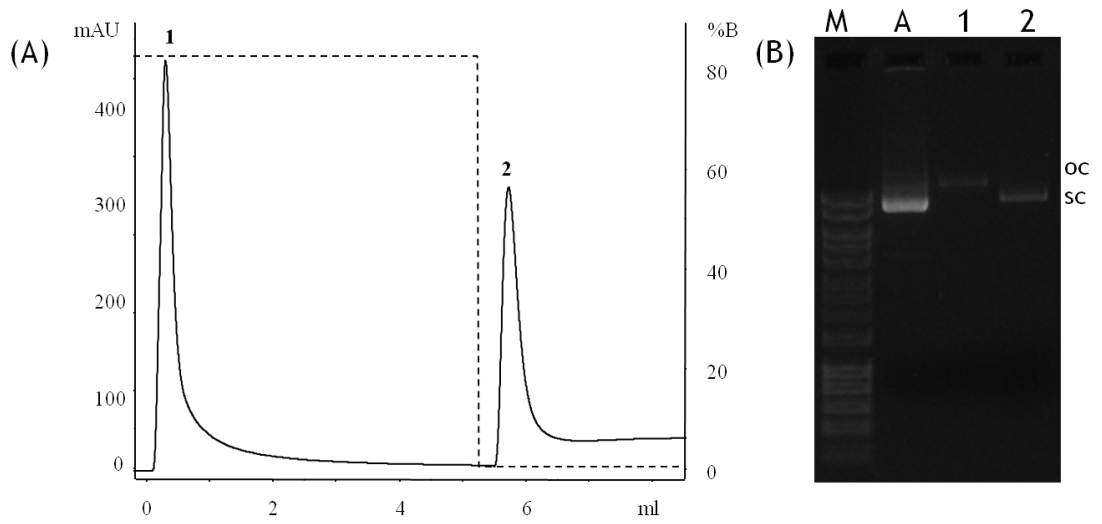

Figure 24. Separation of pcDNA3-based plasmid isoforms with the L-histidine monolith. **(A)** The stepwise gradient was optimized for the isoforms separation. The monolith was equilibrated with 2.91 M ammonium sulfate and after elution of unbound species the buffer was changed to 0 M ammonium sulfate. UV detection at 260 nm. Injection volume was 100 µL. **(B)** Agarose gel electrophoresis of each peak resultant from the respective chromatogram. Lane M: molecular weight marker; lane A: pcDNA3-based plasmid injected onto the column (oc+sc); lane 1: oc isoform; lane 2: sc isoform.

In the pVAX1-*LacZ*, HPV-16 E6/E7 and pcDNA3-based plasmid isoforms, the separation behaviour of oc and sc was similar; the oc isoform was eluted in the flowthrough, whereas the sc pDNA interacted with the L-histidine support. As previously mentioned, the different bases exposition degree, due to the supercoiling phenomenon, explains the preferential interaction occurring between the L-histidine monolith and the sc isoform of pVAX1-*LacZ*, HPV-16 E6/E7 and pcDNA3-based plasmid (Tanigawa and Okada, 1998; Strick *et al.*, 1998; Sousa *et al.*, 2005).Thus, pDNA structure and conformation might have a significant role on the interaction with the L-histidine monolithic support.

Hydrophobic interactions, namely π-π stacking/hydrophobic interactions, are predominant, as previously mentioned. However, van der Walls forces, bifurcate hydrogen bonds and hydrogen π interactions (Sousa *et al.*, 2011) can be involved in the sc pDNA biorecognition.

The plasmids under study present different molecular sizes, namely 6.05 kbp for pVAX1-LacZ, 8.70 kbp for HPV-16 E6/E7 and 14 kbp for pcDNA3-based plasmid. However, it is observed that the ideal ammonium sulfate concentration to separate the isoforms of each plasmid (2.99 M for pVAX1-LacZ, 2.94 M for HPV-16 E6/E7 and 2.91 M for pcDNA3-based plasmid) was decreasing while the plasmid molecular mass was increasing. When hydrophobic interactions are favored, the global hydrophobic character of the molecules slightly increases with the

molecular mass, which is in agreement with previous studies (Sousa *et al.*, 2009). Therefore, the larger plasmid is more hydrophobic, interacts more and needs less salt concentration to promote the retention in the support.

4.5. Effect of flow rates on plasmid isoforms separation

The use of higher flow rates on conventional matrices was limited due to swelling or shrinking of the constituent materials. Nonetheless, monoliths are promising matrices since they are rigid enough to avoid such problems. More rigid stationary phases resist to higher pressures and consequently higher linear velocities, enabling faster separation (Podgornik *et al.*, 2014). Considering the physical and chemical characteristics of monoliths, the separation selectivity should be maintained by employing higher flow rates.

Therefore, to verify the effect of flow rate on separation of plasmid isoforms, decreasing stepwise gradients of ammonium sulfate with pVAX1-*LacZ* were performed. The gradient and elution buffer conditions used to study the effect of flow rate was the same previously established to perform pVAX1-*LacZ* isoforms separation. As shown in figure 25 (A), (B) and (C) the stepwise gradients were performed at a flow rate of 1 mL/min, 2 mL/min and 4 mL/min. The purity of each plasmid isoform at different flow rates was revealed by agarose gel electrophoresis (figure 25 (D)) and as expected, lanes 1, 3 and 5 correspond to the oc isoform, and lanes 2, 4 and 6 correspond to the sc isoform that is isolated for all experiments. All chromatograms were normalized in function of the elution volume, although the experiment performed at 4 mL/min only take 2 min reducing substantially the chromatographic run time of the experiment.

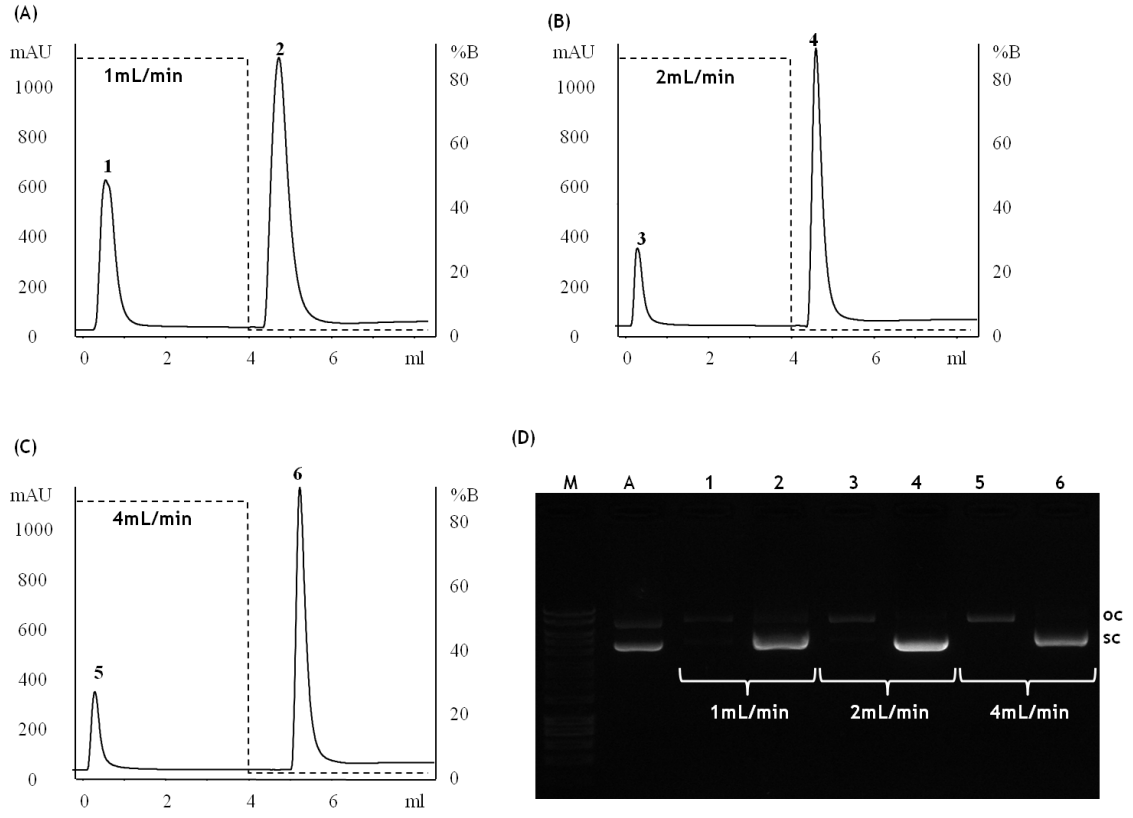

Figure 25. Flow rate effect on pVAX1-*LacZ* isoforms separation. Experiments were performed by decreasing stepwise gradient from 2.99 M to 0 M ammonium sulfate in 10 mM Tris-HCl and 10 mM EDTA, pH 8.0 at different flow rates **(A)** 1 mL/min, **(B)** 2 mL/min and **(C)** 4 mL/min). **(D)** Agarose gel electrophoresis of each peak resultant from the respective chromatogram. Lane M: molecular weight marker; lane A: pVAX1-*LacZ* sample injected onto the column (oc+sc, 100 µL); lanes 1, 3 and 5: oc isoform; lanes 2, 4 and 6: sc isoform.

The results reveal that the modified monolith promotes the pDNA isoforms separation with significant resolution, which is flow-unaffected in the studied range. Besides, the separation procedure can be accomplished much faster (Yamamoto and Kita, 2005), reducing the possible pDNA degradation that may result from longer chromatographic procedures.

4.6. Dynamic binding capacity

In the previous section was demonstrated that with flow rate variations, the plasmid isoforms separation remained unchanged. Therefore, in the dynamic binding capacity studies, to better characterize the modified monolith, it was also interesting to verify the flow rate effect on the monolith binding capacity. The experiments were carried out at 0.5 and 1 mL/min flow rate.

To perform the breakthrough experiments it was necessary to prepare a feedstock solution. After several alkaline lysis and pre-purification with the NZYTech kit a feedstock solution with 0.05 mg/mL of pVAX1-*LacZ* was obtained. The ionic strength of the feedstock solution was corrected for a concentration of 3.5 M ammonium sulfate. Then, the L-histidine monolith was equilibrated with 3.5 M ammonium sulfate in 10 mM Tris-HCl and 10 mM EDTA, pH 8.0. Determination of dynamic binding capacity was carried out by recording breakthrough curves at 260 nm, at 0.5 and 1 mL/min flow rate. The data was normalized and the dynamic binding capacity values were obtained by subtracting the value obtained under non-binding conditions and multiplying by the pDNA concentration. The ratio between the amount of bound pDNA and the support volume (0.34 mL) at 10%, 50% and 100% of the breakthrough was then calculated and the results are present in table 5, where 100% of the breakthrough corresponds to the total column saturation.

Table 5. Dynamic binding capacity results of L-histidine monolith at 0.5 and 1 mL/min. Breakthrough experiments were performed with a 0.05 mg/mL pDNA feedstock solution and the capacity was estimated at 10, 50 and 100% of breakthroughs.

Flow rate	DBC (mg/mL)		
	10%	50%	100%
1 mL/min	3.88	4.96	6.70
0.5 mL/min	4.20	6.24	11.03

The results revealed that for a lower flow rate (0.5 mL/min), a slightly increased on the modified monolith capacity for pDNA binding occurred. It is described that the purification and capacity are independent of the flow rate in the monolithic supports (Mihelic *et al.*, 2000; Podgornik and Krajnc, 2012). Thus, this result is related with the plasmid properties instead of monolith characteristics. The hypothesis that the binding capacity is in part dependent of the pDNA size and conformation (Haber *et al.*, 2004) is reinforced in this study and was previously mentioned in studies using a non-grafted monolith (Sousa *et al.*, 2011;

Bicho *et al.,* 2014), and a histidine-agarose matrix (Sousa *et al.,* 2007).The flow rate decrease implies slower chromatographic runs, and therefore, the contact time between the matrix and the pDNA increases, favoring the attainment of equilibrium and the area occupied by the pDNA becomes smaller since it becomes less extended at lower flow rates (Sousa *et al.,* 2011; Haber *et al.,* 2004).

The dynamic binding capacity achieved for L-histidine monolith was 3.88 mg/mL of column at 10% breakthrough, 1 mL/min with 0.05 mg/mL of plasmid feedstock solution. Comparing this result with the binding capacity obtained for a non-grafted monolith (2.19 mg/mL of column), the L-histidine monolith capacity increased in similar loading conditions (Sousa *et al.,* 2011). The increased binding sites of the monolith after ligand immobilization might explain the L-histidine monolith capacity results, since it is expected an increased capacity after grafting the monolith (Luscombe *et al.,* 2001).

The capacity of L-histidine monolith at 50% breakthrough (6.24 mg/mL) was twenty nine fold higher than the conventional histidine-agarose matrix (0.217 mg/mL), using identical loading conditions and pDNA concentration at 0.5 mL/min (Sousa *et al.*, 2006). This result is in accordance with the expectation, since one of the monolith advantages is to overcome the bottlenecks associated with conventional matrices, such as low binding capacity (Podgornik and Krajnc, 2012).

When compared with L-arginine monolith by using the same parameters but different elution strategy, the L-histidine monolith presents slightly higher binding capacity (6.70 mg/mL of column). The total capacity of L-arginine monolith determined by increasing the sodium chloride concentration was 5.18 mg/mL, using flow rate 1 mL/min and 0.05 mg/mL of plasmid feedstock solution (Soares *et al.,* 2013). Once the loading strategy developed for the L-arginine monolith used low salt concentrations, the capacity differences reported above can be related with a reduced intermolecular repulsion between the pDNA molecules, due to the high salt concentrations used in the L-histidine monolith, which instigate the pDNA molecules to pack more closely on the monolith surface (Bencina *et al.,* 2004).

The capacity results obtained with the L-histidine monolith are satisfactory when compared with other chromatographic supports. Monoliths grafted with suitable ligands are promising strategies to efficiently purify the sc pDNA isoform. Flow-unaffected resolution and high dynamic binding capacity, that enables fast chromatographic procedures with low back pressure (Yamamoto and Kita, 2005), are the monolith properties that can overcome some purification bottlenecks.

Chapter IV-Conclusions and future perspectives

The growing demand of DNA vaccines able to induce the appropriate type of immune responses led to the development of several strategies at different levels, specially, at pDNA purification level. Purification is one important step in order to achieve pDNA suitable for therapeutic applications. The innovations in the purification strategy include chromatographic matrices, such as the monoliths that overcome the problems associated with conventional matrices, and suitable ligands that specifically recognize and interact with the sc pDNA isoform, in order develop purification strategies that enable the sc pDNA isoform separation in a single step.

The analytical concept of affinity chromatography–analysis of the interactions of mobile molecules flowing over surface-immobilized ligands is mimicked by the SPR biosensor, which provides affinity analysis between immobilized amino acids and solution of pDNA. In this work, the ligands L-histidine, Im-benzyl-L-histidine and L-methyl-L-histidine, were immobilized on a carboxymethyl-dextran matrix and studied as affinity ligands for plasmid isoforms separation. The overall affinity with these ligands was significantly higher, $K_D > 10^{-8}$ M, with HEPES 10 mM at pH 7.4 as running buffer. Several running buffers were tested with different plasmid sizes and isoforms. However, no binding response was found using acid HEPES 100 mM, Tris-HCl and ammonium sulfate, due to unspecific interactions of pDNA with the reference cell. ^{1}H NMR experiments were performed to understand the lack of response using HEPES 100 mM, since it was expected to decrease the unspecific interactions. The ^{1}H NMR spectra indicated that the imidazole ring of L-histidine is more involved in binding, concluding that this running buffer affected the strength to the plasmids. Therefore, the ligand selected for immobilization on epoxy monolith was L-histidine, since the maximum response of plasmid isoforms was found for this amino acid while the substituents methyl and benzyl groups in the imidazole ring prevents interaction with pDNA isoforms.

L-histidine was immobilized on the monolithic matrix and when compared with a non-grafted epoxy monolith, the retention time and the chromatographic profile were altered, indicating that the L-histidine ligand was correctly immobilized and interacting with pDNA.

The L-histidine monolith allowed the successful separation of sc pDNA from the oc isoform, with pVAX1-*LacZ,* HPV-16 E6/E7 and pcDNA3-based plasmids, in a single step. The separation of plasmid isoforms was achieved with a decreasing stepwise gradient of ammonium sulfate concentration in the eluent. The global hydrophobic character of pDNA molecules slightly increased with the molecular mass. Thus, sc isoform and plasmids with high molecular weight presented strong interactions with the modified support. The efficiency of plasmid isoforms separation using the modified monolith was assessed by flow rate variations and the results remained unchanged.

In dynamic binding capacity experiments, the values obtained were satisfactory when compared to a histidine-agarose conventional matrix, a non-grafted monolith or a monolith modified with another amino acid. The maximum dynamic binding capacity achieved with the L-histidine monolith was 11.03 mg/mL of column, at 0.5 mL/min and 0.05 mg/mL of plasmid solution.

Thus, the modified L-histidine monolith used in this work can be a promising strategy to efficiently purify the sc pDNA with a therapeutic gene, such as the HPV16 E6/E7, from a lysate sample, with a desirable purity degree. After purification from a complex sample, the sc pDNA obtained should be tested in *in vitro* transfection studies to assess the expression of E6 and E7 proteins encoded in the plasmid. Moreover, in vivo studies could also be interesting to evaluate the immune responses (prophylactic and therapeutic responses) developed by the sc HPV16 E6/E7 pDNA.

Chapter V - Bibliography

Al-Dosari MS, Gao X. Nonviral gene delivery: principle, limitations, and recent progress. AAPS J 2009;11:671–81.

Amourache L, Vijayalakshmi MA. Affinity chromatography of kid chymosin on histidyl-Sepharose. J Chromatogr A 1984;303:285–90.

Benčina M, Podgornik A, Štrancar A. Characterization of methacrylate monoliths for purification of DNA molecules. J Sep Sci 2004;27:801–10.

Biasco L, Baricordi C, Aiuti A. Retroviral integrations in gene therapy trials. Mol Ther 2012;20:709–16.

Bicho D, Sousa A, Sousa F, Queiroz JA, Tomaz CT. Effect of chromatographic conditions and plasmid DNA size on the dynamic binding capacity of a monolithic support. J Sep Sci. 2014; doi: 10.1002/jssc.201400127.

Birnboim HC, Doly J. A rapid alkaline extraction procedure for screening recombinant plasmid DNA. Nucleic Acids Res. 1979; 7:1513-23.

Caramelo-Nunes C, Almeida P, Marcos JC, Tomaz CT. Aromatic ligands for plasmid deoxyribonucleic acid chromatographic analysis and purification: An overview. J Chromatogr A 2014;1327:1– 13.

Carnes AE, Hodgson CP, Williams J a. Inducible Escherichia coli fermentation for increased plasmid DNA production. Biotechnol Appl Biochem 2006;45:155–66.

Carnes AE, Luke JM, Vincent JM, Schukar A, Anderson S, Hodgson CP, et al. Plasmid DNA fermentation strain and process-specific effects on vector yield, quality, and transgene expression. Biotechnol Bioeng 2011;108:354–63.

Clonis YD, Labrou NE, Kotsira VP, Mazitsos C, Melissis S, Gogolas G. Biomimetic dyes as affinity chromatography tools in enzyme purification. J Chromatogr A 2000;891:33–44.

Coban C, Koyama S, Takeshita F, Akira S, Ishii KJ. Molecular and cellular mechanisms of DNA vaccines. Hum. Vaccin. 2008;:453–6.

Davis HL, Schleef M, Moritz P, Mancini M, Schorr J, Whalen RJ. Comparison of plasmid DNA preparation methods for direct gene transfer and genetic immunization. Biotechniques 1996;21:92-4.

Defilippis RA, Goodwin EC, Wu L, Dimaio D, Defilippis RA, Goodwin EC, et al. Endogenous Human Papillomavirus E6 and E7 Proteins Differentially Regulate Proliferation, Senescence, and Apoptosis in HeLa Cervical Carcinoma Cells. J Virol 2003;77:1551–63.

Diogo MM, Queiroz JA, Prazeres DMF. Assessment of purity and quantification of plasmid DNA in process solutions using high-performance hydrophobic interaction chromatography. J Chromatogr A 2003;998:109–17.

Doorslaer K Van, Burk RD. Evolution of Human Papillomavirus Carcinogenicity. Adv Virus Res 2010;77:41–62.

Dunne EF, Unger ER, Sternberg M, McQuillan G, Swan DC, Patel SS, et al. Prevalence of HPV infection among females in the United States. JAMA 2007;297:813–9.

Endres HN, Johnson JAC, Ross CA, Welp JK, Etzel MR. Evaluation of an ion-exchange membrane for the purification of plasmid DNA. Biotechnol Appl Biochem 2003;37:259–66.

Fabre JW, Grehan A, Whitehorne M, Sawyer GJ, Dong X, Salehi S, et al. Hydrodynamic gene delivery to the pig liver via an isolated segment of the inferior vena cava. Gene Ther 2008;15:452–62.

Ferraro B, Morrow MP, Hutnick N, Shin TH, Lucke CE, Weiner DB. Clinical applications of DNA vaccines: current progress. Clin Infect Dis 2011;53:296–302.

Ferreira GNM. Chromatographic Approaches in the Purification of Plasmid DNA for Therapy and Vaccination. Chem Eng Technol 2005;28:1285–94.

Ferreira GN, Monteiro GA, Prazeres DM, Cabral JM. Downstream processing of plasmid DNA for gene therapy and DNA vaccine applications. Trends Biotechnol 2000;18:380–8.

Fischer MJE. Amine Coupling Through EDC/NHS: A Practical Approach. Method Mol Biol 2010;627:55–73.

Ghanem A, Healey R, Adly FG. Current trends in separation of plasmid DNA vaccines: a review. Anal Chim Acta 2013;760:1–15.

Ginn SL, Alexander IE, Edelstein ML. Gene therapy clinical trials worldwide to 2012 – an update. 2013;15:65–77.

Gupta BD, Verma RK. Surface Plasmon Resonance-Based Fiber Optic Sensors: Principle, Probe Designs, and Some Applications. J Sensors 2009;1–12.

Haber C, Skupsky J, Lee A, Lander R. Membrane chromatography of DNA: conformation-induced capacity and selectivity. Biotechnol Bioeng 2004;88:26–34.

Haritha PN, Devi SKU, Nagaratna DP, Chaitanya PSK, Gunasekharan V. Gene Therapy- A Review. Int J Biopharm 2012;3:55–64.

Hoffman MM, Khrapov MA, Cox JC, Yao J, Tong L, Ellington AD. AANT: the Amino Acid-Nucleotide Interaction Database. Nucleic Acids Res 2004;32:D174–81.

Holmes DS, Quigley M. A Rapid Boiling Method for the Preparation of Bacterial Plasmids. Anal Biochem 1981;114:193–7.

Horn NA, Meek JA, Budahazi G, Marquet M. Cancer Gene Therapy Using Plasmid DNA : Purification o f DNA for Human Clinical Trials. Hum Gene Ther 1995;6:565–73.

Howie HL, Katzenellenbogen RA, Galloway DA. Papillomavirus E6 proteins. Virology 2009;384:324–34.

Howley PM, Lowry DR. Fields Virology: Papillomavirus. Knipe DM, Howley PM (eds) 2007.

Huang S, Kamihira M. Development of hybrid viral vectors for gene therapy. Biotechnol Adv 2013;31:208–23.

Iuliano S, Fisher JR, Chen M, Kelly WJ. Rapid analysis of a plasmid by hydrophobic-interaction chromatography with a non-porous resin. J Chromatogr A 2002;972:77–86.

Kamimura K, Suda T, Zhang G, Liu D. Advances in Gene Delivery Systems. Pharmaceut Med 2011;25:293–306.

Kay MA. State-of-the-art gene-based therapies: the road ahead. Nat Rev Genet 2011;12:316–28.

Kaufmann KB, Büning H, Galy A, Schambach A, Grez M. Gene therapy on the move. EMBO Mol Med 2013;5:1642–61.

Liao S-M, Du Q-S, Meng J-Z, Pang Z-W, Huang R-B. The multiple roles of histidine in protein interactions. Chem Cent J 2013;7:44.

Liu M . DNA vaccines: an historical perspective and view to the future. Immunol Rev. 2011;239:62–84.

Liu M. Immunologic basis of vaccine vectors. Immunity 2010;33:504–15.

Luscombe NM, Laskowski R a, Thornton JM. Amino acid-base interactions: a three-dimensional analysis of protein-DNA interactions at an atomic level. Nucleic Acids Res 2001;29:2860–74.

Lyddiatt A, O'Sullivan D A. Biochemical recovery and purification of gene therapy vectors. Curr Opin Biotechnol 1998;9:177–85.

Majka J, Speck C. Analysis of protein-DNA interactions using surface plasmon resonance. Adv Biochem Eng Biotechnol 2007;104:13–36.

Marti G, Ferguson M, Wang J, Byrnes C, Dieb R, Qaiser R, et al. Electroporative transfection with KGF-1 DNA improves wound healing in a diabetic mouse model. Gene Ther 2004;11:1780–5.

Merhar M, Podgornik A, Barut M, Žigon M, Štrancar A. Methacrylate monoliths prepared from various hydrophobic and hydrophilic monomers - Structural and chromatographic characteristics. J Sep Sci 2003;26:322–30.

McLaughlin-Drubin ME, Münger K. Oncogenic activities of human papillomaviruses. Virus Res 2009;143:195–208.

Mihelic I, Koloini T, Podgornik A, Strancar A. Dynamic Capacity Studies of CIM (Convective Interaction Media) Monolithic Columns. J High Resol Chromatogr 2000;23:39–43.

Morille M, Passirani C, Vonarbourg A, Clavreul A, Benoit J-P. Progress in developing cationic vectors for non-viral systemic gene therapy against cancer. Biomaterials 2008;29:3477–96.

Münger K, Phelps WC, Bubb V, Howley PM, Schlegel R. The E6 and E7 genes of the human papillomavirus type 16 together are necessary and sufficient for transformation of primary human keratinocytes. J Virol 1989;63:4417–21.

Naldini L. Ex vivo gene transfer and correction for cell-based therapies. Nat Rev Genet 2011;12:301–15.

Nomikou N, Feichtinger GA, Redl H, Mchale AP. Ultrasound-mediated gene transfer (sonoporation) in fibrin-based matrices : potential for use in tissue regeneration. J Tissue Eng Regen Med 2013. doi: 10.1002/term.1730.

Ongkudon CM, Danquah MK. Anion exchange chromatography of 4.2kbp plasmid based vaccine (pcDNA3F) from alkaline lysed E. coli lysate using amino functionalised polymethacrylate conical monolith. Sep Purif Technol 2011;78:303–10.

Patil SD, Rhodes DG, Burgess DJ. DNA-based therapeutics and DNA delivery systems: a comprehensive review. AAPS J 2005;7:E61–77.

Podgornik A, Krajnc NL. Application of monoliths for bioparticle isolation. J Sep Sci 2012;35:3059–72.

Podgornik A, Savnik A, Jančar J, Krajnc NL. Design of monoliths through their mechanical properties. J Chromatogr A 2014;1333:9–17.

Prather KJ, Sagar S, Murphy J, Chartrain M. Industrial scale production of plasmid DNA for vaccine and gene therapy: plasmid design, production, and purification. Enzyme Microb Technol 2003;33:865–83.

Prazeres DMF, Ferreira GNM. Design of flowsheets for the recovery and purification of plasmids for gene therapy and DNA vaccination. Chem Eng Process Process Intensif 2004;43:609–24.

Quaak SGL, Nuijen B, Haanen JB a G, Beijnen JH. Development and validation of an anion-exchange LC-UV method for the quantification and purity determination of the DNA plasmid pDERMATT. J Pharm Biomed Anal 2009;49:282–8.

Ren S, Li M, Smith JM, DeTolla LJ, Furth P a. Low-volume jet injection for intradermal immunization in rabbits. BMC Biotechnol 2002;2:10.

Ritzefeld M, Sewald N. Real-Time Analysis of Specific Protein-DNA Interactions with Surface Plasmon Resonance. J Amino Acids 2012;2012:816032.

Roque ACA, Lowe CR. Affinity chromatography: methods and protocols. History, perspectives, limitations and prospects. Zachariou M (ed) 2008

Saade F, Petrovsky N. Technologies for enhanced efficacy of DNA vaccines. Expert Rev Vaccines 2012;11:189–209.

Schiffman M, Castle PE, Jeronimo J, Rodriguez AC, Wacholder S. Human papillomavirus and cervical cancer. 2007;370:890–907.

Schlecht NF, Kulaga S, Robitaille J, Ferreira S, Santos M, Miyamura R a, et al. Persistent human papillomavirus infection as a predictor of cervical intraepithelial neoplasia. JAMA 2001;286:3106–14.

Soares A, Queiroz JA, Sousa F, Sousa A. Purification of human papillomavirus 16 E6/E7 plasmid deoxyribonucleic acid-based vaccine using an arginine modified monolithic support. J Chromatogr A 2013;1320:72– 79.

Sousa A, Bicho D, Tomaz C. Performance of a non-grafted monolithic support for purification of supercoiled plasmid DNA. J Chromatogr A 2011;1218:1701–6.

Sousa A, Sousa F, Prazeres DMF, Queiroz JA. Histidine affinity chromatography of homo-oligonucleotides. Role of multiple interactions on retention. Biomed Chromatogr 2009;23:745–53.

Sousa A, Sousa F, Queiroz JA. Advances in chromatographic supports for pharmaceutical-grade plasmid DNA purification. J Sep Sci 2012;35:3046–58.

Sousa A, Sousa F, Queiroz JA. Biorecognition of supercoiled plasmid DNA isoform in lysine-affinity chromatography. J Chromatogr B Analyt Technol Biomed Life Sci 2009;877:3257–60.

Sousa F, Cruz C, Queiroz JA. Amino acids-nucleotides biomolecular recognition: from biological occurrence to affinity chromatography. J Mol Recognit 2010;23:505–18.

Sousa F, Freitas S, Azzoni RA, Queiroz JA, Prazeres DMF. Selective purification of supercoiled plasmid DNA from clarified cell lysates with a single histidine–agarose chromatography step. Biotechnol Appl Biochem 2006;45:131–40.

Sousa F, Matos T, Prazeres DMF, Queiroz JA. Specific recognition of supercoiled plasmid DNA in arginine affinity chromatography. Anal Biochem 2008b;374:432–4.

Sousa F, Prazeres DMF, Queiroz JA. Affinity chromatography approaches to overcome the challenges of purifying plasmid DNA. Trends Biotechnol 2008a;26:518–25.

Sousa F, Prazeres DMF, Queiroz JA. Dynamic binding capacity of plasmid DNA in histidine–agarose chromatography. 2007;21:993–8.

Sousa F, Queiroz JA. Circular dichroism investigation of the effect of plasmid DNA structure on retention in histidine chromatography. Arch Biochem Biophys 2007;467:154–62.

Sousa F, Tomaz CT, Queiroz JA. Separation of supercoiled and open circular plasmid DNA isoforms by chromatography with a histidine–agarose support. Anal Biochem 2005;343:183–5.

Stadler J, Lemmens R, Nyhammar T. Plasmid DNA purification. J Gene Med 2004;6 Suppl 1:S54–66.

Strick TR, Allemand JF, Bensimon D, Croquette V. Behavior of supercoiled DNA. Biophys J 1998;74:2016–28.

Tanigawa M, Okada T. Atomic force microscopy of supercoiled DNA structure on mica. Anal Chim Acta 1998;365:19–25. Thomas CE, Ehrhardt A, Kay M a. Progress and problems with the use of viral vectors for gene therapy. Nat Rev Genet 2003;4:346–58.

Thillaivinayagalingam P, Gommeaux J, McLoughlin M, Collins D, Newcombe AR. Biopharmaceutical production: Applications of surface plasmon resonance biosensors. J Chromatogr B 2010;878:149–53.

Thomas CE, Ehrhardt A, Kay MA. Progress and problems with the use of viral vectors for gene therapy. Nat Rev Genet 2003;4:346–58.

Tota JE, Chevarie-Davis M, Richardson L A, Devries M, Franco EL. Epidemiology and burden of HPV infection and related diseases: implications for prevention strategies. Prev Med 2011;53 Suppl 1:S12–21.

Tolmachov O. Gene therapy of cancer. Designing Plasmid Vectors. Wolfgang W, Stein US (eds) 2009;117–29.

Trottier H, Burchell AN. Epidemiology of mucosal human papillomavirus infection and associated diseases. Public Health Genomics 2009;12:291–307.

Uchida M, Natsume H, Kobayashi D, Sugibayashi K, Morimoto Y. Effects of particle size, helium gas pressure and microparticle dose on the plasma concentration of indomethacin after bombardment of indomethacin-loaded poly-L-lactic acid microspheres using a Helios gun system. Biol Pharm Bull 2002;25:690–3.

Vlakh EG, Tennikova TB. Preparation of methacrylate monoliths. J Sep Sci 2007;30:2801–13.

Walther W, Stein U. Viral vectors for gene transfer: a review of their use in the treatment of human diseases. Drugs 2000;60:249–71.

Williams J, Carnes AE, Hodgson CP. Plasmid DNA vaccine vector design: impact on efficacy, safety and upstream production. Biotechnol Adv 2009a;27:353–70.

Williams J, Luke J, Langtry S, Anderson S, Hodgson CP, Carnes AE. Generic plasmid DNA production platform incorporating low metabolic burden seed-stock and fed-batch fermentation processes. Biotechnol Bioeng 2009b;103:1129–43.

Williams J. Vector Design for Improved DNA Vaccine Efficacy, Safety and Production. Vaccines 2013;1:225–49.

Wirth T, Ylä-Herttuala S. History of gene therapy. Gene 2013;525:162–9.

Woo MS, Ohta Y, Rabinovitz I, Stossel TP, Blenis J. Ribosomal S6 Kinase (RSK) Regulates Phosphorylation of Filamin A on an Important Regulatory Site. 2004;24:3025–35.

Yamamoto S, Kita A. Theoretical background of short chromatographic layers. J Chromatogr A 2005;1065:45–50.

Zhaohui P. Current Status of Gendicine in China : Recombinant Human Ad-p53 Agent for Treatment of Cancers. Hum Gene Ther 2005;16:1016–27.

Chapter VI – Appendix: submitted manuscript

Purification of supercoiled plasmid DNA from different plasmids using L-histidine monolith

L.F.A. Amorim, F. Sousa, J.A. Queiroz, C. Cruz, A. Sousa*

CICS-UBI – Centro de Investigação em Ciências da Saúde, Universidade da Beira Interior, Av. Infante D. Henrique,6200-506 Covilhã, Portugal

*corresponding author:
Ângela Sousa
CICS-UBI – Centro de Investigação em Ciências da Saúde, Universidade da Beira Interior, Av. Infante D. Henrique, 6200-506 Covilhã, Portugal
Tel.: +351 275 329 002; Fax: +351 275 329 099
E-mail: angela@fcsaude.ubi.pt

Abstract

The growing demand of pharmaceutical grade plasmid DNA suitable for bio therapeutic applications fostered the development of new purification strategies.

The surface plasmon resonance technique was employed for a fast screening of histidine and derivatives, Im-benzyl-L-histidine and L-methyl-L-histidine as potential ligands for the biorecognition of three plasmids with different sizes (6.05, 8.70 and 14 kilo base pairs). The binding analyses were performed with different isoforms of each plasmid (supercoiled, open circular and linear) separately. The results revealed that the overall affinity of plasmids to histidine ligand and their derivatives was high ($K_D > 10^{-8}$ M^1) and the highest affinity was found for HPV-16 E6/E7/L-histidine interaction, with a K_D value of $3.34 \times 10^{-10} \pm 0.0209$ M.

Therefore, the L-histidine ligand was selected to combine its specificity and selectivity with the versatility of monolithic supports. Chromatographic studies of the L-histidine monolith were also performed with the aforementioned samples. In general, the supercoiled isoform had strong interactions with the support. The separation of plasmid isoforms was achieved by decreasing the ammonium sulfate concentration in the eluent. The efficiency of plasmid isoforms separation remained unchanged with flow rate variations. The binding capacity for plasmid DNA achieved with the L-histidine monolith was twenty nine fold higher than the obtained with conventional L-histidine matrix in previous studies.

Overall, the combination of L-histidine ligand with the monolithic support can be a promising strategy to purify the supercoiled isoform from different plasmids with suitable purity degree for pharmaceutical applications.

Keywords: Affinity ligands; Dynamic binding capacity; L-histidine monolith; Supercoiled plasmid DNA; Surface plasmon resonance.

1. Introduction

Over the last years, the demand of clinical-grade plasmid DNA (pDNA), to be used as a biotherapeutic agent, has increased due to its safety, versatility and low risk of immunogenic reactions when compared with the viral vectors approach [1].

Large-scale and cost-effective production of pDNA is a constant challenge to the biotechnological industry. The pDNA quality has to be maintained in order to meet the international regulatory agency requirements. Thus, for the successful expression of the encoded protein, the final plasmid sample should be free from host impurities and present more than 97 % of the supercoiled (sc) isoform [2].

Several chromatographic techniques have been exploited over the years to achieve the sc pDNA separation from other non-effective topoisomers and host impurities. Anion exchange chromatography [3], size exclusion chromatography [4], hydrophobic interaction chromatography [5] were commonly used with that purpose. However, these chromatographic strategies did not achieve efficient pDNA isoforms separation from the lysate sample, due to their structural and chemical similarities. On the other hand, the application of affinity chromatography allows the reduction of the purification steps needed to accomplish the final purified product [6] without compromising its quality, developing a specific biorecognition by the sc pDNA isoform [7].

Affinity chromatography can be used to specifically isolate pDNA, based on biological function or individual chemical structure of a specific ligand immobilized on the chromatographic matrix [8]. However, a suitable ligand has to be chosen to improve the selectivity for pDNA [9]. Multiple studies have described the successful use of amino acids as affinity ligands to separate pDNA isoforms with conventional agarose-matrices, namely arginine [10], lysine [11], and histidine [12]. Therefore, characterization studies of amino acid ligands with plasmid molecules are important tools to understand the biorecongnition mechanisms and the affinity interactions that can be developed between the ligand and the target molecule.

Moreover, Surface Plasmon Resonance (SPR) biosensor has been used to yield information regarding amino acid immobilized on surface and pDNA molecules. Interaction of nucleotides with several amino acids, such as lysine, arginine [14] and histidine [15], has already been reported and the binding responses were analyzed in order to understand the underlying mechanisms of biorecognition. A recent study,

employing SPR, exploited the interaction between immobilized L-arginine and different plasmids topologies to provide further knowledge for affinity chromatography purification [16].

Nuclear magnetic resonance (NMR) was also used to study structural aspects of chromatographic supports with the aforementioned amino acids [14]. These techniques can be employed in fast screening of suitable ligands to be applied in chromatographic experiments.

Beyond the study and choice of a ligand with high selectivity, also a suitable chromatographic support should be selected. Low capacity and low diffusivity for pDNA are disadvantages that remain in the aforementioned conventional matrices [17]. These problems are overcome by monoliths, which are considered advantageous supports to purify large biomolecules due to their tridimensional characteristics of interconnected pores, which allows good mass transfer properties and binding capacity [18].

Thus, the aim of this work was to perform a fast screening by SPR technique of L-histidine, Im-benzyl-L-histidine and L-methyl-L-histidine as possible affinity ligands for immobilization on a monolithic support. Additionally, the modified monolith was characterized in terms of functionality, elution strategy (type and salt concentration, type of buffer and pH effect), recognition of sc pDNA isoform of different plasmids and dynamic binding capacity.

2. Experimental

2.1 Materials

All solutions, used in SPR and chromatographic experiments, were freshly prepared using deionized ultra-pure grade water, purified with a Milli-Q system from Millipore (Billerica, MA, USA) and analytical grade reagents were used. All experiments were conducted at room temperature unless otherwise stated.

The 6.05 kbp pVAX1-*LacZ* plasmid was provided by Invitrogen (Carlsband, CA, USA). The 8.702 kbp HPV-16 E6/E7 plasmid, Addgene plasmid 8641 [19], and the 14 kbp pcDNA3-myc-FLNa S2152A plasmid, Addgene plasmid 8983, (pcDNA3-based plasmid) [20] were provided by Addgene (Cambrige, USA). The Hind III restriction enzyme, the GreenSafe Premium and the NZYTech Plasmid Maxi Columns were purchased from NZYTech (Lisbon, Portugal). Hyper Ladder I (Bioline, London, UK) was used as a DNA molecular weight marker.

The elution buffers were filtered through a 0.20 μm pore size membrane (Schleicher Schuell, Dassel, Germany) and degassed ultrasonically. Sodium chloride and ammonium sulfate were purchased from Panreac (Barcelona, Spain), tris(hydroxymethyl) aminomethane (Tris) from Merck (Darmstadt, Germany), and 4-(2-hydroxyethyl)-1-piperazineethanesulfonic acid (HEPES) and borate buffer were from Sigma Aldrich (St.Louis, MO, USA). Chromatographic experiments were carried out with monolithic disks of 0.34 mL bed volume (average pore size of 1500 nm in diameter) modified with histidine amino acid, which were kindly provided by BIA Separations (Ajdovščina, Slovenia).

2.2 Methods

2.2.1 Plasmids amplification by bacterial production

The pVAX1-*LacZ,* HPV-16 E6/E7 and pcDNA3-based plasmids amplification was performed by autonomous replication in *Escherichia coli* (*E. coli*) DH5α. The fermentation was carried out overnight at 37 ºC under 250 rpm shaking. Terrific Broth medium was used (20 g/L tryptone, 24 g/L yeast extract, 4 mL/L glycerol, 0.017 M KH_2PO_4 and 0.072 M K_2HPO_4) and in order to ensure the exclusive growth of

transformed cells, antibiotics were applied as selection markers. The culture medium was supplemented with 30 µg kanamycin/mL for cells transformed with pVAX1-*LacZ*, 100 µg ampicillin/mL for cells transformed with HPV-16 E6/E7 and 100 µg ampicillin/mL and 50 µg Neomycin/mL for cells transformed with pcDNA3-based plasmid. Growth was suspended at the log phase [OD_{600}~7] and cell pellets recovered by centrifugation were stored at – 20 ºC.

2.2.2 Alkaline lysis and pre-purification of pDNA samples

The lysis of pelleted bacteria was performed by a modified alkaline lysis method and the plasmid samples were pre-purified according to NZYTech Plasmid Maxi kit manufacturer's instructions. Briefly, after the alkaline lysis, the lysate is cleared by centrifugation, and then, the impurities are removed by a medium-salt wash after plasmid DNA binding to the NZYTech anion-exchange resin. pDNA elution occurs when a high-salt buffer is added. In last, the pDNA is concentrated by isopropanol precipitation.

2.2.3 Plasmid isoforms preparation

Three plasmid conformations, namely sc, linear (ln) and open circular (oc) isoforms of each plasmid, were prepared to be used in SPR and chromatographic experiments. The sc-enriched samples of pVAX1-*LacZ*, HPV-16 E6/E7 and pcDNA3-based plasmid directly obtained by alkaline lysis, as described above, were also used to prepare ln and oc pure samples. In order to convert sc into oc isoform, the plasmids were incubated at room temperature, and monitored over the time by agarose electrophoresis, until total sample conversion (about 3 days). To prepare ln samples of each plasmid, an enzymatic digestion with Hind III at 37ºC was performed.

2.2.4 Agarose gel electrophoresis

The conformation and the purity of different samples used for this study, as well as the fractions recovered in each chromatographic experiment, were analyzed by horizontal electrophoresis using 15-cm-long 0.8% agarose gels (Hoefer, San Francisco, CA, USA), stained with GreenSafe Premium (1µg/mL). Electrophoresis was performed at 100 V, for 30 minutes, with TAE buffer (40 mM Tris base, 20 mM acetic acid and 1 mM EDTA, pH 8.0). Agarose gels were revealed under UV light in a transilluminator system (ILC Lda, Lisbon, Portugal).

2.2.5 SPR measurements

All SPR experiments were performed using a BIAcore T200 system and the BIAevaluation software was used for data analysis.

L-Histidine, Im-benzyl-L-histidine and L-methyl-L-histidine, were immobilized on a carboxymethylated dextran-coated sensor chip (CM5 research grade). After detector normalization with BIAnormalizing solution (70% glycerol, GE Healthcare), the amino acids were covalently attached to the surface of this sensor chip, using the amine-coupling method. The running buffer for ligands immobilization was HBS-EP (10 mM HEPES, 150 mM NaCl, 0.05% P20 surfactant, 3 mM EDTA, pH 7.4), purchased from Biacore. The sensor chip surface was activated with 1-ethyl-3-(3-dimethylaminopropyl) carbodiimide (EDC) and N-hydroxysuccinimide (NHS). L-histidine, Im-benzyl-L-histidine and L-methyl-L-histidine, were dissolved in 100 mM borate solution, at pH 9 with a final concentration of 340 mM, 21 mM and 350 mM, respectively. The sensor surface was blocked with ethanolamine and injections with HBS-EP were performed to stabilize the baseline.

The CM5 chip flow cell 1 was left unmodified to act as reference and samples were tested for binding in duplicate.

To collect affinity data, samples of pVAX1-*LacZ*, HPV-16 E6/E7 and pcDNA3-based plasmid isoforms (sc, oc and ln), separately, in HEPES 10 mM pH 7.4 were injected at concentrations ranging from 0.55µM to 4.3×10^{-6} µM. After each run the plasmid was removed from the surface without requiring a regeneration solution.

A steady state affinity study was performed with the binding data collected, averaging the resonance unit values (RU) in the plateau region of the sensograms over 350-400 s and the data were fit to a 1:1 interaction model.

2.2.6 ^{1}H NMR experiments

The L-histidine 0.34 M was dissolve in solution of HEPES (10 mM and 100 mM) with 10 % D_2O at pH 7.4. The proton resonances of L-histidine were first assigned. The ^{1}H NMR spectra were recorded at a temperature of 298 K on a Bruker Avance III 600 MHz spectrometer operating at 14.09 Tesla observing ^{1}H at 600.13 MHz. The spectrometer was equipped with a four-channel Quadruple (QXI) resonance probe and all spectra were processed with the software topspin 3.1 (Bruker).

2.2.7 Chromatographic experiments

Chromatographic experiments were performed in a AKTA Purifier system (GE Healthcare Biosciences Uppsala, Sweden) and the control system software was Unicorn version 5.11.

L-histidine amino acid was immobilized in a CIM^{TM} epoxy disk by pumping the ligand solution (1 g L-histidine dissolved in 4 mL of NaOH) through the monolithic disk followed by 72h thermostating of the column at 60 ºC. Finally, the monolithic disk was washed with water and the remaining epoxy groups were hydrolyzed in diol groups by soaking with 0.5 M H_2SO_4 for 30 min.

L-histidine monolith was equilibrated, at a flow rate of 1 mL/min, with appropriate binding buffer, as described below. Plasmid samples pre-purified with the NZYTech kit were injected (100 µL) at the same flow rate. Linear gradients were performed by decreasing the ammonium sulfate concentration from 3.5 to 0 M and increasing the sodium chloride concentration from 0 to 3 M. Afterwards, stepwise gradient of decreasing ammonium sulfate concentration was also explored to separate isoforms of pVAX1-*LacZ*, HPV-16 E6/E7 and pcDNA3-based plasmid. All chromatographic runs were monitored at 260 nm and the pooled fractions were concentrated and desalted for further analysis by agarose electrophoresis.

The monolith regeneration was conducted after some chromatographic experiments by washing with deionized water followed by 5 column volumes of 0.5 M NaOH at a flow rate of 0.5 mL/min. Finally, L-histidine monolith was again thoroughly washed with the deionized water until the proper pH is restored.

2.2.8 Dynamic binding capacity

Breakthrough experiments were conducted to assess the L-histidine monolith dynamic binding capacity for pDNA. A pVAX1-*LacZ* solution with 0.05 mg/mL was prepared to perform the monolith overload at the flow rates of 1 mL/min and 0.5 mL/min. Briefly, L-histidine monolith was equilibrated with 3.5 M ammonium sulfate in 10 mM Tris-HCl buffer and 10 mM EDTA, pH 8. After the column saturation with the pDNA prepared in the same binding buffer, the elution was obtained by decreasing the ammonium sulfate concentration to 0 M. Dynamic binding capacity assessment was carried out by the amount of bound pDNA per mL of support at 10%, 50% and 100% of breakthrough curves and subtracting the respective value obtained under non-binding conditions.

3. Results and discussion

3.1 SPR binding experiments

L-histidine, Im-benzyl-L-histidine and L-methyl-L-histidine were immobilized on a carboxymethylated dextran-coated sensor chip via amine coupling [21]. After immobilization, different running buffers were tested such as 10 mM Tris-HCl, pH 8, 500 mM ammonium sulfate in 10 mM Tris-HCl, pH 8, 500 mM ammonium sulfate and 100 mM of HEPES, pH 7.4. However no signal was detected when plasmid isoforms were injected.

The affinity data was collected with running buffer HEPES 10 mM, pH 7.4 when different plasmid isoforms were injected over the surfaces. The steady-state results are carried out by averaging the resonance unit values (RU) in the plateau region of the sensorgrams over a 350 to 400 s. The SPR binding profile was identical for all complexes indicating rapid association and dissociation for steady-state binding studies (examples of sensorgrams and binding curves in supplementary information). Even with running buffer 10 mM of HEPES pH 7.4 non-specific binding was detected between the reference surface (blocked dextran) with the ligand surfaces specially Im-benzyl-L-histidine and L-methyl-L-histidine indicating that plasmid isoforms have significant affinity for blocked dextran. This makes affinity calculations of some plasmid isoforms unfeasible (see Table 1). The equilibrium dissociation constants (K_D) presented in Table 1 are significantly high (10^{-10}-10^{-8} M range) with the highest affinity found for HPV-16 E6/E7 linear/L-histidine, 3.34×10^{-10} ±0.0209 M, while the pcDNA3-based supercoiled plasmid showed the lowest binding affinity. Also the results suggest a non-linear tendency between plasmid size and binding, since the linear pcDNA3-based plasmid have lowest affinity than linear HPV-16 E6/E7 plasmid. HEPES acid was the running buffer used which promoted less unspecific binding with blank cell. However for some cases like HPV-16 E6/E7 sc especially in L-methyl-L-histidine the profile obtained shows that the pDNA binds to L-methyl-L-histidine but the dissociation starts right away at 350s (data not shown).

Since it has been described that increasing the running buffer concentration might help decreasing unspecific interactions [22], several injections were performed with HEPES 100 mM, pH 7.4. No binding responses were also detected. In order to

understand the concentration effect of HEPES buffer in the interaction with L-histidine, ^{1}H NMR experiments were performed in solutions of HEPES 10 mM and HEPES 100 mM at pH 7.4. L-histidine was dissolved in solution of HEPES (10 mM and 100 mM) with 10 % D_2O at pH 7.4. The ^{1}H NMR spectra shows chemical shift variation in imidazole protons only in HEPES 100 mM (data not shown). Only the imidazole ring of L-histidine interacted with HEPES buffer 100 mM meaning that maybe this ring is not free to interact with other molecules. This might also be the explanation for the results in Table 1 using running buffer HEPES 10 mM pH 7.4. Also the main interaction between the plasmid isoforms and the ligands seems to be mostly through the imidazole ring [23]. This can explain the decrease of the affinity for the L-histidine derivatives with methyl and benzyl groups replace in position 1 in the imidazole ring. In general, the maximum response was found for L-histidine surface, when compared with its derivatives indicating that L-histidine might be a promising ligand for purification of pVAX1-*LacZ*, HPV-16 E6/E7 and pcDNA3-based plasmids. Moreover, an L-histidine-agarose matrix was already employed in the purification of pVAX1-*LacZ* sc isoform [24]. However, due to the bottlenecks associated with conventional matrices, the conjugation of L-histidine ligand with other chromatographic supports, such as monoliths, can be a more promising and efficient strategy.

3.2 Preliminary chromatographic experiments

The use of monoliths has increased in the last years, since they overcome many of the conventional matrices limitations. Thus, the combination of the specificity and selectivity of the L-histidine ligand with the versatility of monolithic supports can be a promising strategy to develop a suitable chromatographic support for sc pDNA purification.

Several preliminary chromatographic tests were performed in order to verify the modification of L-histidine monolith and to choose suitable conditions for the plasmid retention (Fig. 1). First of all, a decreasing linear gradient of ammonium sulfate, from 3.5 M to 0 M in 10 mM Tris-HCl and 10 mM EDTA pH 8.0, was tested with the non-grafted epoxy monolith, loading a pVAX1-*LacZ* plasmid sample (100 µL) at 1mL/min. The binding condition allowed the pDNA retention to the epoxy groups, being eluted during the linear gradient (data not shown). Then, the same strategy was applied to the L-histidine monolith in order to compare the elution profile with the one achieved with

the non-grafted monolith. The results showed a different elution profile as well as a different retention time for pDNA, which indicates that the different elution behavior is due to the presence of L-histidine ligand on the modified monolith (Fig. 1 (A)).

Afterwards, the influence of elution buffer composition in the plasmid retention to the L-histidine monolith was studied in order to select the elution strategy that should be used for further separation of plasmid isoforms. Since HEPES 10 mM was the most suitable buffer to perform the SPR experiments, the same elution gradient with ammonium sulfate in 10 mM HEPES and 10 mM EDTA pH 7.4 was evaluated and the elution profile was similar to the previous result with the Tris-HCl buffer (data not shown).

Previous studies reported the pH influence on oligonucleotides retention to the histidine-agarose matrix [25]. Therefore, the pH effect in the plasmid retention was also a parameter evaluated in these preliminary tests. A solution with 3.5 M $(NH_4)_2SO_4$ in 10 mM Tris-HCl buffer and 10 mM EDTA, pH 6.0 was prepared and a decreasing linear gradient was established from 3.5 M to 0 M. The obtained result is presented in Fig. 1 (B) and reveals a slight increase on the plasmid retention time (5.59) when compared with the same assay performed at pH 8.0 (5.21). This behavior suggests that besides the predominant action of hydrophobic interactions, owing to the salt concentration used, other interactions can be present, affecting the plasmid retention. Given that the pKa of L-histidine is 6.5, acidic pH environment can favor the protonation of imidazole ring, which enables the additional involvement of ring stacking interactions and cation π interactions with plasmid aromatic bases [23], especially with guanine [25,26].

Finally, an increasing linear gradient from 0 to 3 M of sodium chloride in 10 mM Tris-HCl and 10 mM EDTA, pH 8.0 was also tested (Fig.1 (C)). After pDNA injection onto the L-histidine monolith, all species were eluted in a single peak in the flowthrough, at 0 M of sodium chloride. Therefore, these conditions disfavor the plasmid retention, indicating that ionic interactions are not established between the pDNA and the modified monolith.

3.3 Plasmid isoforms separation

Similarly to what was explored in SPR study, also in the characterization of the chromatographic support, a screening of different isoforms (oc, sc and ln) of pVAX1-*LacZ*, HPV-16 E6/E7 and pcDNA3-based plasmid, was performed. According to the

preliminary studies, the decreasing linear gradient from 3.5 M to 0 M $(NH_4)_2SO_4$ in 10 mM Tris-HCl and 10 mM EDTA pH 8.0 was the elution condition chosen. The results revealed that only the sc isoform of the three plasmids binds effectively to the histidine monolith under the conditions established, while the ln and oc isoforms did not show an effective retention, being mostly eluted in the flowthrough (data not shown). The retention behavior of each pDNA isoform suggests that it can be possible the separation of the respective sc pDNA when present in a mixture of isoforms. Therefore, some experiments were performed to find the best strategy to separate the pDNA isoforms of different plasmids by using decreasing stepwise gradients of ammonium sulfate. The chromatographic profile of the sc pDNA purification from plasmid samples pre-purified with the NZYTech kit is shown in Fig. 2. First, the L-histidine monolith was equilibrated with 2.99 M, 2.94 M or 2.91 M ammonium sulfate in 10 mM Tris-HCl buffer and 10 mM EDTA, pH 8.0, to the pVAX1-*LacZ* (Fig.2 (A)), HPV-16 E6/E7 (Fig.2 (B)) and pcDNA3-based plasmid (Fig.2 (C)) assays, respectively, at a flow rate of 1 mL/min. After the injection of the respective plasmid (100 µL), a first peak was obtained, corresponding to unbound species. Then, a second step was established with 0 M of ammonium sulfate for elution of bound species in a second peak. Additional washing steps were performed between each experiment. The fractions pooled from each peak were analyzed by agarose gel electrophoresis (Fig.2 (D)). The elution of oc isoforms occurred in the first peak (Fig.2 (D), lanes 1,3 and 5) with high ionic strength, and the sc isoform of each plasmid was recovered in the second peak with the decrease of ionic strength (Fig.2 (D), lanes 2, 4 and 6).

The preferential interaction of the L-histidine monolith with the sc isoform of each plasmid can be explained by the different bases exposure degree. The supercoiling phenomenon is a consequence of deformations induced by the torsional strain [27], and as a consequence, the bases of the sc isoform are more exposed and available to interact with the ligand than the bases of the oc isoform [12] [28]. As a matter of fact, besides the predominance of hydrophobic interactions, namely ring stacking/hydrophobic interactions, other elementary and non-covalent forces can be involved in the sc pDNA biorecognition, such as van der Waals forces, bifurcate hydrogen bonds and hydrogen π interactions [17].

The plasmids under study present different molecular sizes, namely 6.05 kbp for pVAX1-*LacZ*, 8.70 kbp for HPV-16 E6/E7 and 14 kbp for pcDNA3-based plasmid. However, it is observed that the ideal ammonium sulfate concentration to separate the

isoforms of each plasmid (2.99 M for pVAX1-*LacZ*, 2.94 M for HPV-16 E6/E7 and 2.91 M for pcDNA3-based plasmid) was decreasing while the plasmid molecular mass was increasing (Fig. 2). These results are in agreement with previous works, which describe that when hydrophobic interactions are favored, the global hydrophobic character of the molecules slightly increases with the molecular mass [25]. Therefore, the larger plasmid is the most hydrophobic, interacts more and so the salt concentration needed to promote its retention is the lowest.

3.4 Effect of flow rate on plasmid isoforms separation

Monolithic supports are characterized by a single piece with highly interconnected pores where mass transport is based on convection by laminar flow, enabling very fast separations [29]. Given that the stability, integrity and pDNA biological activity are important parameters for the pDNA application and can be affected by the time of chromatographic run, it can be considered a crucial factor in purification strategies to be controlled in order to avoid pDNA structural damages.

To verify the effect of flow rate on separation of plasmid isoforms, decreasing stepwise gradients of ammonium sulfate with pVAX1-*LacZ* were studied. The gradient and elution buffer conditions used to study the effect of flow rate were similar to the conditions used to separate pVAX1-*LacZ* isoforms. As shown in Fig. 3 (A), the stepwise gradients were performed at a flow rate of 1mL/min, 2mL/min and 4mL/min. The peaks content was revealed by agarose gel electrophoresis (Fig.3 (B)) and as expected, lanes 1, 3 and 5 correspond to the oc isoform, and lanes 2, 4 and 6 correspond to the sc isoform that is isolated for all experiments. All chromatograms were normalized in function of the elution volume, although the experiment performed at 4 mL/min took only 2 min.

These results show that also the modified L-histidine monolith exerts the pDNA isoforms separation with good resolution, which is maintained at different flow rates, in the studied range.

3.5 Dynamic binding capacity

In order to better characterize the modified L-histidine monolith, dynamic binding capacity studies were carried out. Since it was demonstrated that at different

flow rates the plasmid isoforms separation remained unchanged, it was also interesting to verify the flow rate effect on the monolith binding capacity.

Breakthrough experiments were performed at 0.5 and 1 mL/min using a pDNA feedstock solution with 0.05 mg/mL, obtained after alkaline lysis and pre-purification with the NZYTech kit. The L-histidine monolith was equilibrated with 3.5 M ammonium sulfate in 10 mM Tris-HCl and 10 mM EDTA, pH 8.0 and the same ionic strength was used to prepare the 0.05 mg/mL plasmid feedstock solution. Determination of dynamic binding capacity was carried out by recording breakthrough curves at 260 nm. The dynamic binding capacity values were obtained, after data normalization, by subtracting the value obtained under non-binding conditions and multiplying by the pDNA concentration. The ratio between the amount of bound pDNA and the support volume (0.34 mL) at 10%, 50% and 100% of the breakthrough was then calculated and the results are present in Table 2.

It is generally described for monolithic supports that the purification and capacity are independent of the flow rate [30, 31]. However, the present work indicates a smooth increase of capacity for the low flow rate assays. This result cannot be related with the monolith characteristics but with the plasmid properties. The increasing contact time between the matrix and pDNA favors the attainment of equilibrium and a smaller area is occupied by the pDNA, which becomes less extended at lower flow rates [32, 33]. Similar conclusions about how the pDNA conformation and the flow rate affect the capacity were reported in previous studies using a non-grafted monolith [17], and an histidine-agarose matrix [32]. Thus, these particular studies reinforce the hypothesis that the support capacity is in part dependent of the pDNA size and conformation [33, 34].

Overall these results are very satisfactory, since an increased capacity was achieved for the L-histidine monolith (3.88 mg/mL of column) at 10% breakthrough, 1 mL/min with 0.05 mg/mL of plasmid feedstock solution, when compared to the non-grafted monolith (2.19 mg/mL of column), with identical loading conditions [17]. This increased capacity might be related with the increased binding sites of the monolith after ligand immobilization [26], since it is expected an increased capacity after grafting the monolith. In addition, the capacity of L-histidine monolith (6.24 mg/mL) was twenty nine fold higher than the conventional histidine-agarose matrix (0.217 mg/mL) at 50% breakthrough, using identical loading conditions and pDNA concentration at 0.5 mL/min [32].

The results obtained with the L-histidine monolith are also satisfactory when compared with another monolith immobilized with arginine amino acid. The total capacity of arginine monolith determined in a sodium chloride-based elution strategy,, at 1 mL/min of flow rate and 0.05 mg/mL of plasmid feedstock solution was 5.18 mg/mL of column [35]. This value is slightly lower in comparison with the achieved for the L-histidine monolith with the same parameters (6.70 mg/mL of column). Once the loading strategy used for the arginine monolith was performed with low salt concentration, the capacity differences reported above can be related with a reduced intermolecular repulsion between the DNA molecules. Otherwise, the capacity of the L-histidine monolith increased because DNA molecules pack more closely on the surface due to the high salt concentrations used [36].

The capacity results obtained with the L-histidine monolith contradict the affinity chromatography association with low capacity, indicating that the combination of a suitable ligand, like L-histidine, with an appropriate chromatographic support, like monolith, can overcome some purification bottlenecks.

4. Conclusions

SPR, NMR and affinity chromatography are three distinct research areas, however, the knowledge of affinity interactions and the functional groups involved in interactions obtained through SPR and NMR analysis are valuable tools to provide information regarding the interactions that can be explored in affinity chromatographic strategies.

In this study, L-histidine, Im-benzyl-L-histidine and L-methyl-L-histidine, were immobilized on a carboxymethyl-dextran matrix and studied by SPR as affinity ligands for plasmid isoforms separation. The overall affinity with these ligands was significantly high, 10^{-10}-10^{-8} M range, in presence of running buffer 10 mM HEPES at pH 7.4. The maximum response for different plasmid samples was found for L-histidine. No binding response was found using acid HEPES 100 mM or other buffers like Tris-HCl and ammonium sulfate. The ^{1}H NMR spectra suggested that the imidazole ring of L-histidine is more involved in binding and the running buffer affected their strength to the plasmids. The ligand selected for immobilization on epoxy monolith was L-histidine.

L-histidine monolith allowed the successful separation of sc pDNA from the oc isoform, with pVAX1-*LacZ*, HPV-16 E6/E7 and pcDNA3-based plasmids. The separation of plasmid isoforms was achieved by decreasing the ammonium sulfate concentration in the eluent. The three plasmids present different sizes, and the global hydrophobic character slightly increases with the molecular mass. Thus, plasmids with high molecular weight and exhibiting the supercoiled isoform develop strong interactions with the modified support. In addition, the efficiency of plasmid isoforms separation remained unchanged with flow rate variations.

The maximum dynamic binding capacity achieved with the L-histidine monolith was 11.03 mg/mL of column, at 0.5 mL/min and 0.05 mg/mL of plasmid solution. The capacity values were satisfactory when compared to a histidine-agarose conventional matrix, a non-grafted monolith or a monolith modified with arginine amino acid. Therefore, the L-histidine monolith solved some drawbacks associated with conventional matrices where L-histidine ligand has already been used to purify pDNA.

Thus, the monolith modified in this work can be a promising strategy to efficiently purify the sc plasmid DNA with a therapeutic gene, such as the HPV16 E6/E7, from a lysate sample.

Acknowledgments

This work was supported by FCT, the Portuguese Foundation for Science and Technology (PTDC/EBB-BIO/114320/2009) and PEst-C/SAU/UI0709/2011 COMPETE. A. Sousa and C. Cruz acknowledge the post-doctoral fellowships (SFRH/BPD/79106/2011 and SFRH/BPD/46934/2008, respectively) from FCT. The authors acknowledge to Karl Münger for the HPV16 E6/E7 Addgene plasmid, to John Blenis for the pcDNA3-myc-FLNa S2152A Addgene plasmid, to BIA Separations for having kindly provided monolithic supports and especially to Dr. Urh Černigoj for the valuable help in the L-histidine amino acid immobilization to the epoxy monolithic disc.

References

[1] C. Vox, Biotechnol Annu. Rev.13 (2007) 201.

[2] J. Stadler, R. Lemmens, T. Nyhammar, J. Gene Med. 6 (2004) S54.

[3] A. Eon-Duval, G. Burke, J. Chromatogr. B 804 (2004) 327.

[4] D.R. Latulippe, A.L. Zydney, J. Chromatogr. A 1216 (2009) 6295.

[5] F. Smrekar, A. Podgornik, M. Ciringer, S. Kontrec, P. Raspor, A. Strancar, M. Peterka, Vaccine 28 (2010) 2039.

[6] Y. Han, G.M. Forde, J. Chromatogr. B 874 (2008) 21.

[7] V.B. Pillai, M. Hellerstein, T. Yu, R.R. Amara, H.L. Robinson, Vaccine 26 (2008) 1136.

[8] A. Ghanem, R. Healey, F.G. Adly, Anal. Chim. Acta 760 (2013) 1.

[9] F. Sousa, C. Cruz, J.A. Queiroz, J. Mol. Recognit. (2010) 505.

[10] F. Sousa, T. Matos, D.M.F. Prazeres, J.A. Queiroz, Anal. Biochem. 374 (2008) 432.

[11] A. Sousa, F. Sousa, J.A. Queiroz, J. Chromatogr. B 877 (2009) 3257.

[12] F. Sousa, C.T. Tomaz, D.M.F. Prazeres, J.A. Queiroz, Anal. Biochem. 343 (2005) 183.

[13] M. Ritzefeld, N. Sewald, Amino Acids 2012 (2012).

[14] C. Cruz, E. J. Cabrita, J.A. Queiroz, Anal. Bioanal. Chem. 401 (2011) 983.

[15] C. Cruz, S.D. Santos, E.J. Cabrita, J.A. Queiroz, Int. J. Biol. Macromol. 56 (2013) 175-180.

[16] C. Cruz, A. Sousa, F. Sousa, J.A. Queiroz, Anal. Methods, 5 (2013) 1682.

[17] A. Sousa, D. Bicho, C.T. Tomaz, F. Sousa, J.A. Queiroz, J. Chromatogr. A 1218 (2011) 1701.

[18] A. Sousa, F. Sousa, J.A. Queiroz, J. Sep. Sci. 35 (2012) 3046.

[19] K. Münger, W. Phelps, V. Bubb, P. Howley, R. Schlegel, J. Virol. 63 (1989) 4417.

[20] M.S. Woo, Y. Ohta, I. Rabinovitz, T.P. Stossel, J. Blenis, Mol. Cell. Biol. 24 (2004) 3025.

[21] A. McWhirter, S. Löfås, Springer Ser. Chem. Sens. Biosens. (2006) 117.

[22] M. Fischer, Method. Mol. Biol. 627 (2010) 55.

[23] C. Caramelo-Nunes, P. Almeida, J. Marcos, C. Tomaz, J. Chromatogr. A 1327 (2014) 1.

[24] F. Sousa, S. Freitas, R.A. Azzoni, J.A. Queiroz, D.M.F. Prazeres, Biotechnol. Appl. Biochem. 45 (2006) 131.

[25] A. Sousa, F. Sousa, D.M.F. Prazeres, J.A. Queiroz, Biomed. Chromatogr. 23 (2009) 745.

[26] N.M. Luscombe, R.A. Laskowski, J.M. Thornton, Nucleic Acids Res. 29 (2001) 2860.

[27] M. Tanigawa, T. Okada, Anal. Chim. Acta 365 (1998) 19.

[28] T.R. Strick, J.F. Allemand, D. Bensimon, V. Croquette, Biophys. J. 74 (1998) 2016.

[29] A. Podgornik, A. Savnik, J. Jančar, N.L. Krajnc, J. Chromatogr. A 1333 (2014) 9.
[30] T. Koloini, I. Mihelic, J. High Resol. Chromatogr. 2000 (1) 39.
[31] A. Podgornik, N.L. Krajnc, J. Sep. Sci. 35 (2012) 3059.
[32] F. Sousa, D.M.F. Prazeres, J.A. Queiroz, Biomed. Chromatogr. 21 (2007) 993.
[33] C. Haber, J. Skupsky, A. Lee, R. Lander, Biotechnol. Bioeng. 88 (2004) 26.
[34] D. Bicho, A. Sousa, F. Sousa, J.A. Queiroz, C.T. Tomaz, J. Sep. Sci. (2014). Doi:10.1002/jssc.201400127.
[35] A. Soares, J.A. Queiroz, F. Sousa, A. Sousa, J. Chromatogr. A 1320 (2013) 72.
[36] M. Bencina, A. Podgornik, A. Strancar, J. Sep. Sci. 27 (2004) 801.

555

556 **Table 1.** Equilibrium data analysis of plasmids in 10 mM of HEPES pH 7.4.

Plasmid samples		K_D(M) ± SD		
		L-methyl-L-histidine	**Im-benzyl-L-histidine**	**L-histidine**
pVAX1-*LacZ*	sc	5.05×10^{-8}±0.00613	6.03×10^{-9}±0.00595	5.79×10^{-8}±0.0131
	oc	*	5.62×10^{-8}±0.00607	8.18×10^{-8}±0.00441
	ln	*	*	*
HPV-16 E6/E7	sc	*	*	*
	oc	1.1×10^{-10}±0.00573	*	*
	ln	*	*	3.34×10^{-10}±0.0209
pcDNA3-based plasmid	sc	*	2.95×10^{-8}±0.00734	4.2×10^{-8}±0.00629
	oc	*	*	*
	ln	*	1.68×10^{-9}±0.00702	2.44×10^{-9}±0.00848

557 K_D-dissociation constant; **SD**-standard deviation

558

559 **Table 2.** Dynamic binding capacity results of L-histidine monolith at 0.5 and 1 mL/min.
560 Breakthrough experiments were performed with a 0.05 mg/mL pDNA solution pre-
561 purified and the capacity was estimated at 10, 50 and 100% of breakthroughs.

Flow rate	DBC (mg/mL)		
	10%	50%	100%
1 mL/min	3.88	4.96	6.70
0.5 mL/min	4.20	6.24	11.03

562

563

Figure captions

Figure 1. Chromatographic profiles of L-histidine monolith with the pVAX1-*LacZ* plasmid sample, pre-purified with NZYTech kit, under different elution conditions. (A) Decreasing linear gradient from 3.5 M to 0 M $(NH_4)_2SO_4$ in 10 mM Tris-HCl and 10 mM EDTA, pH 8.0; (B) decreasing linear gradient from 3.5 M to 0 M $(NH_4)_2SO_4$ in 10 mM Tris-HCl and 10 mM EDTA, pH 6.0; (C) increasing linear gradient from 0 M to 3 M NaCl in 10 mM Tris-HCl and 10 mM EDTA, pH 8.0. The assays were performed at 1 mL/min and labels in the peaks represent the pDNA retention time.

Figure 2. Separation of plasmid isoforms of different sizes with the histidine monolith. The $(NH_4)_2SO_4$ concentrations optimized for the isoforms separation of each plasmid were (A) 2.99 M for pVAX1-*LacZ* (6.05 kbp), (B) 2.94 M for HPV-16 E6/E7 (8.70 kbp) and (C) 2.91 M for pcDNA3-based plasmid (14 kbp). UV detection at 260 nm. Injection volume was 100 µL. (D) Agarose gel electrophoresis of each peak resultant from the respective chromatogram. Lane M: molecular weight marker; lanes A, B and C: pDNA samples injected onto the column (oc+sc); lanes 1, 3 and 5: oc isoform; lanes 2, 4 and 6: sc isoform.

Figure 3. (A) Flow rate effect on pVAX1-*LacZ* isoforms separation. Experiments were performed by decreasing stepwise gradient from 2.99 M to 0 M $(NH_4)_2SO_4$ in 10 mM Tris-HCl and 10 mM EDTA, pH 8.0 at different flow rates (1, 2 and 4 mL/min). (B) Agarose gel electrophoresis of each peak resultant from the respective chromatogram. Lane M: molecular weight marker; lane A: pVAX1-*LacZ* sample injected onto the column (oc+sc); lanes 1, 3 and 5: oc isoform; lanes 2, 4 and 6: sc isoform.

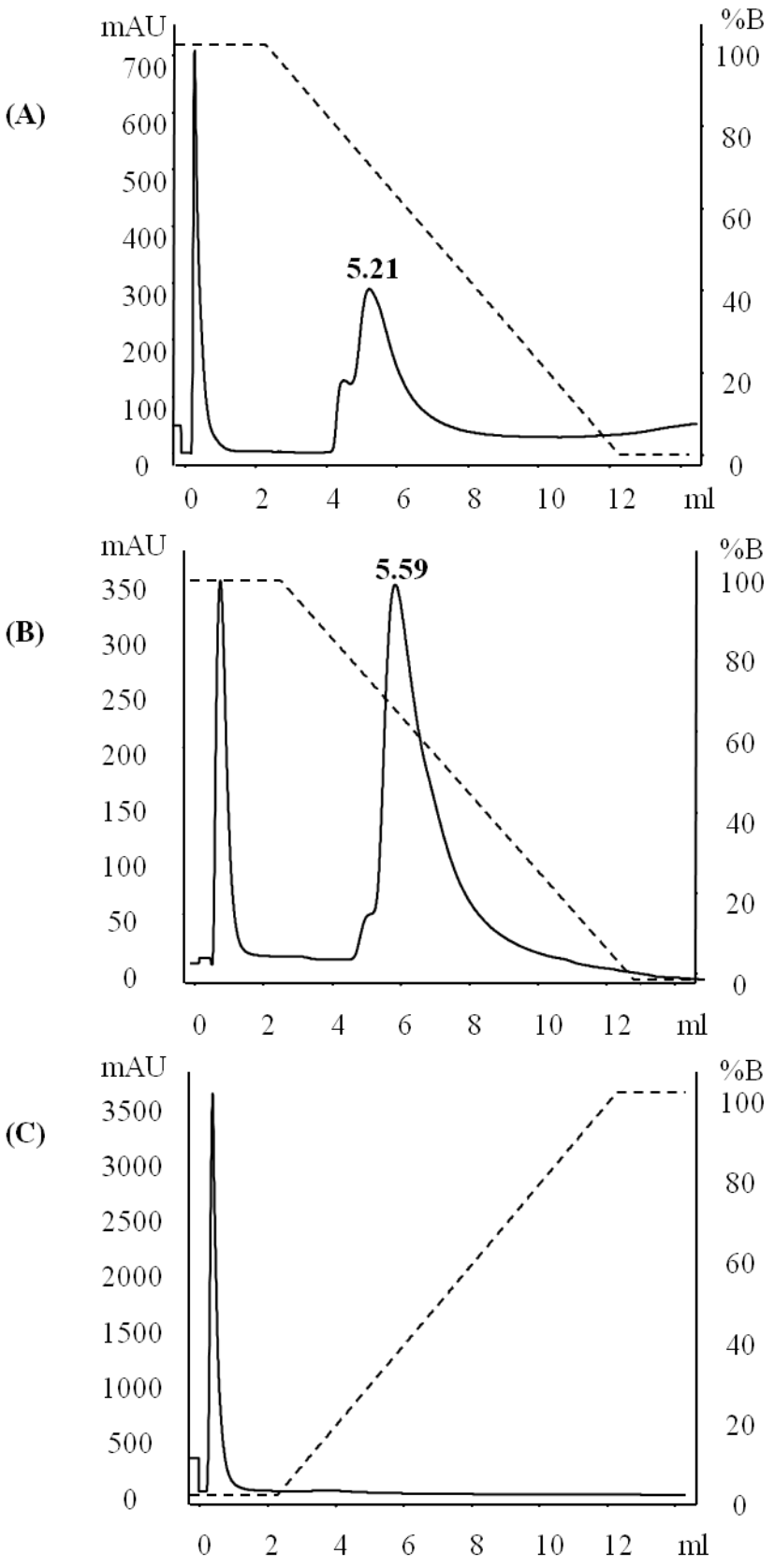

590

591

592 **Fig. 1**

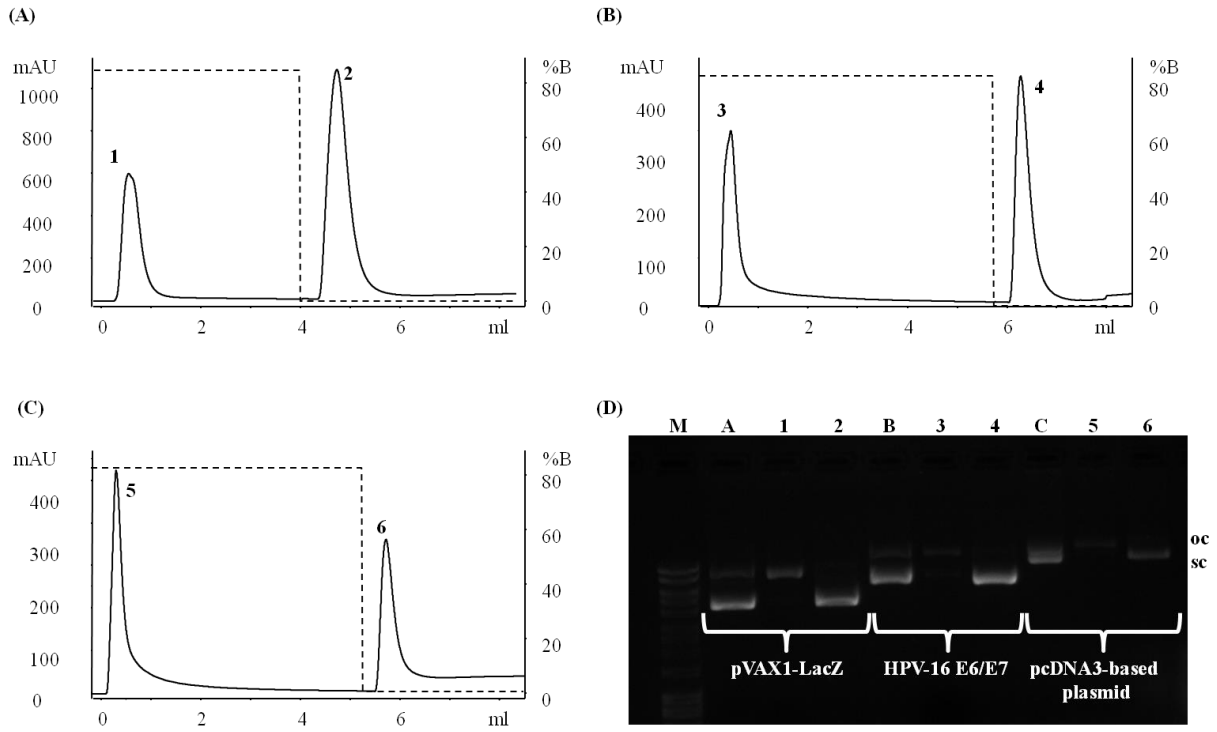
(A)
mAU
%B
ml
1
2
(B)
3
4
(C)
5
6
(D)
M A 1 2 B 3 4 C 5 6
oc
sc
pVAX1-LacZ
HPV-16 E6/E7
pcDNA3-based plasmid

Fig. 2

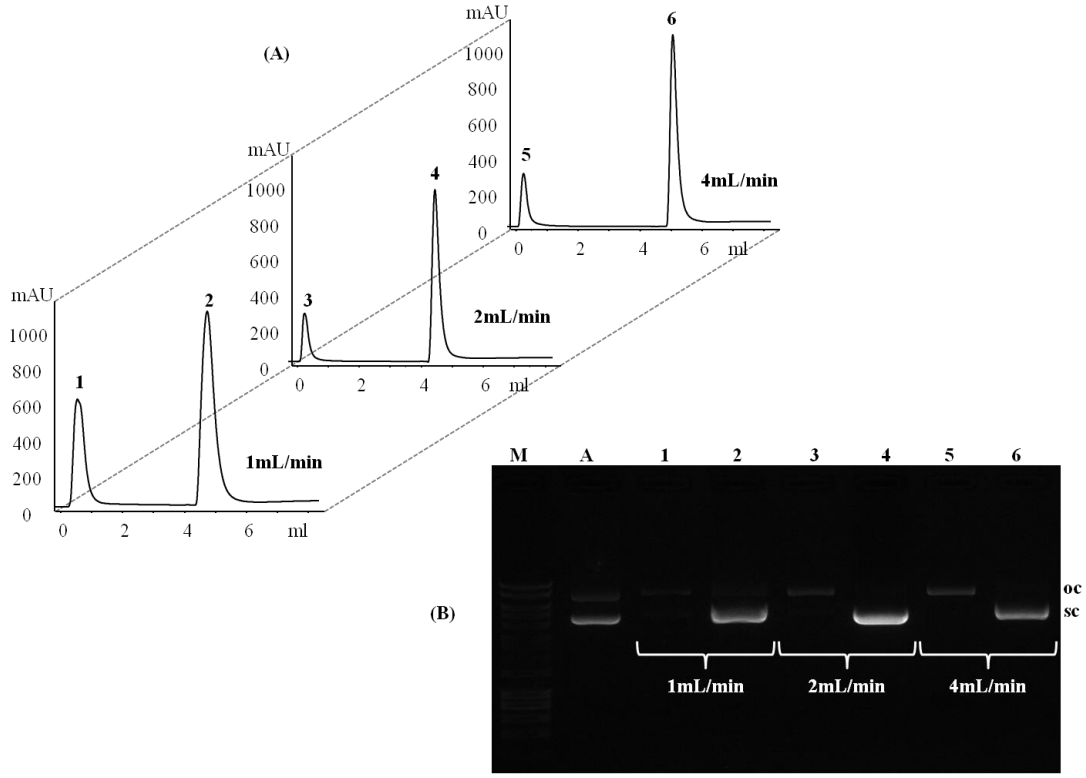
(A)
mAU
ml
1
2
1mL/min
3
4
2mL/min
5
6
4mL/min
(B)
M A 1 2 3 4 5 6
oc
sc
1mL/min
2mL/min
4mL/min

Fig. 3

Supplementary information

A)

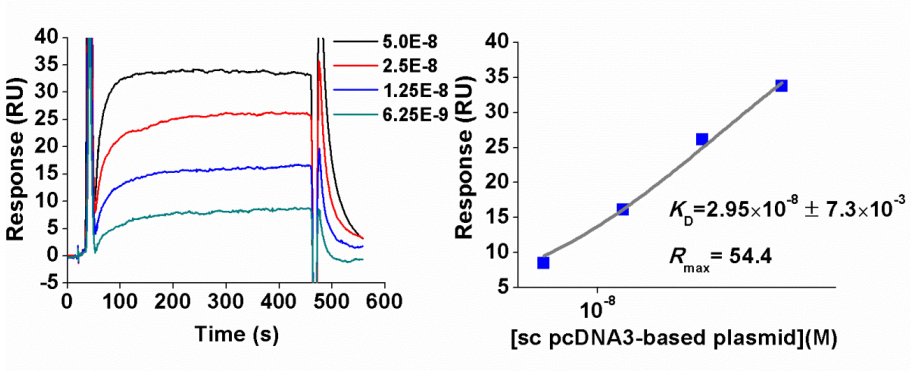

B)

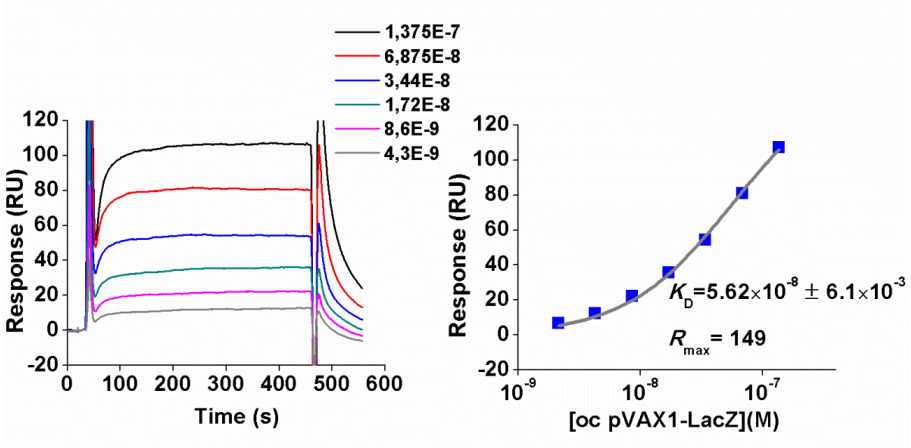

C)

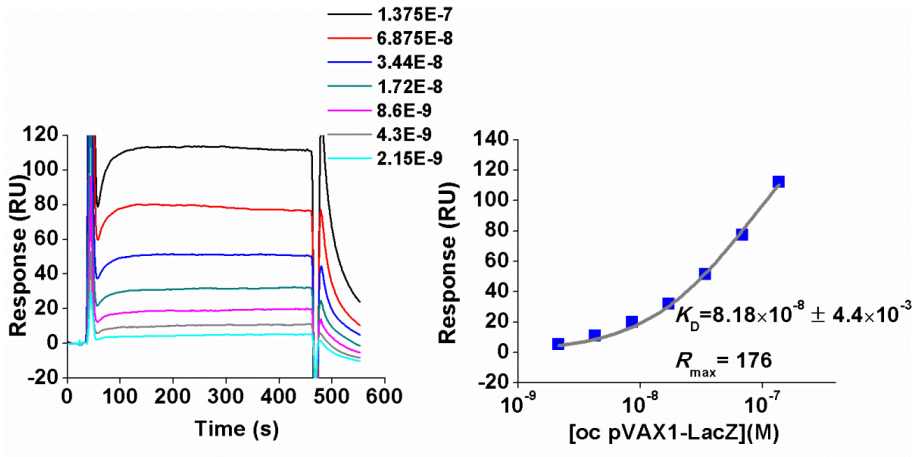

D)

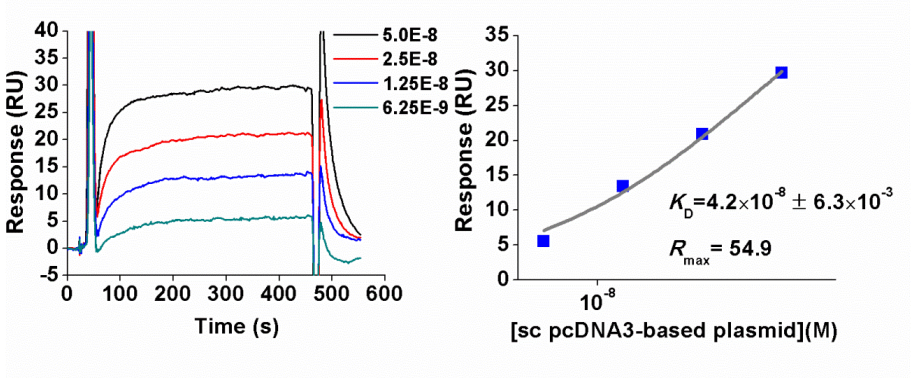

620 **S1.** Sensorgrams and equilibrium-binding analysis of immobilized Im-benzyl-L-
621 histidine to A**)** sc isoform of pcDNA3-based plasmid B**)** oc isoform of pVAX1-*LacZ*
622 and immobilized L-histidine to **C)** oc isoform of pVAX1-*LacZ* and **D)** sc isoform of
623 pcDNA3-based plasmid in HEPES 10mM pH 7.4.

624
625